UNIVERSITY OF TURKU

TURUN YLIOPISTON MAANTIETEEN JA GEOLOGIAN LAITOKSEN JULKAISUJA
PUBLICATIONS OF THE DEPARTMENT OF GEOGRAPHY AND GEOLOGY OF UNIVERSITY OF TURKU

No. 26

CHARACTERISTICS OF SPATIO-TEMPORAL TEMPERATURE VARIABILITY IN RELATION TO POPULATION AND VARIOUS ENVIRONMENTAL PARAMETERS

A case study of Turku, SW Finland

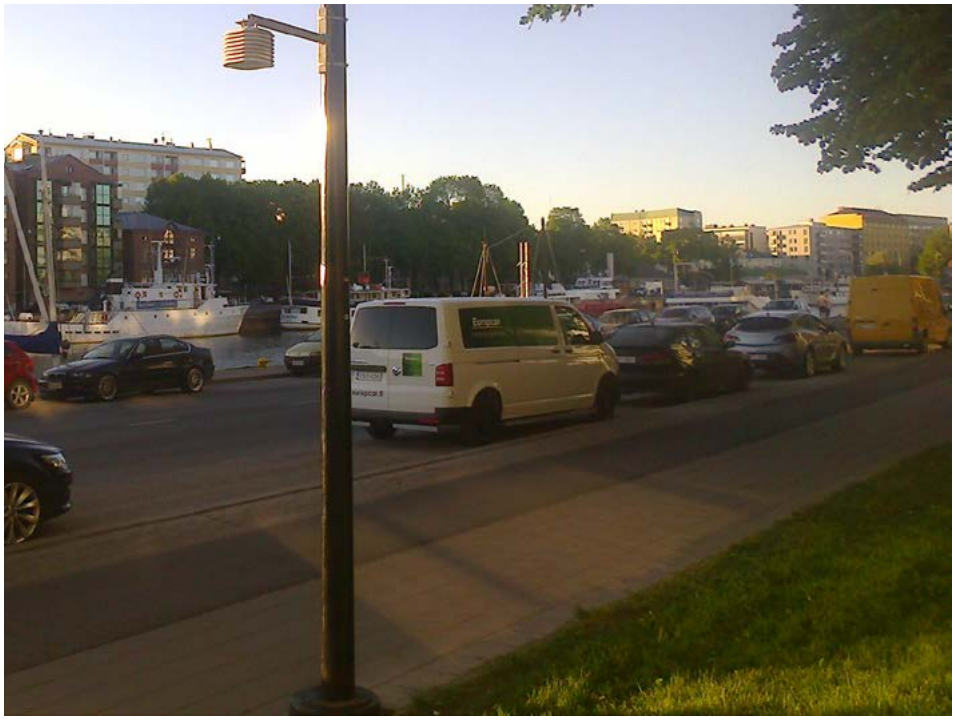

Juuso Suomi, Krista Väätäinen & Jukka Käyhkö

CHARACTERISTICS OF SPATIO-TEMPORAL TEMPERATURE VARIABILITY IN RELATION TO POPULATION AND VARIOUS ENVIRONMENTAL PARAMETERS

A case study of Turku, SW Finland

Juuso Suomi, Krista Väätäinen & Jukka Käyhkö

Turku 2025
University of Turku
Department of Geography and Geology
Division of Geography

TURUN
YLIOPISTO
UNIVERSITY
OF TURKU

This project has received funding from the European Union's Horizon 2020 research and innovation programme under Grant Agreement nº 957751. The document represents the views of the authors only and is their sole responsibility: it cannot be considered to reflect the views of the European Commission and/or the European Climate, Infrastructure and Environment Executive Agency (CINEA). The European Commission and the Agency do not accept responsibility for the use that may be made of the information it contains.

ISBN ISBN 978-952-02-0383-2 (PDF)
ISSN 2324-0369 (Electronic)
Painosalama, Turku, Finland 2025

CONTENTS

ABSTRACT

This study investigates the local climate of Turku, a coastal city in southwestern Finland, and its surrounding areas. The Turku Student Village, located in the study area approximately two kilometres to the northeast of the city centre, is under more specific consideration. The study area consists of various urban and rural land cover types. The study is based on open-access GIS data on air pressure, land cover, elevation and water bodies, and GIS data on population and building floor area. The temperature data of the study consists of temperature observations of 77 loggers measuring temperatures and relative humidity (T/RH) in the study area at half-an-hour interval. The loggers are part of a continuous project monitoring the local climate in the Turku area, managed by the Turku Urban Climate Research Group (TURCLIM) of the Geography Division at the Department of Geography and Geology at the University of Turku. The study is conducted in the context of the RESPONSE research project (https://h2020response.eu/) funded by the European Commission's Horizon 2020 Framework Programme. The study is based on the half-an-hour interval temperature observations of the calendar year 2024. For the purposes of the RESPONSE project, the TURCLIM observation network was densified in the Turku Student Village area with nine additional loggers in the beginning of the RESPONSE project in 2020. Before that, the Turku Student Village had only one T/RH logger. This dense local cluster enables examining spatio-temporal temperature differences also inside the Turku Student Village area. This study compares the weather conditions of the year 2024 with the long-term climate of the Turku region, represented by the 30-year reference period 1991–2020. The study focuses on temperature observations and spatially continuous temperature maps. The maps are produced as part of a research process using a linear regression model based on the temperature observations and open-access GIS data on environmental factors relevant for spatial temperature differences. The observed temperatures are analysed on both monthly and diurnal scales within two spatial scales: the Turku region as a whole and the more localized Turku Student Village area. Compared to the coverage of the TURCLIM observation network, the regression model results and related temperature maps are examined even in a broader regional scale in order to assess spatial temperature patterns in a regional scale in and around the city of Turku. The results demonstrate significant spatial and temporal variability of temperature across the Turku region in 2024, with the Turku city centre being consistently as the warmest area. A temperature difference of on average 2 °C occurred between the warmest (Kauppatori) and coolest (Niuskala) sites, aligning with longer-term averages between the respective sites located in the Turku city centre and on the forested uninhabited area approximately 10 km to the north-northeast of the Turku city centre. The main factors influencing spatial temperature variability in the Turku area were land cover and urban morphology, proximity to water bodies and elevation. Urban land cover, related large building mass and high population density had almost persistent warming effect resulting in the urban heat island (UHI) phenomenon. Water bodies had seasonally varying impacts appearing mostly as cooling during spring days and warming in autumn and winter nights. Elevation effects were generally weaker but notable during nocturnal inversion conditions. Large-scale atmospheric patterns, wind speed, and cloudiness

further modulated spatial differences. These findings underscore the importance of fine-scale environmental heterogeneity as an agent behind spatial temperature differences and support the need for climate-sensitive urban planning to mitigate heat stress and improve energy efficiency.

Keywords: urban heat island, spatio-temporal temperature variability, regression model, population, building floor area, land cover

1
THEORETICAL BACKGROUND

Urban and other densely built areas promote a unique environment with a diverse climate that is distinctive of surrounding rural areas. Typical characteristics of urban climate include weaker wind speed compared to rural areas due to buildings disturbing the passing of wind, air pollutants due to anthropogenic activity, such as traffic and industries, and lower humidity (Kuttler & Weber, 2023). On the contrary to the average wind speed slowing effect of buildings, they can cause wind tunnels, in which bursts of wind reach higher than average speeds between buildings. Humidity is lower in cities compared to the countryside due to effective sewer systems where rainwater quickly drains and decreases evaporation from surfaces. Moreover, urban areas often have less vegetation than rural areas, resulting in reduced evapotranspiration in the cities.

A common feature of urban climates is the urban heat island (UHI) effect, where urban and other built-up areas usually appear warmer than the surrounding rural areas (Oke, 1987). Cities are warmer than the countryside due to anthropogenic heat release, differences in evapotranspiration between the urban and rural areas and due to the stored solar heat in buildings and pavements that is released typically during the night. The heat released at night slows the cooling process of the cities resulting in higher temperatures compared to the countryside. Key factors in anthropogenic heat production are heating of buildings, vehicle traffic and nearby industries. Environmental factors like terrain and distance from the coastline also shape the unique features of the UHI effect in various cities (Reinwald et al., 2024). This study investigates the influence of elevation, water bodies, and land cover on UHI intensity and examines the spatial characteristics of the UHI effect during the year 2024 in the city of Turku, southwestern Finland.

2
STUDY AREA

The study area consists of the city of Turku and surrounding areas and municipalities (Figure 1). Turku, located in southwestern Finland, is a mid-sized coastal city with 206 655 inhabitants (at the end of June 2025). The southwest parts of the area are surrounded by the brackish Baltic Sea with a broad and substantial archipelago consisting of nearly 40 000 islands. The city centre (60°27′ N, 22°16′ E) is built around the River Aura that runs through the centrum from Oripää eskers and discharges into the Baltic Sea. The coastal location next to the Baltic Sea and the River Aura has an effect on the climate of Turku.

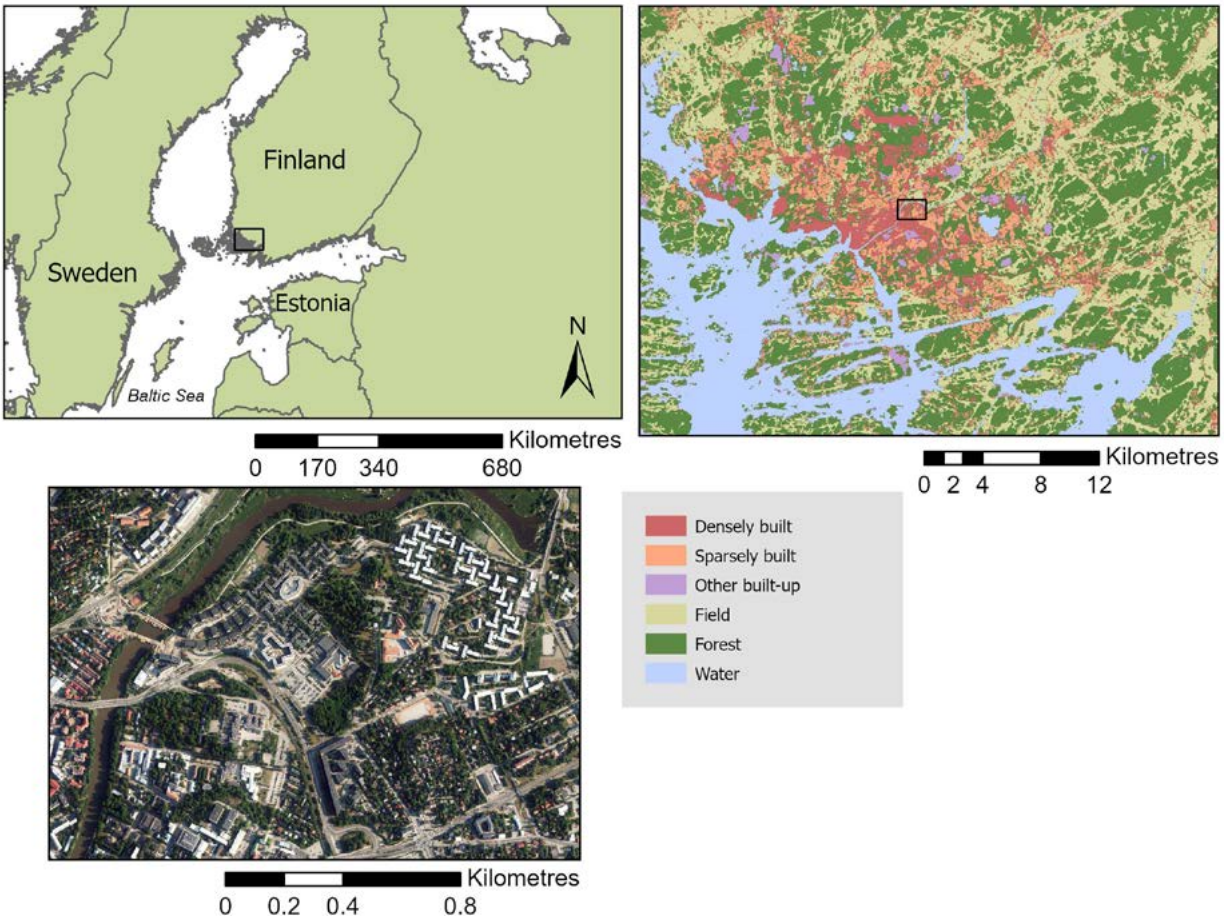

Figure 1. The study area presenting the geographical location of southwest Finland (upper left), the land cover of southwest Finland and Turku region with Turku Student Village's geographical location indicated (upper right) and an ortho aerial photo of the Turku Student Village area (bottom left). The land cover map is based on the CORINE Land Cover 2018 dataset. The aerial photo is produced by the National Land Survey of Finland.

According to Köppen's climate classification, Turku has a Dfb climate, characterized as a humid continental climate with warm summers and no major seasonal variation in precipitation. Between 1991 and 2020, the average annual temperature at Turku Airport was 5.8 °C (Jokinen et al., 2021). February is typically the coldest month, averaging –4.5 °C, while July is the warmest, with an average temperature of 17.5 °C. The city receives an average of 684 mm of precipitation annually, with July being the wettest month (74 mm) and April the driest (32 mm). The mean annual wind speed is 3.4 m/s, peaking in December at 3.7 m/s and reaching its lowest in July, August, and September at 3.1 m/s.

3
DATA AND METHODS

This study was conducted with the temperature observations of the TURCLIM research group observation network owned by the Geography Division of the University of Turku and consisting of 85 observation sites monitoring the local climate around Turku at half-an-hour interval on 3-meter elevation above the ground. The observation sites are located around Turku and neighbouring municipalities creating an extensive network (Figure 2 & 3). In this study, the half-an-hour interval air temperature data of 2024 recorded by 77 Onset Hobo Pro v2 U23-001 T/RH loggers placed inside Onset RS1 radiation shields are used. The data includes temperature observations of nine additional loggers installed in the Turku Student Village in December 2020 to densify the observation network for the purposes of the RESPONSE project (Figure 4). The TURCLIM dataset supports comprehensive research into the spatial and temporal variability of temperature. The observation sites represent a wide range of various environmental settings (Table 1) which, when combined with diverse GIS data, allow for the assessment of the impacts of environmental factors, such as topography, land cover, and distance to sea areas, on spatial temperature variations across different seasons and weather patterns.

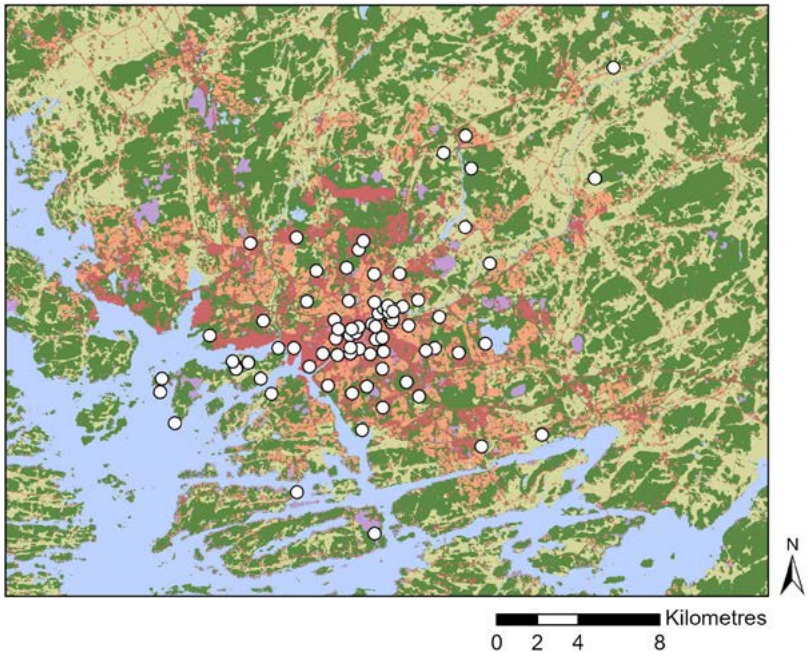

Figure 2. The TURCLIM observation site locations (white circles) in and around the city of Turku. Background map: CORINE Land Cover 2018, reclassified.

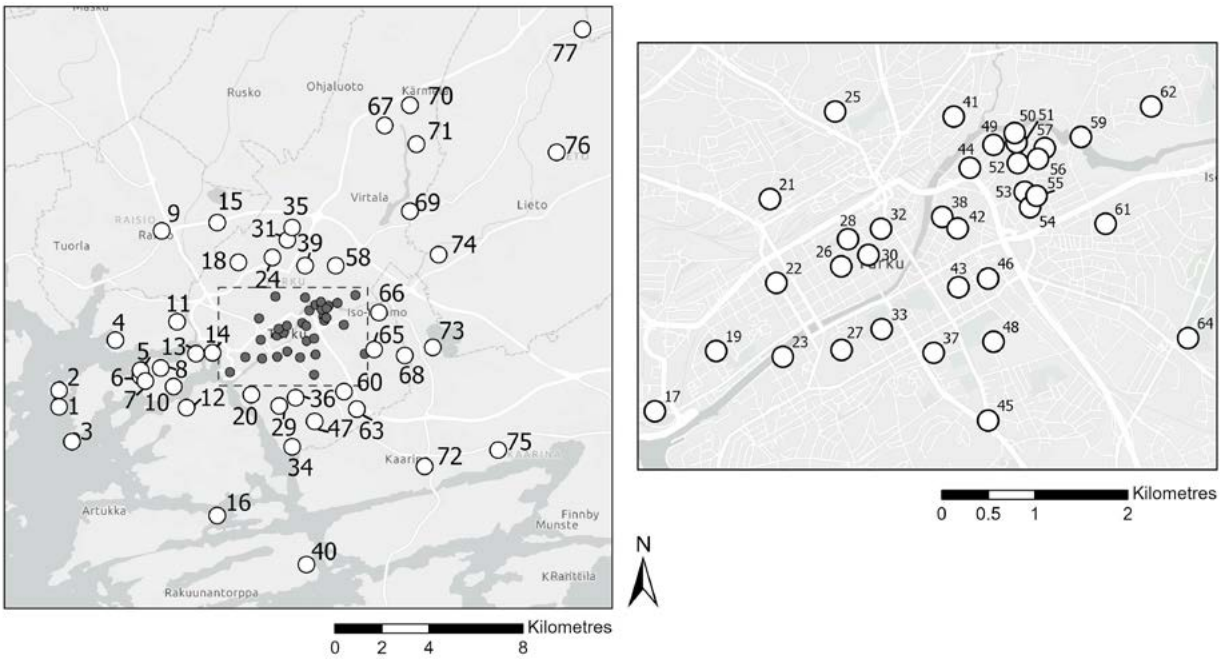

Figure 3. Zoomed view of the TURCLIM observation site network. The loggers are numbered consecutively based on the eastern coordinate. For information on the observation site elevation and land cover, see Table 1.

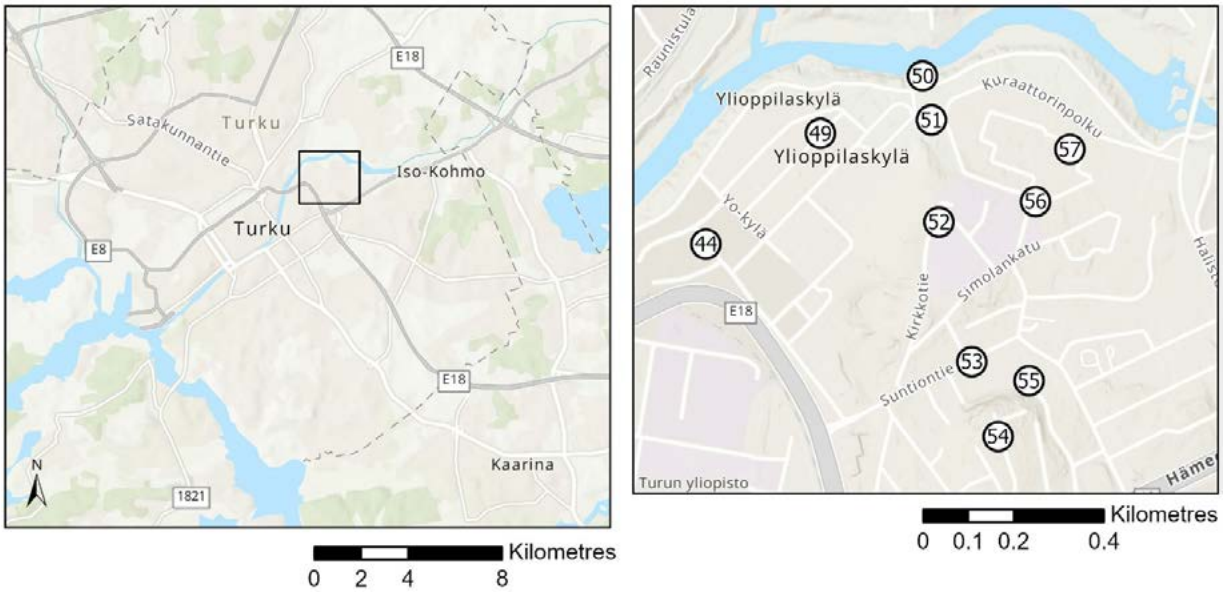

Figure 4. Observation sites of the Turku Student Village area. For information on the observation site elevation and land cover, see Table 1.

Monthly inspection of 2024 temperatures was performed with various types of analyses. Data of a 1991–2020 climate reference period provided by the Finnish Meteorological Institute (FMI) (Jokinen et al., 2021) was used to relate the 2024 temperatures to the long-term average conditions. FMI has three observation sites in Turku: Artukainen, Rajakari and Turku airport. In this study, the observations of Turku airport during the climate reference period were utilized. In visualizing the maps, ortho-aerial photographs and CORINE Land Cover 2018 data provided by the National Land Survey of Finland were used.

Table 1. Elevation and urban land cover proportion in the surroundings of the TURCLIM observation sites.

No	Logger Name	Elevation (m)*	Urban land cover proportion (%)**
1	Kolkka	0.5	0.0
2	Camping	1.4	19.8
3	Kuuva	4.8	0.0
4	Pansio	3.5	0.0
5	Hiiriluoto ranta	0.5	0.0
6	Hiiriluoto mäki	36.3	0.0
7	Hiiriluoto manner	17.3	0.0
8	Kasvitieteellinen	4.6	0.0
9	Raisio	14.5	95.1
10	Ruissalo	1.0	0.0
11	Messukeskus	6.0	85.2
12	Hirvensalo	0.8	0.0
13	Marjaniemi	17.0	56.8
14	Vapaavarasto	2.5	25.9
15	Mylly	20.8	76.5
16	Satava	1.2	12.3
17	Linna	2.3	49.4
18	Metsäkyla	22.4	3.7
19	Kakola	18.0	49.4
20	Heikkilänkasarmi	4.1	25.9
21	Kähäri	20.9	32.1
22	Mikaelinkirkko	9.8	76.5
23	Martti	2.5	55.6
24	Impivaara	31.1	0.0
25	Rieskalähde	31.4	28.4
26	Betel	16.9	100.0
27	Urheilupuisto	23.3	0.0
28	Puolalanmäki	28.9	86.4
29	Ispoinen	16.5	1.2
30	Kauppatori	7.7	97.5
31	Runosmäki	37.6	98.8
32	Puutori	18.1	100.0
33	Luostarivuori	33.5	81.5
34	Katariina	6.5	0.0
35	Vahdontie	40.1	45.7
36	Luolavuori	43.5	0.0
37	Saarnitie	16.8	16.0
38	Piispankatu	9.7	25.9
64	Pääskyvuori WS	15.2	21.0
65	Pääskyvuori	47.7	21.0
66	Kurala	13.5	0.0
67	Ylijoki	33.8	0.0
68	Varissuo	46.2	80.2
69	Metsämäki	21.3	0.0
70	Jäkärlä	56.6	69.1
71	Niuskala	32.4	0.0
72	Kaarina	17.3	56.8
73	Rauhanniemi	39.7	0.0
74	Vanhalinna	22.2	9.9
75	Tuorla	14.1	14.8
76	Lieto	30.8	0.0
77	Sikilä	43.3	16.0

* Metres above sea level.
** Urban land cover proportion is calculated within a 100 metre radius around the observation site. Urban land cover consists the following three CORINE Land Cover 2018 classes: blocks of flats areas, commercial areas and road and rail networks and associated lands.

For each month, multiple linear regression models were constructed with temperature, as measured by the TURCLIM observation network, serving as the response variable, and various environmental factors as explanatory variables. These factors included land cover, topography, and water bodies, each derived from high-resolution spatial datasets. The land cover variable was based on the CORINE Land Cover 2018 dataset (20 × 20 m resolution) (Syke, 2024), while the topography variable came from the national elevation model (10 × 10 m resolution) (National Land Survey of Finland, 2019), and the water bodies variable was obtained from the SLICES 2010 land use classification (10 × 10 m resolution) (National Land Survey of Finland, 2020). Each explanatory variable was calculated within an optimally sized buffer zone, selected individually for each case using Pearson's correlation coefficients between the variable and observed temperatures (see Table 2). The land cover variable represents the proportion of urban land cover types within the buffer area, calculated as the ratio of urban land cover, defined by three CORINE classes: blocks of flats, commercial areas, and transport-related areas, to the total buffer area. The water bodies variable measures the share of water-covered areas within a buffer. The topographic variable reflects the site's relative elevation, determined by subtracting the average elevation of the buffer from the elevation of the observation site, resulting in positive values for elevated locations (e.g., hilltops) and negative values for low-lying areas (e.g., valleys). In addition to estimating the effects of environmental factors on temperatures, these regression models were applied in producing high-resolution (100 m) spatial temperature maps for each study case. By using the Enter method, all explanatory variables were included in the regression models, regardless of their statistical significance. A significance threshold of $p \leq 0.05$ was used when interpreting model results.

To complete the information on the impacts of urban morphology and population density on spatial temperature differences and to assess the usability of the Grid Data of Community Structure Monitoring (known as YKR data) (Statistics Finland, 2023) in temperature modelling, the month-specific regression models, in which a YKR data based variable acted as an urban variable, were calibrated. The YKR data used in this study include the total population and total building floor area. Of those, a combined standardized variable was formed, in which both have equal weights. The original YKR data consists of 250 m x 250 m grid cells. In this study, a combined variable on population and building floor area was tested against temperature with Pearson correlation coefficients with three spatial resolutions: 1 x 1 (250 m x 250 m), 3 x 3 (750 m x 750 m) and 5 x 5 (1250 m x 1250 m) grid cells. Similarly, as for the CORINE data, the results of the Pearson's correlation analyses were utilised in the selection of the most optimal buffer sizes of the explanatory variables for the regression model (Table 2). Linear regression models including the YKR based variable as an urban explanatory variable were calibrated with the same explanatory variables on the water bodies and relative elevation that were used in the corresponding models in which the CORINE based urban land cover variable acted as an urban variable. Also the buffer sizes of the variables were the same. Temperature maps, however, were only conducted based on the regression models in which the urban explanatory variable was based on CORINE Land Cover dataset. Also in the regression models including YKR based explanatory variable, all explanatory variables were incorporated into the

models regardless of their individual statistical significance using the Enter method. Similar to the regression models including the CORINE based explanatory variable, a significance level of $p \leq 0.05$ was applied when interpreting the results of the models.

Maps depicting the 500 hPa geopotential height and surface air pressure, obtained from the Wetterzentrale CFS reanalyses, were used in describing and interpreting the weather conditions in the larger area in the Northern Europe (Wetterzentrale, 2025). The maps are available at the standard synoptic times of 00:00, 06:00, 12:00, and 18:00 UTC. As the temperature data are reported in UTC+2, this time offset was accounted for when selecting the appropriate pressure maps. The maps closest to the times of the largest momentary maximum temperature range were selected for the analyses. Additionally, wind speed and cloud cover data corresponding to these maximum temperature range situations were utilised. These wind and cloudiness observations were obtained from the FMI Turku Artukainen station and they represent mean values of the 30-minute period preceding the occurrence of the maximum temperature range. Wind speed is expressed in metres per second (m/s), while cloudiness is reported on the okta scale ranging from 0 (clear sky) to 8 (completely overcast).

Table 2. The optimal buffer radii for the explanatory variables used in the multiple linear regression models were determined based on Pearson's correlation coefficients between each variable and temperature. These buffer sizes represent the spatial scale at which each environmental factor most strongly correlates with temperature and were applied accordingly in the regression models. For the YKR data, one pixel is equivalent to 250 m x 250 m.

	Monthly average temperature				Monthly averages of daily minimums				Monthly averages of daily maximums				Momentary maximum temperature range			
Month	Land cover	YKR**	Water body	Elevation	Land cover	YKR	Water body	Elevation	Land cover	YKR	Water body	Elevation	Land cover	YKR	Water body	Elevation
January	700 m	3 × 3	2 km	300 m	700 m	3 × 3	2 km	500 m	400 m	3 × 3	5 km	100 m	700 m	3 × 3	2 km	500 m
February	1000 m	5 × 5	5 km	100 m	1000 m	5 × 5	2 km*	300 m	400 m	3 × 3	2 km*	500 m	1000 m	5 × 5	5 km	300 m
March	1000 m	5 × 5	2 km	200 m	1000 m	5 × 5	5 km	300 m	500 m	3 × 3	2 km	100 m	700 m	5 × 5	2 km*	300 m
April	700 m	5 × 5	2 km	200 m	700 m	5 × 5	1000 m	300 m	1000 m	3 × 3	2 km	500 m	1000 m	3 × 3	5 km	200 m
May	700 m	5 × 5	1500 m	300 m	700 m	5 × 5	1000 m	300 m	200 m	1 × 1	1500 m	200 m	100 m	3 × 3	500 m	300 m
June	400 m	5 × 5	1500 m	300 m	100 m	5 × 5	2 km	500 m	500 m	3 × 3	1500 m	200 m	700 m	5 × 5	2 km*	100 m
July	400 m	5 × 5	500 m	300 m	400 m	5 × 5	2 km	500 m	700 m	3 × 3	2 km*	200 m	100 m	5 × 5	2 km	300 m
August	400 m	5 × 5	500 m	300 m	100 m	3 × 3	2 km	500 m	300 m	3 × 3	2 km*	300 m	100 m	5 × 5	2 km	500 m
September	400 m	3 × 3	500 m	300 m	100 m	3 × 3	2 km	500 m	300 m	3 × 3	2 km*	100 m	100 m	3 × 3	2 km	300 m
October	400 m	3 × 3	2 km*	300 m	100 m	3 × 3	2 km	500 m	400 m	3 × 3	700 m	500 m	100 m	1 × 1	2 km*	500 m
November	400 m	5 × 5	2 km*	100 m	400 m	5 × 5	2 km*	500 m	400 m	5 × 5	700 m	500 m	100 m	1 × 1	5 km	500 m
December	400 m	5 × 5	5 km	300 m	400 m	3 × 3	5 km	500 m	400 m	3 × 3	5 km	100 m	700 m	1 × 1	2 km	500 m

* The square root of the original value has been applied.
** The pixel size in the YKR data is 250 m x 250 m.

4
RESULTS

4.1 Monthly summaries of temperature variability

4.1.1 January

At the FMI weather station located at Turku Airport, the average temperature in January 2024 was –7.6 °C, which is 3.8 °C colder than the average January temperature for the 1991–2020 climate reference period (Jokinen et al., 2021).

Observing the TURCLIM observation network in January 2024, the warmest and coldest average temperatures were measured in Betel (–6.2 °C) and Sikilä (–8.2 °C) (Figure 5). For the averages of daily minimum temperatures, the sites remained the same but with temperatures –9.2 °C (Betel) and –13.0 °C (Sikilä). In the case of the monthly averages of daily maximum temperatures the coldest site was Niuskala with the average temperature of –4.9 °C and the warmest Kauppatori with the average temperature of –3.5 °C. The maximum momentary temperature range occurred on January 21st at midnight 00.00 between the Halinen and Luostarivuori sites. Halinen measured –26.0 °C and Luostarivuori –11.8 °C resulting in a 14.3 °C temperature difference.

Looking at the ten loggers located in the Turku Student Village in January 2024 the lowest average temperature of –7.6 °C occurred in Aurajokiranta while the highest values were recorded in Pispalantie and Kuuvuori with –7.1 °C, respectively (Figure 6). For the monthly averages of daily minimum temperatures, the highest value –10.3 °C occurred in Kuuvuori while the lowest value of –12.6 °C revolved around Aurajokiranta, respectively. In the case of the monthly averages for daily maximum temperatures the dispersion was minimal. The highest value of –4.1 °C was recorded in Pispalantie, while the lowest of –4.3 °C was recorded in four observation sites: Kirkkotie, Kuikkulankatu, Kuuvuori and Yo-kylä itä, respectively. The momentary maximum temperature range in January reached a difference of 11.3 °C between Kuuvuori and Aurajokiranta on the 21st of January at 00.00. One possible explanation for the temperature difference is the presence of inversion conditions, during which elevation differences become more pronounced, particularly between the hilltop site at Kuuvuori and the low-lying Aurajokiranta site located near the river.

The CORINE-based regression model for the monthly average temperatures has an explanatory power (Adjusted R Square) 0.733, while the YKR-based regression model 0.684 with the land cover, building floor area and population and water bodies being statistically significant out of the explanatory variables (Table 3). The variable vl_3_5_700 represents the proportion of urban land cover, specifically apartment building areas, service areas, and traffic areas, within a 700-metre radius. The variable tkuwaters500m indicates the proportion of water bodies within a 500-metre radius. The variable relelev200 refers to relative elevation, calculated as the difference between the elevation of the observation site and the average elevation within a 200-metre buffer surrounding the site. The variable rakvae_3x3

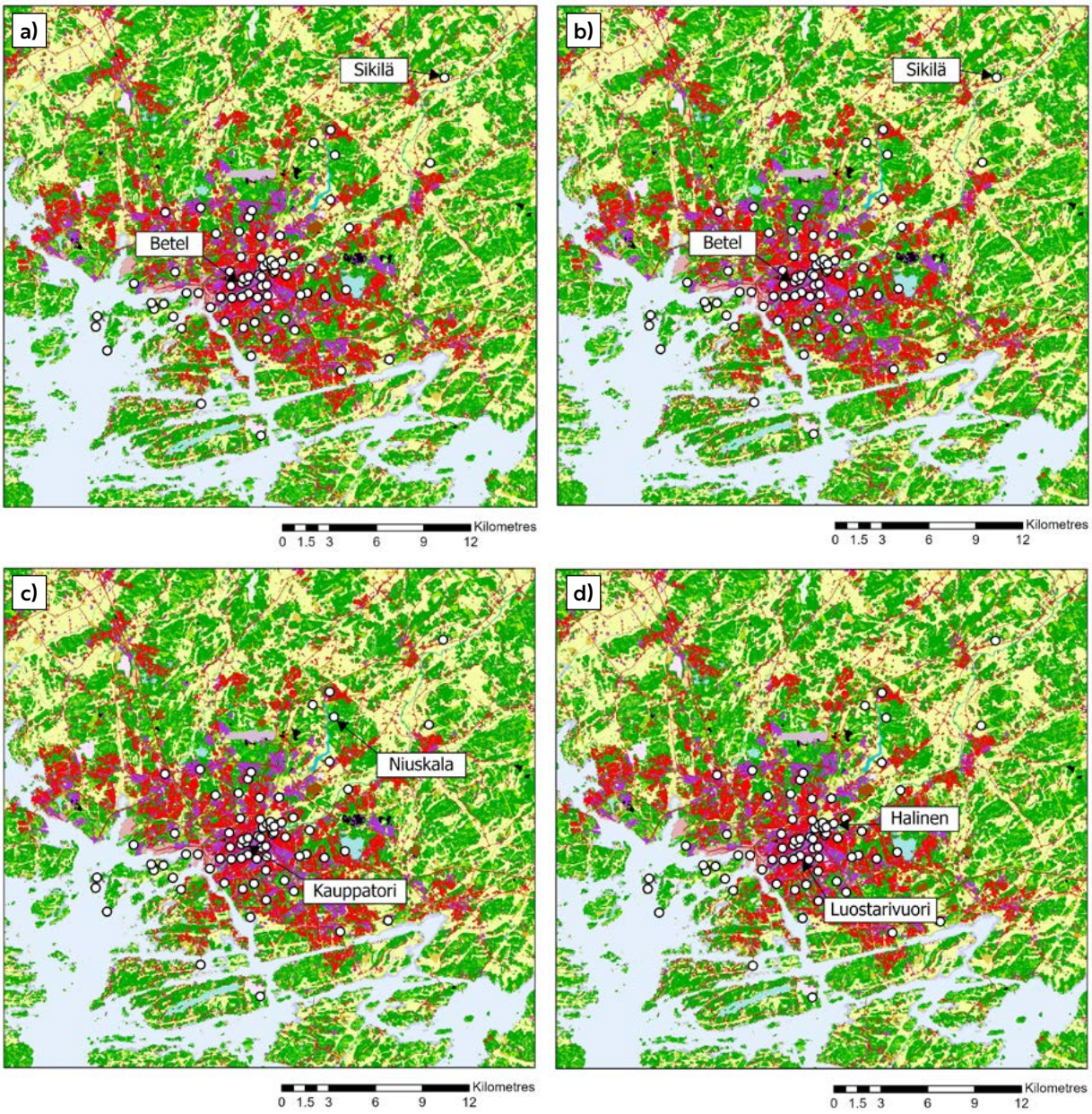

Figure 5. The locations of the logger sites of the highest and lowest a) monthly average temperatures (Betel –6.2 °C, Sikilä –8.2 °C), b) monthly averages of daily minimum temperatures (Betel –9.2 °C, Sikilä –13.0 °C), c) monthly averages of daily maximum temperatures (Kauppatori –3.5 °C, Niuskala –4.9 °C) and d) momentary maximum temperature range on January 21st at 00.00 with the difference of 14.2 °C (Luostarivuori –11.8 °C, Halinen –26.0 °C). Background map: CORINE Land Cover 2018. For information on CORINE level 4 classes and respective colours, used in this Figure and subsequent CORINE based Figures, see Suomi et al. 2024, Appendix A.

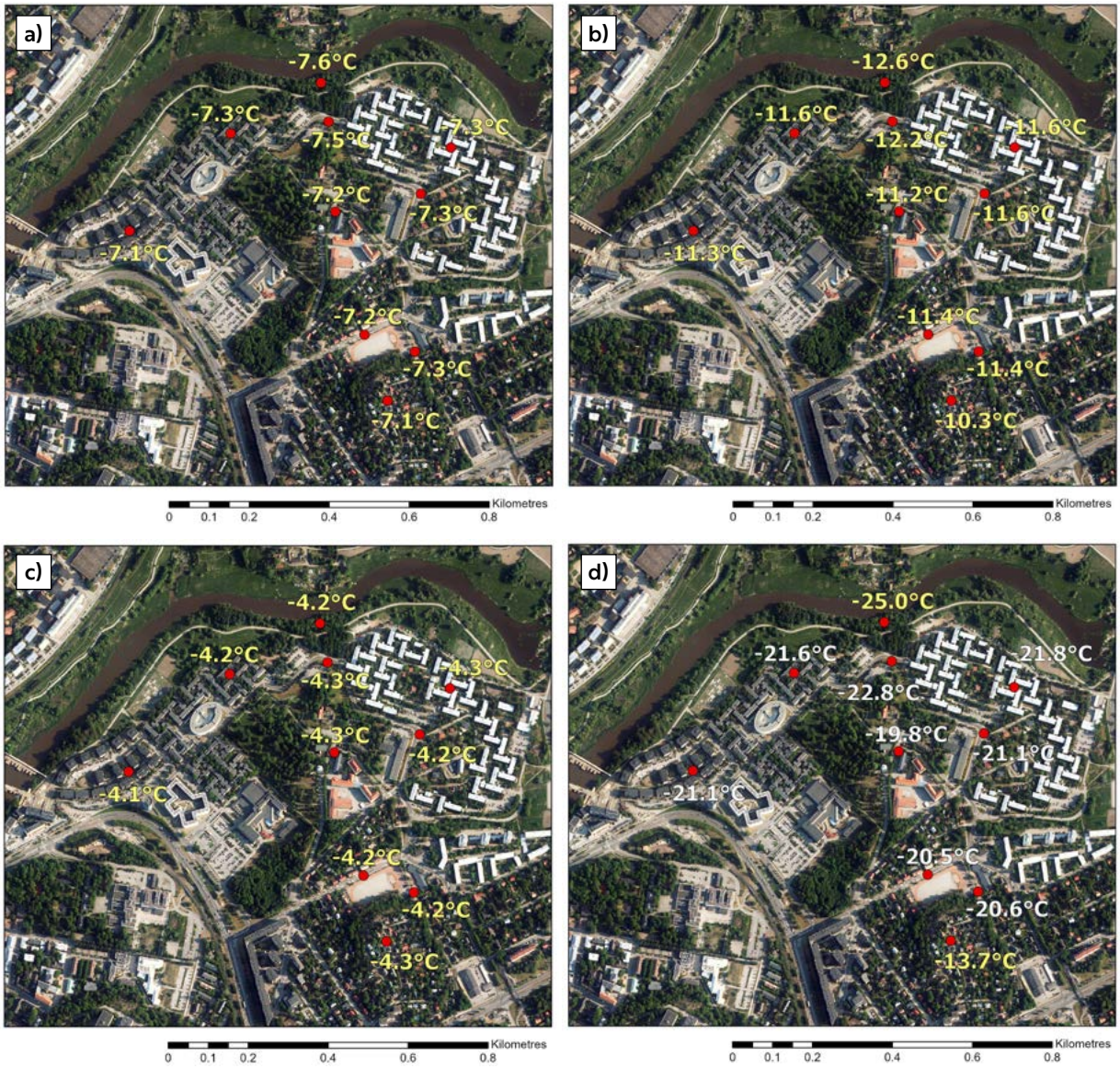

Figure 6. The Student Village logger sites with a) monthly average temperatures, b) monthly averages of daily minimum temperatures, c) monthly averages of daily maximum temperatures and d) the momentary maximum temperature range on January 21st at 00.00 in 2024 with the difference of 11.3 °C between Kuuvuori and Aurajokiranta. For individual logger site names, see Figure 4.

refers to the community structure (total building area and population) inside a 3×3 grid of 250 m × 250 m pixels. All explanatory variables had a warming effect with the strongest being the land cover and building floor area and population variable. The same applied to both monthly averages of daily minimum and maximum temperatures regression models (Table 4 & 5). In these, however, elevation was also statistically significant having a weak warming effect with the minimums and a weak cooling effect with the maximums. The explanatory

Table 3. The regression models for the monthly average temperatures in January 2024. vl_3_5_700 = proportion of urban land cover inside a 700-metre radius buffer, tkuwaters_2km = proportion of water bodies inside a 2-kilometre radius buffer, relelev_300 = elevation of the observation site minus the average elevation of the 300-metre radius buffer around the observation site, rakvae_3x3 = proportion of building floor area and population inside a 3×3 grid (1 pixel = 250 m × 250 m). The variable abbreviations of the other respective tables follow the same nomination principles.

CORINE-based regression model

R Square	0.745
Adjusted R Square	0.733

Variable	Standardized Coefficients Beta	Significance
Constant		<0.001
vl_3_5_700m	0.881	<0.001
tkuwaters_2km	0.701	<0.001
relelev_300m	0.131	0.049

YKR-based regression model

R Square	0.698
Adjusted R Square	0.684

Variable	Standardized Coefficients Beta	Significance
Constant		<0.001
rakvae_3x3	0.788	<0.001
tkuwaters_2km	0.560	<0.001
relelev_300m	0.154	0.033

Table 4. The regression models for the monthly averages of daily minimum temperatures in January 2024.

CORINE-based regression model

R Square	0.748
Adjusted R Square	0.737

Variable	Standardized Coefficients Beta	Significance
Constant		<0.001
vl_3_5_700m	0.777	<0.001
tkuwaters_2km	0.547	<0.001
relelev_500m	0.370	<0.001

YKR-based regression model

R Square	0.740
Adjusted R Square	0.728

Variable	Standardized Coefficients Beta	Significance
Constant		<0.001
rakvae_3x3	0.721	<0.001
tkuwaters_2km	0.432	<0.001
relelev_500m	0.377	<0.001

Table 5. The regression models for the monthly averages of daily maximum temperatures in January 2024.

CORINE-based regression model

R Square	0.523
Adjusted R Square	0.500

Variable	Standardized Coefficients Beta	Significance
Constant		<0.001
vl_3_5_400m	0.673	<0.001
tkuwaters_5km	0.662	<0.001
relelev_100m	-0.063	<0.001

YKR-based regression model

R Square	0.510
Adjusted R Square	0.487

Variable	Standardized Coefficients Beta	Significance
Constant		<0.001
rakvae_3x3	0.648	<0.001
tkuwaters_5km	0.609	<0.001
relelev_100m	-0.081	0.371

Table 6. The regression models for the momentary maximum temperature range in January 2024.

CORINE-based regression model

R Square	0.558
Adjusted R Square	0.537

Variable	Standardized Coefficients Beta	Significance
Constant		<0.001
vl_3_5_700m	0.492	<0.001
tkuwaters_2km	0.304	0.002
relelev_500m	0.515	<0.001

YKR-based regression model

R Square	0.569
Adjusted R Square	0.549

Variable	Standardized Coefficients Beta	Significance
Constant		<0.001
rakvae_3x3	0.476	<0.001
tkuwaters_2km	0.238	0.009
relelev_500m	0.516	<0.001

powers for the minimums are 0.737 and 0.728 and for the maximums 0.500 and 0.487. For the momentary maximum temperature range the land cover, building floor area and population and elevation were statistically significant and the explanatory powers being 0.537 and 0.549 (Table 6). All had a warming effect but with the strongest effect being with elevation.

In the temperature maps produced with the linear regression models, coastal areas appear to be the warmest areas in all four cases: average temperatures, averages of daily minimum and maximum temperatures and the momentary maximum temperature range (Figure 7). In all cases the Turku city centre is also visible in red or yellow appearing as a warmer area than its surrounding areas. In some cases, such as the average temperatures and averages of daily maximum temperatures major roads appear also warmer than the surrounding environment. The coldest areas in the average temperatures and averages of daily maximums models divide evenly across the surface on the mainland while coldest areas in the momentary maximum temperature range and averages of daily minimum temperatures maps appear to be the low-lying sites where cooler air drains. In these two maps the limestone quarry locat-

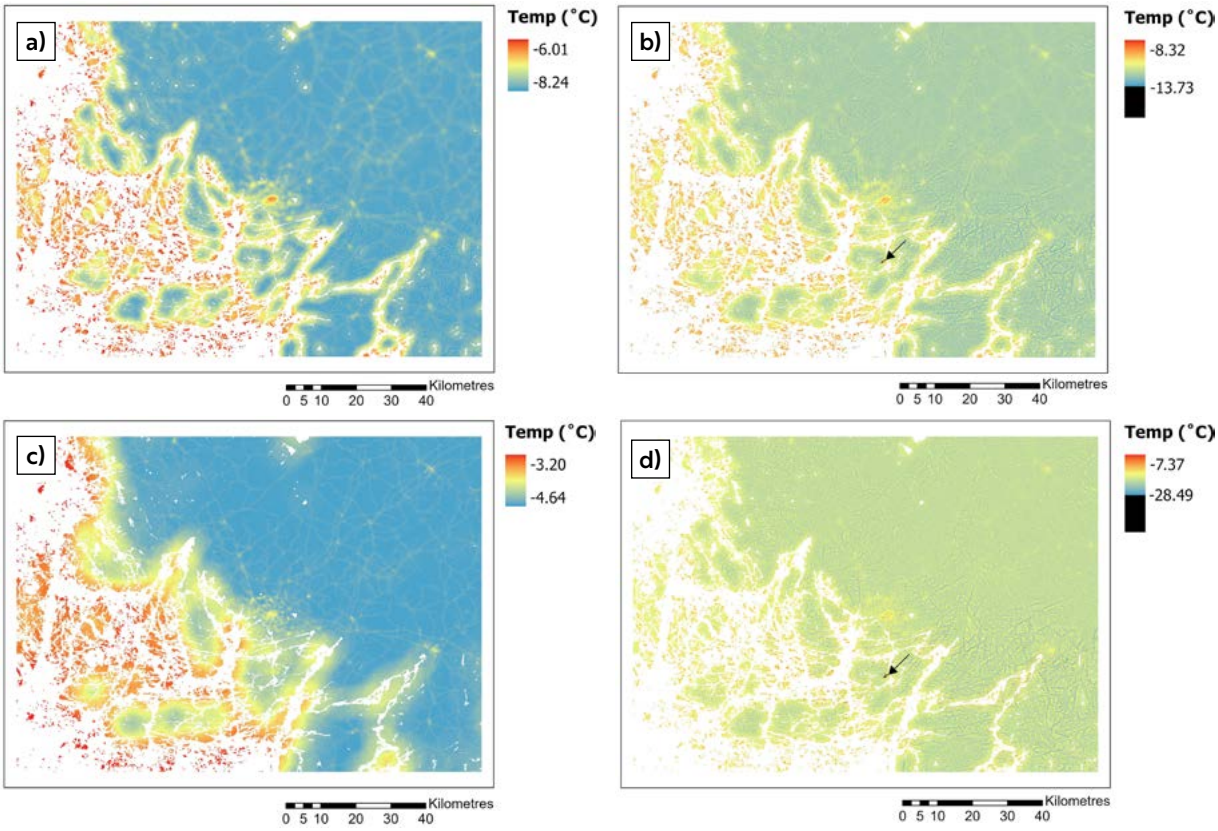

Figure 7. High-resolution (100 m) temperatures based on linear regression model depicting January 2024 a) monthly average temperatures, b) monthly averages of daily minimum temperatures, c) monthly averages of daily maximum temperatures and d) temperatures of momentary maximum temperature range on January 21st, 2024, at 00.00. The abnormally low temperature area in the limestone quarry located in Parainen is marked in black (arrow).

ed in Parainen distorts the temperature ranges due to high topographic variability. The temperature range that is distorted by the quarry is marked in black. A black arrow is also added to indicate the location of the quarry. This distortion did not appear with all of the maps such as with average temperatures and averages of daily maximum temperatures maps in January.

During the maximum momentary temperature difference on January 21st at 00.00 (map is timed at 00.00 UTC) the Student Village and whole Turku region are located on the northern edge of a high-pressure ridge with the centre of the high-pressure zone located over Belarus and northern Ukraine (Figure 8). Another high-pressure zone is visible over Kazan, Russia north of the Kazakhstan border. Quite strong low-pressure zones appear north of Novaya Zemlya, over Greenland and around Iceland on the North Atlantic Ocean. The 500 hPa pressure surface height was about 532–536 decametres over the Turku region at this time. The average wind speed on January 21st at 00.00 was1.85 m/s whereas the average cloudiness was 1.25 oktas.

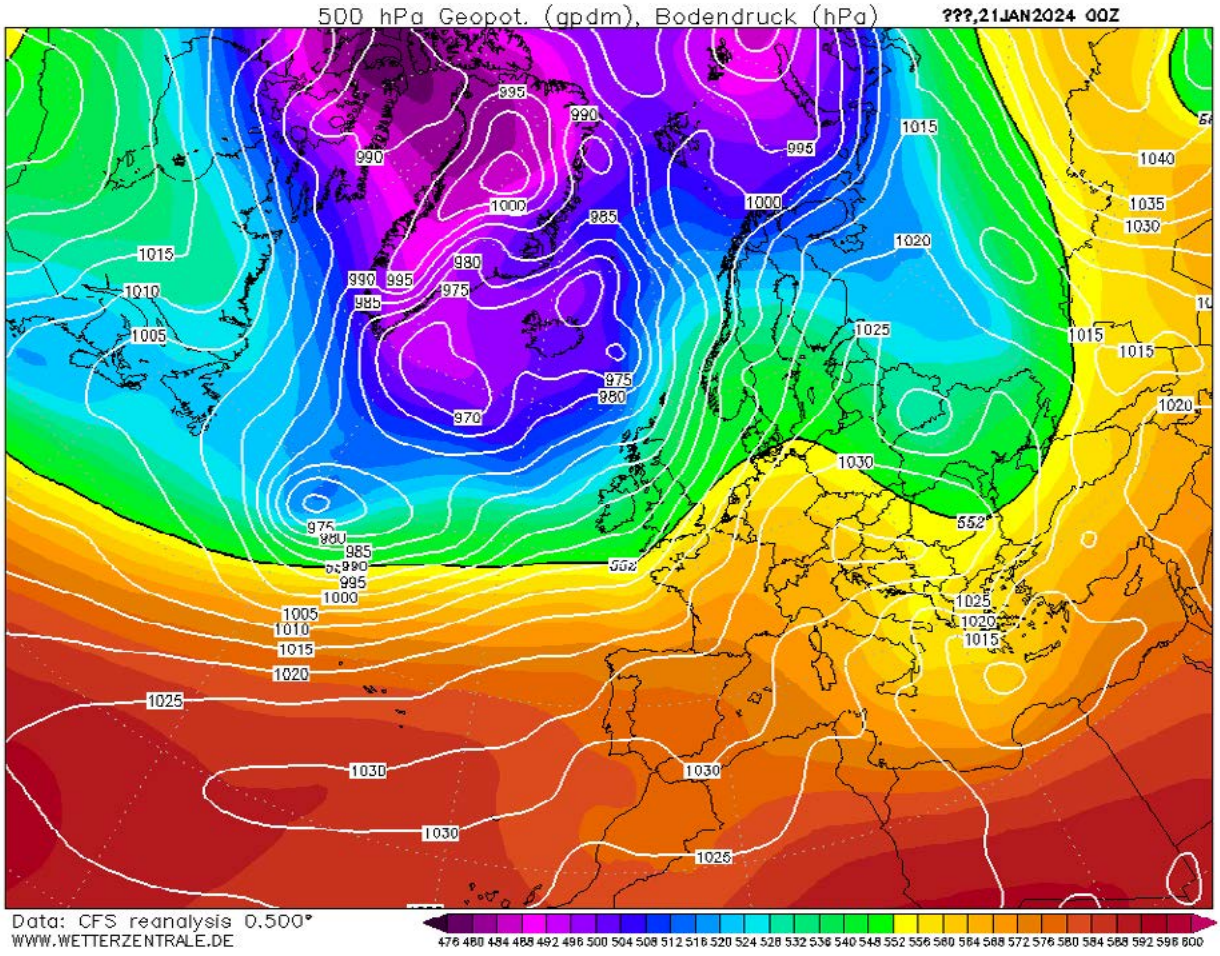

Figure 8. Sea level air pressure (white contours) and height of 500 hectopascal pressure level in decametres (colour ramp) for January 21st at 00.00 UTC. Retrieved from Wetterzentrale (https://www.wetter-zentrale.de/en/reanalysis.php?model=cfsr).

4.1.2 February

In February 2024, the average temperature at the Turku airport was –2.8 °C which was 1.7 °C warmer than the average temperature recorded for February in the 1991–2020 climate reference period (Jokinen et al., 2021).

For the average temperature around the whole observation network in February, the warmest site Kauppatori measured –1.7 °C and the coldest Sikilä –3.2 °C (Figure 9). The coldest site for the averages of daily minimum temperatures was also Sikilä measuring –5.6 °C while the warmest site Betel measured –3.5 °C in February 2024. In the case of averages of daily maximums, the highest and lowest averages were achieved in Kauppatori (0.3 °C) and Sikilä (–1.0 °C). The maximum momentary temperature difference in February occurred on the 8th at 05.00 between Betel and Sikilä. The difference during these during the maximum difference time was 7.0 °C. Betel is a site located in the centrum where warmer temperatures can be measured with the effect of the UHI while Sikilä is a clear rural site located on the mainland further from the centrum and the coast.

For the Student Village observation network the highest average temperature in February was –2.2 °C recorded by the Pispalantie logger while the coldest average temperature of –2.5 °C was measured in three locations: Aurajokiranta, Kuikkulankatu and Kuuvuori, respectively (Figure 10). The highest value for the monthly average of daily minimum temperatures was –4.1 °C recorded again in Pispalantie while the lowest value of –4.7 °C occurred in Aurajokiranta, respectively. In the case of the monthly average of daily maximum temperatures the lowest value was –0.6 °C and it was recorded in Aurajokiranta, Kuikkulankatu, Kuuvuori and Kuuvuori kenttä, respectively. For the highest value it was –0.4 °C recorded in Pispalantie, Suntiontie and Yo-kylä länsi, respectively. In the case of the momentary maximum temperature range it occurred between Aurajokiranta and Kuuvuori on February 5th at 07.30 with the difference between these sites being 3.9 °C. Similarly to January, elevation differences can be a possible factor in the temperature differences between Aurajokiranta and Kuuvuori

In February the explanatory powers for the monthly average temperatures regression model are 0.600 for the CORINE-based regression model and 0.583 for the YKR-based regression model, monthly averages of daily minimum temperatures are 0.728 and 0.677, for the equivalent maximum temperatures 0.327 and 0.350 and for the momentary maximum temperature range the explanatory powers are 0.540 and 0.469 (Tables 7–10). Out of explanatory variables land cover and building floor area and population were statistically significant and had a warming effect in all the regression models. They were also the strongest variables in all cases. For all except the monthly averages of daily maximum temperatures regression model, the water body variable was also statistically significant and had a warming effect although being weaker than the effect of the land cover and building floor area and population.

Similarly to January the coastal areas and islands appear warmer than the mainland in all regression model temperature maps in February 2024 (Figure 11). The heat effect of the city centre can be noticed in every map although it is most clear in the averages of daily minimum and maximum temperature models. Additionally, major roads appear warmer in every map although they have the warmest effect in the averages of daily minimum and maximum tempera-

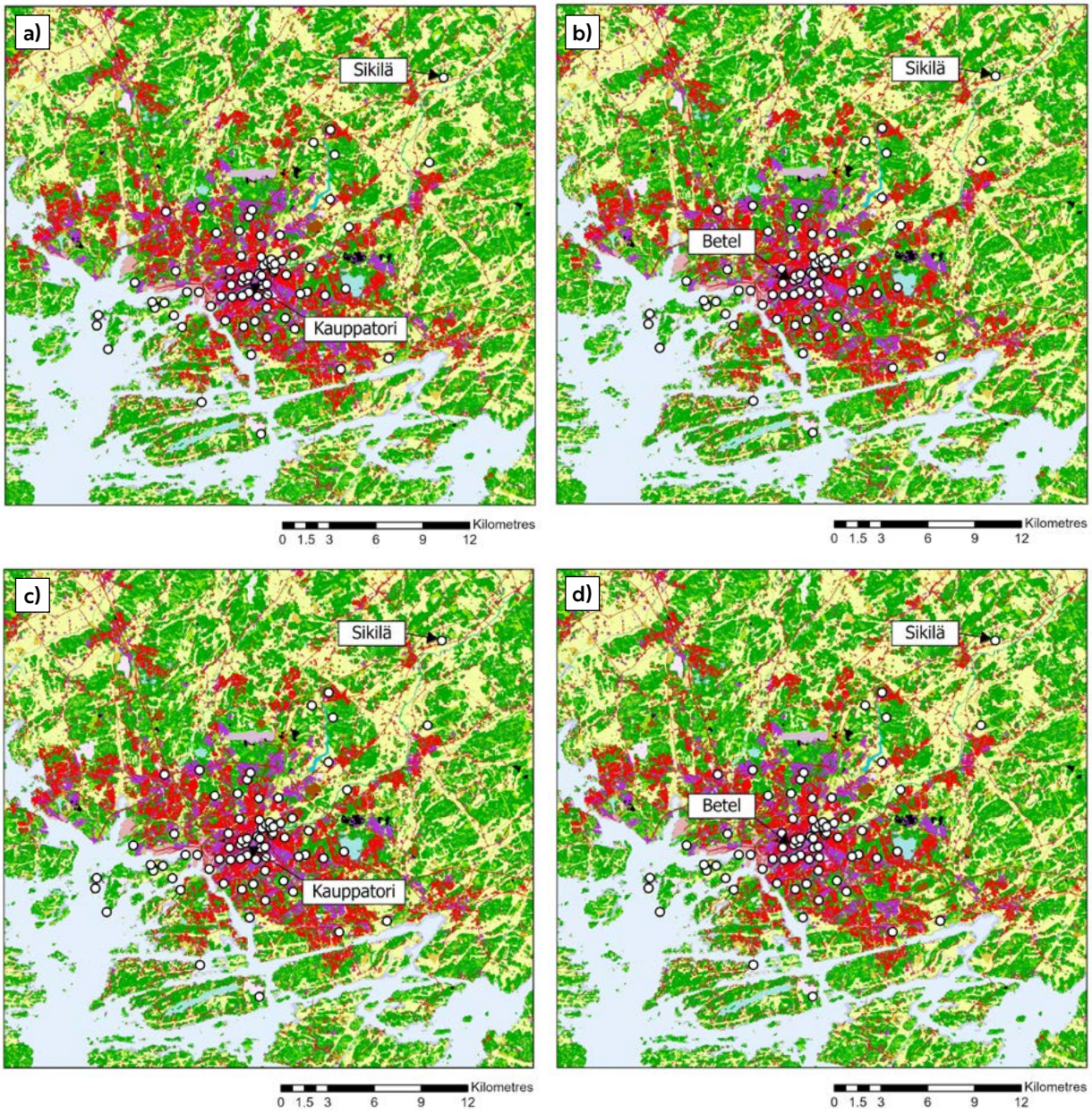

Figure 9. The locations of the logger sites of the highest and lowest a) monthly average temperatures (Kauppatori –1.7 °C, Sikilä –3.2 °C), b) monthly averages of daily minimum temperatures (Betel –3.5 °C, Sikilä –5.6 °C), c) monthly averages of daily maximum temperatures (Kauppatori 0.3 °C, Sikilä –1.0 °C) and d) momentary maximum temperature range on February 8th at 05.00 with the difference of 7.0 °C (Betel –12.9 °C, Sikilä –19.9 °C). Background map: CORINE Land Cover 2018. For information on CORINE level 4 classes and respective colours, used in this Figure and subsequent CORINE based Figures, see Suomi et al. 2024, Appendix A.

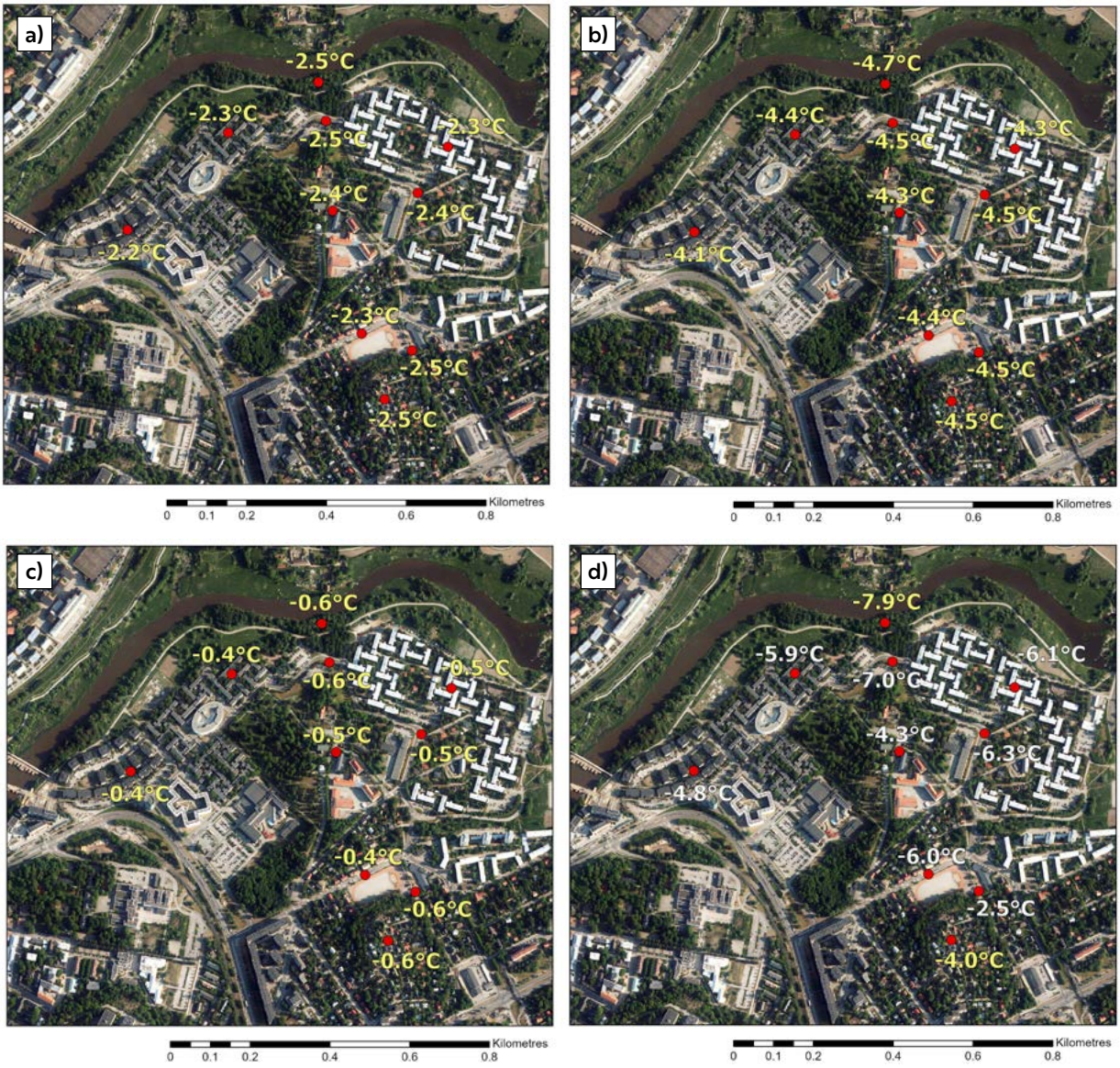

Figure 10. The Student Village logger sites with a) monthly average temperatures, b) monthly averages of daily minimum temperatures, c) monthly averages of daily maximum temperatures and d) the momentary maximum temperature range on February 5th at 07.30 in 2024 with the difference of 3.9 °C between Kuuvuori and Aurajokiranta. For individual logger site names, see Figure 4.

Table 7. The regression models for the monthly average temperatures in February 2024.

CORINE-based regression model		
R Square	0.618	
Adjusted R Square	0.600	
Variable	**Standardized Coefficients Beta**	**Significance**
Constant		<0.001
v1_3_5_1000m	0.862	<0.001
tkuwaters_5km	0.627	<0.001
relelev_100m	-0.089	0.272

YKR-based regression model		
R Square	0.602	
Adjusted R Square	0.583	
Variable	**Standardized Coefficients Beta**	**Significance**
Constant		<0.001
rakvae_5x5	0.814	<0.001
tkuwaters_5km	0.535	<0.001
relelev_100m	-0.085	0.303

Table 8. The regression models for the monthly averages of daily minimum temperatures in February 2024.

CORINE-based regression model		
R Square	0.740	
Adjusted R Square	0.728	
Variable	**Standardized Coefficients Beta**	**Significance**
Constant		<0.001
v1_3_5_1000m	0.942	<0.001
tkuwaters_2kmsqrt	0.758	<0.001
relelev_300m	0.010	0.885

YKR-based regression model		
R Square	0.691	
Adjusted R Square	0.677	
Variable	**Standardized Coefficients Beta**	**Significance**
Constant		<0.001
rakvae_5x5	0.841	<0.001
tkuwaters_2kmsqrt	0.613	<0.001
relelev_300m	0.040	0.578

Table 9. The regression models for the monthly averages of daily maximum temperatures in February 2024.

CORINE-based regression model		
R Square	0.358	
Adjusted R Square	0.327	
Variable	**Standardized Coefficients Beta**	**Significance**
Constant		<0.001
v1_3_5_400m	0.653	<0.001
tkuwaters_2kmsqrt	0.360	0.002
relelev_500m	-0.176	0.087

YKR-based regression model		
R Square	0.379	
Adjusted R Square	0.350	
Variable	**Standardized Coefficients Beta**	**Significance**
Constant		<0.001
rakvae_3x3	0.662	<0.001
tkuwaters_2kmsqrt	0.322	0.004
relelev_500m	-0.224	0.030

Table 10. The regression models for the momentary maximum temperature range in February 2024.

CORINE-based regression model		
R Square	0.561	
Adjusted R Square	0.540	
Variable	**Standardized Coefficients Beta**	**Significance**
Constant		<0.001
v1_3_5_1000m	0.784	<0.001
tkuwaters_5km	0.621	<0.001
relelev_300m	0.005	0.957

YKR-based regression model		
R Square	0.493	
Adjusted R Square	0.469	
Variable	**Standardized Coefficients Beta**	**Significance**
Constant		<0.001
rakvae_5x5	0.687	<0.001
tkuwaters_5km	0.517	<0.001
relelev_300m	0.036	0.700

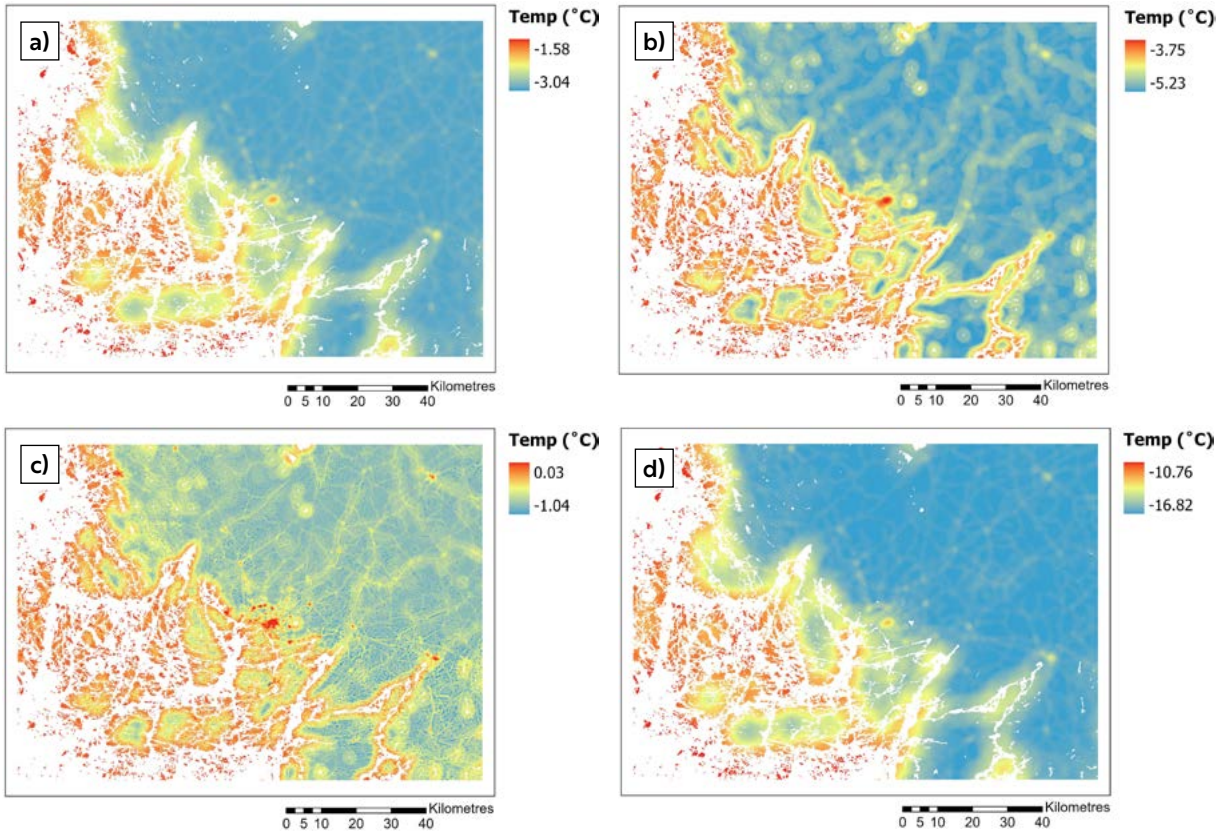

Figure 11. High-resolution (100 m) temperatures based on linear regression model depicting February 2024 a) monthly average temperatures, b) monthly averages of daily minimum temperatures, c) monthly averages of daily maximum temperatures and d) temperatures of momentary maximum temperature range on February 8th, 2024, at 05.00. The abnormally low temperature area in the limestone quarry located in Parainen is marked in black (arrow).

tures maps. In the maximum temperatures map the low-lying areas seem to be the coolest with cold air drainage. The same effect is not as visible in the other cases.

During the momentary maximum temperature range for the whole Turku region on the 8th of February at 05.00 (map is timed at 00.00 UTC) Turku is located between two low-pressure zones (Figure 12). Low-pressure zones are located over the Norwegian Sea close to the coast of northern Norway and over Moscow. The 500 hPa pressure surface height during this time in Turku was about 504–508 decametres. For the equivalent Student Village situation which occurred on the 5th of February at 07.30 (map is timed at 06.00 UTC) a low-pressure zone extends from Russia to southern Finland (Figure 13). A low-pressure was over Turku during this time with another low-pressure zone situated over the Norwegian Sea northwest from northern Norwegian coastline. The 500 hPa surface pressure height over Turku was 500–504 decametres. On February 8th at 05.00 the average wind speed was 1.175 m/s and average cloudiness 5.5 oktas. During the Student Village maximum difference on the 5th at 07.30 the average cloudiness was 0 oktas and average wind speed 1.45 m/s.

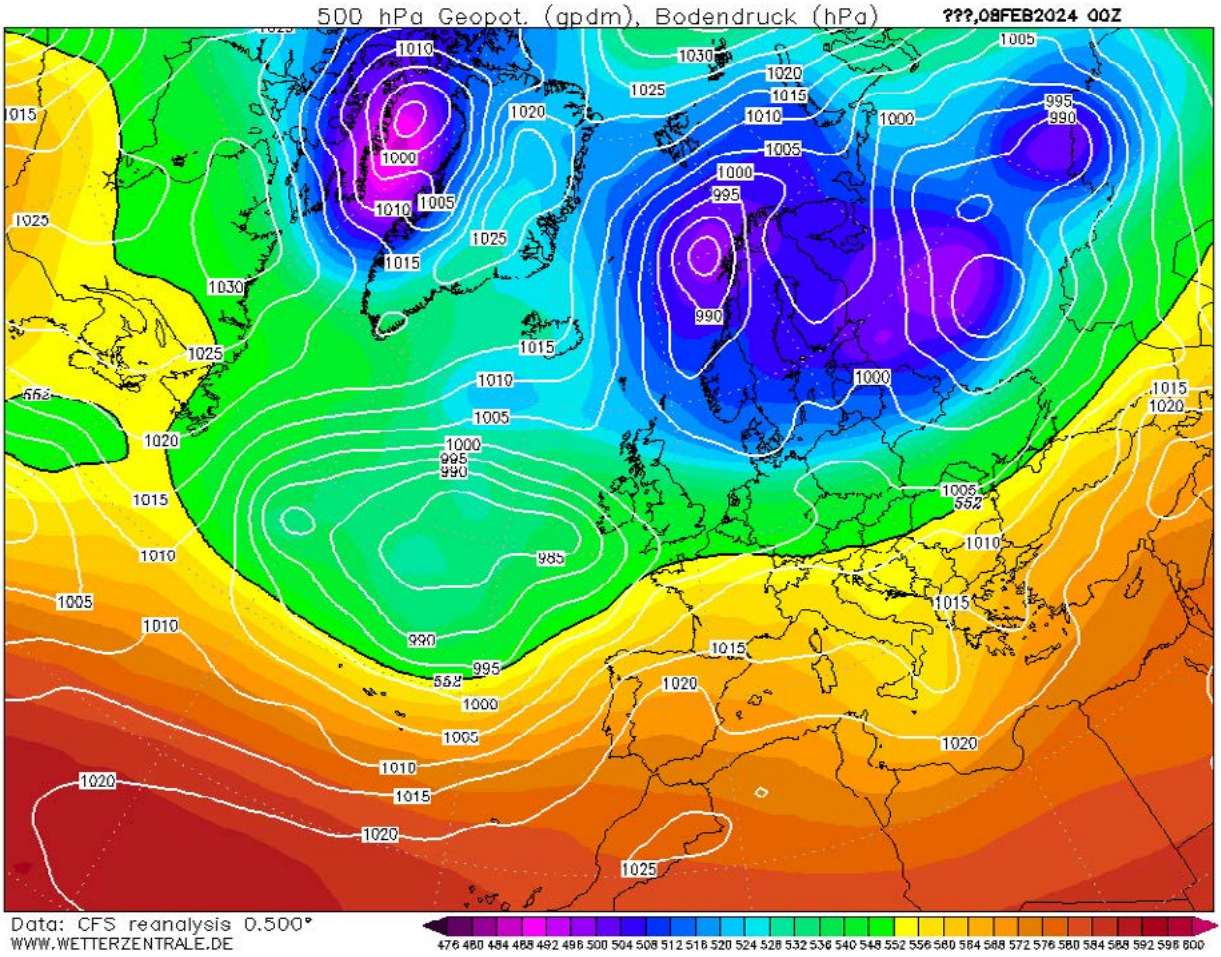

Figure 12. Sea level air pressure (white contours) and height of 500 hectopascal pressure level in decametres (colour ramp) for February 8th at 00.00 UTC. Retrieved from Wetterzentrale (https://www.wetter-zentrale.de/en/reanalysis.php?model=cfsr).

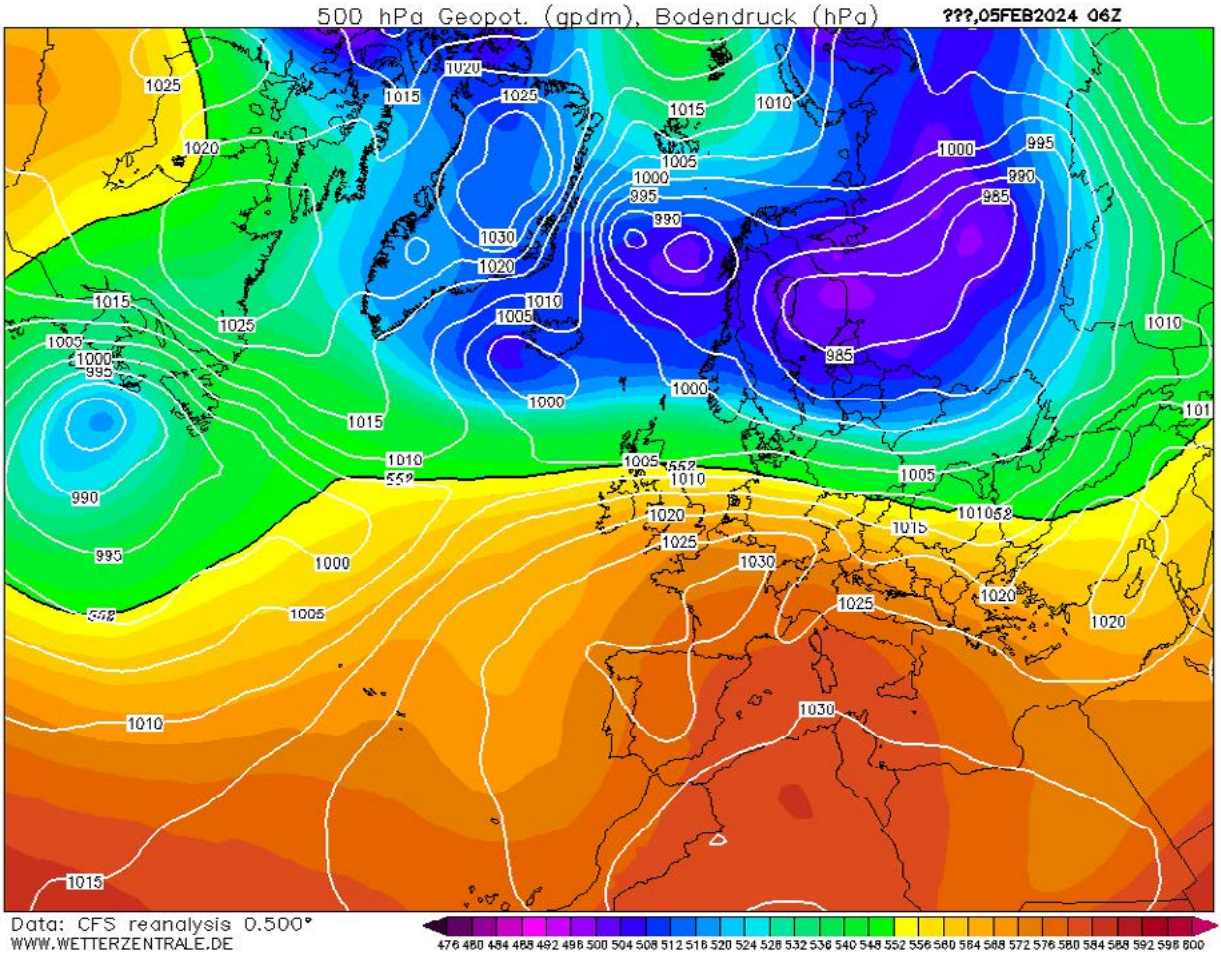

Figure 13. Sea level air pressure (white contours) and height of 500 hectopascal pressure level in decametres (colour ramp) for February 5th at 06.00 UTC. Retrieved from Wetterzentrale (https://www.wetter-zentrale.de/en/reanalysis.php?model=cfsr).

4.1.3 March

The average temperature in March 2024 recorded 0.4 °C at the Turku airport observation site which was 0.9 °C warmer than during the climate reference period in 1991–2020 (Jokinen et al., 2021).

The highest and lowest average temperatures and averages for daily minimum temperatures were measured in Betel and Niuskala with Betel being the warmer site and Niuskala the colder one (Figure 14). In the monthly averages case Niuskala measured 0.1 °C and Betel 1.6 °C while for the minimums they measured –3.1 °C (Niuskala) and –0.8 °C (Betel). For the averages for daily maximum temperatures the warmest site Betel had an average of 4.4 °C and the coldest site being Kolkka had an average of 3.1 °C in March 2024. For the greatest momentary temperature difference the difference of 6.6 °C occurred between Betel and Sikilä, similarly as to the prior month. This difference occurred on March 18th at 22.30.

In March the highest average temperature in the Student Village was 1.0 °C recorded in Pispalantie while the lowest average temperature was recorded in Aurajokiranta with the value 0.6 °C, respectively (Figure 15). The highest monthly average of daily minimum temperatures was –1.8 °C in Pispalantie while the lowest was –2.3 °C in Aurajokiranta, respectively. Again, for the monthly averages of daily maximum temperatures the dispersion is minimal with the highest value being 3.8 °C in Kirkkotie, Kuuvuori, Pispalantie, Suntiontie, Yo-kylä länsi and Yo-kylä and the lowest value being 3.6 °C in Aurajokiranta and Kuuvuori kenttä, respectively. The difference between Aurajokiranta and Kuuvuori was 3.2 °C in the momentary maximum temperature range observation. This occurred on March 12th at 23.00 in 2024. Difference in elevation is a possible cause here as well for the temperature differences.

The explanatory power in the regression model for the monthly average temperatures is 0.682 in the CORINE-based regression model and 0.670 in the YKR-based model (Table 11). Only the land cover and building floor area and population variables were statistically significant both having a warming effect. In the case of the monthly averages of daily minimums the explanatory powers are 0.713 and 0.712 (Table 12). Land cover, building floor area and population and water bodies were statistically significant having a warming effect. Out of these the land cover and building floor area and population had a stronger effect than the water bodies. For the regression model of the monthly averages for daily maximum temperatures the explanatory power is 0.171 for the CORINE-based regression model and 0.360 for the YKR-based model (Table 13). In the CORINE-based regression model water bodies had a cooling effect while in the YKR-based regression model the building floor area and population variable had a warming effect. In the momentary maximum temperature difference model, the explanatory power is 0.475 for the CORINE-based regression model and 0.441 for the YKR-based regression model (Table 14). In both cases land cover, building floor area and population and water bodies were statistically significant all having a warming effect. The effect of water bodies was weaker.

In March, the coast areas and archipelago appear as the warmest areas with the average temperatures, averages of daily minimum temperatures and momentary maximum temperature range models (Figure 16). In these cases, the UHI effect in the Turku city centre is also clear. In the

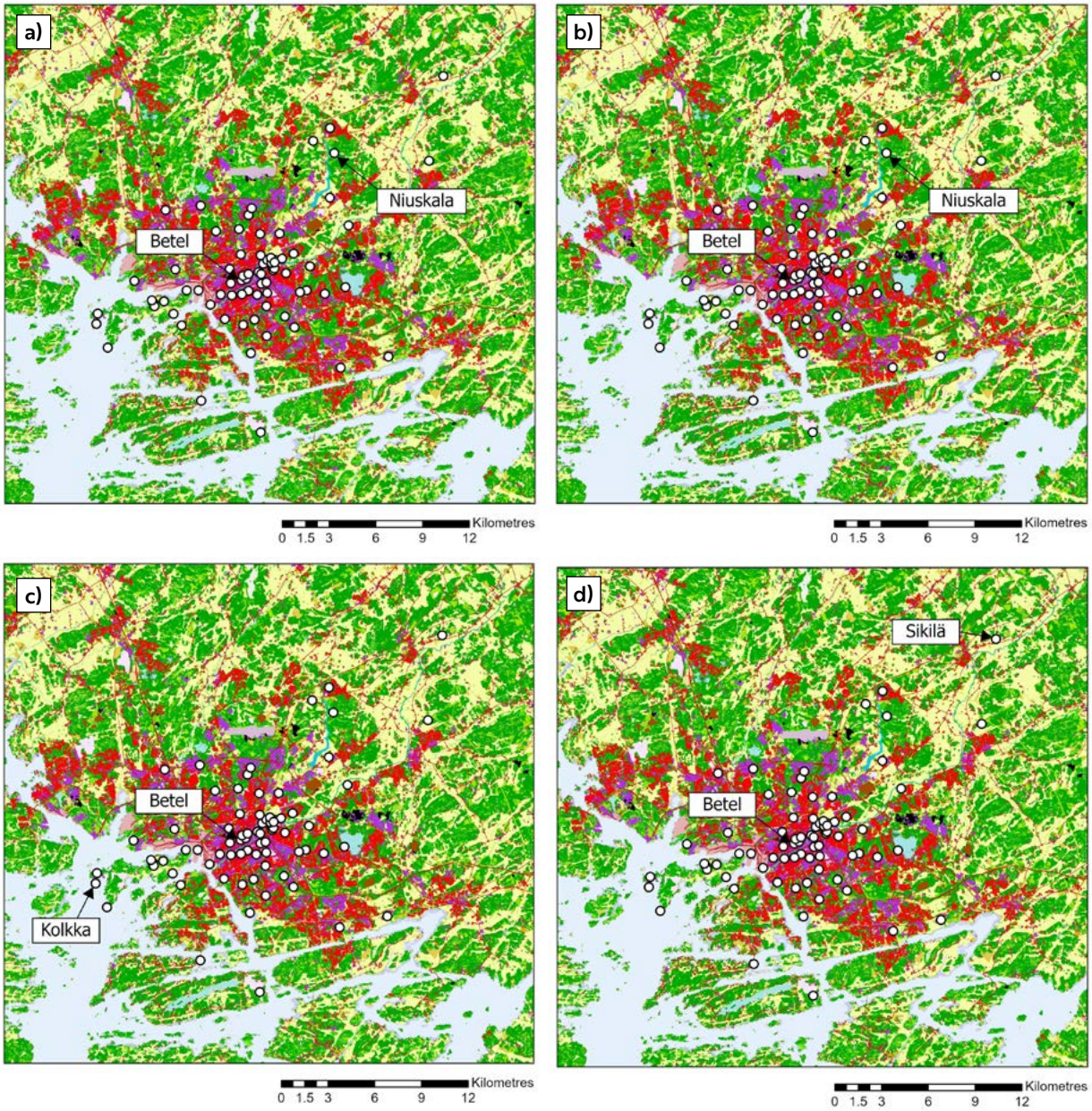

Figure 14. The locations of the logger sites of the highest and lowest a) monthly average temperatures (Betel 1.6 °C, Niuskala 0.1 °C), b) monthly averages of daily minimum temperatures (Betel –0.8 °C, Niuskala –3.1 °C), c) monthly averages of daily maximum temperatures (Betel 4.4 °C, Kolkka 3.1 °C) and d) momentary maximum temperature range on March 18th at 22.30 with the difference of 6.6 °C (Betel –0.9 °C, Sikilä –7.5 °C). Background map: CORINE Land Cover 2018. For information on CORINE level 4 classes and respective colours, used in this Figure and subsequent CORINE based Figures, see Suomi et al. 2024, Appendix A.

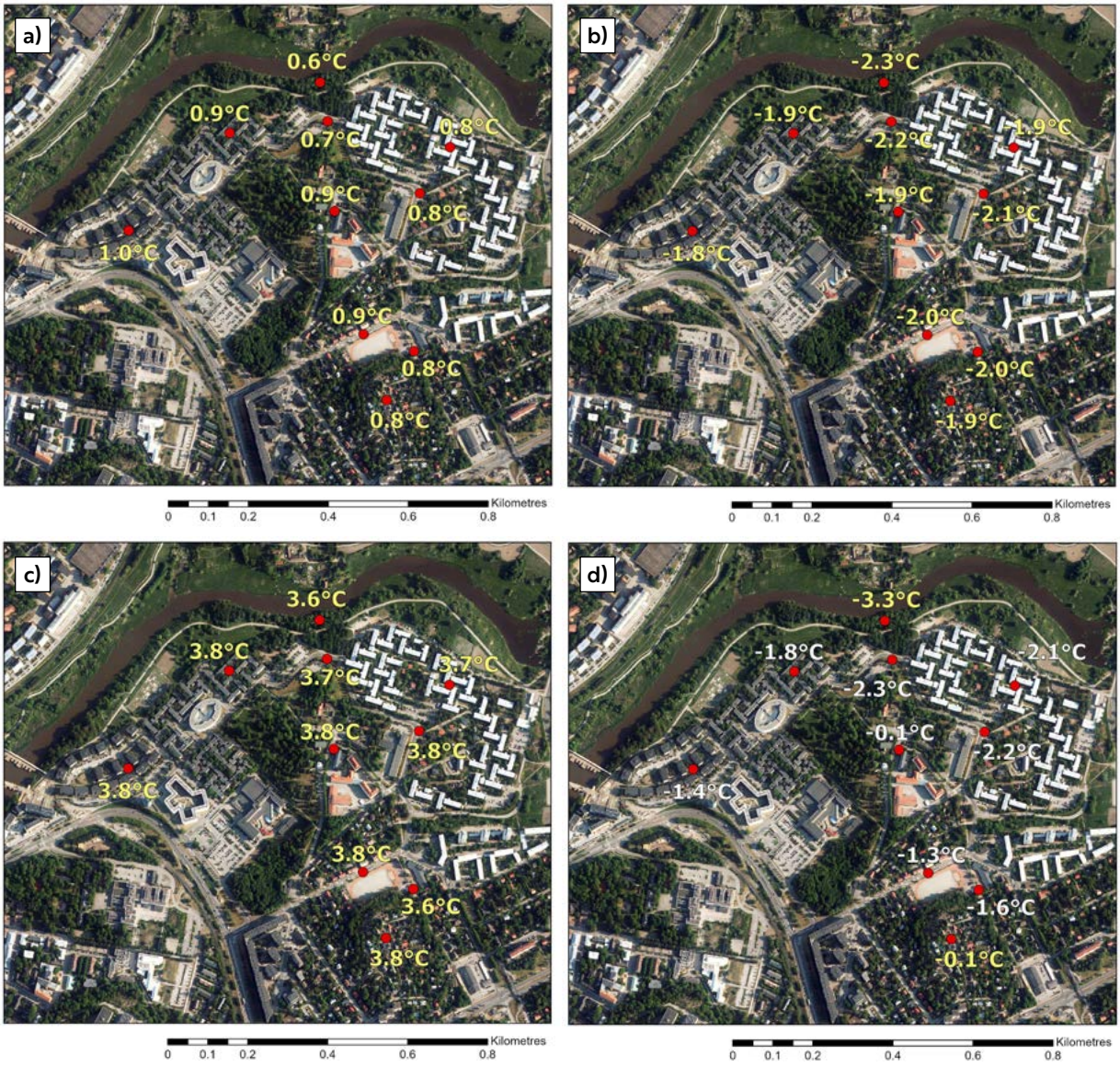

Figure 15. The Student Village logger sites with a) monthly average temperatures, b) monthly averages of daily minimum temperatures, c) monthly averages of daily maximum temperatures and d) the momentary maximum temperature range on March 12th at 23.00 in 2024 with the difference of 3.2 °C between Kuuvuori and Aurajokiranta. For individual logger site names, see Figure 4.

average temperatures model the neighbouring municipalities appear also rather warm. Some cities further away from Turku such as Salo, appears also warmer than the surrounding areas. Major roads and the biggest urban areas are warmer than the surrounding environment in these three models. In the averages of daily maximum temperatures model the coast is the coolest while the whole mainland appears as warmer. No distinctive UHI effect is visible in this model.

Table 11. The regression models for the monthly average temperatures in March 2024.

CORINE-based regression model		
R Square	0.696	
Adjusted R Square	0.682	
Variable	**Standardized Coefficients Beta**	**Significance**
Constant		<0.001
vl_3_5_1000m	0.911	<0.001
tkuwaters_2km	0.215	0.009
relelev_200m	0.028	0.701

YKR-based regression model		
R Square	0.685	
Adjusted R Square	0.670	
Variable	**Standardized Coefficients Beta**	**Significance**
Constant		<0.001
rakvae_5x5	0.851	<0.001
tkuwaters_2km	0.103	0.183
relelev_200m	0.041	0.576

Table 12. The regression models for the monthly averages of daily minimum temperatures in March 2024.

CORINE-based regression model		
R Square	0.726	
Adjusted R Square	0.713	
Variable	**Standardized Coefficients Beta**	**Significance**
Constant		<0.001
vl_3_5_1000m	0.894	<0.001
tkuwaters_5km	0.501	<0.001
relelev_300m	0.131	0.062

YKR-based regression model		
R Square	0.725	
Adjusted R Square	0.712	
Variable	**Standardized Coefficients Beta**	**Significance**
Constant		<0.001
rakvae_5x5	0.851	<0.001
tkuwaters_5km	0.407	<0.001
relelev_300m	0.148	0.034

Table 13. The regression models for the monthly averages of daily maximum temperatures in March 2024.

CORINE-based regression model		
R Square	0.208	
Adjusted R Square	0.171	
Variable	**Standardized Coefficients Beta**	**Significance**
Constant		<0.001
vl_3_5_500m	0.101	0.379
tkuwaters_2km	-0.430	<0.001
relelev_100m	-0.067	0.552

YKR-based regression model		
R Square	0.388	
Adjusted R Square	0.360	
Variable	**Standardized Coefficients Beta**	**Significance**
Constant		<0.001
rakvae_3x3	0.477	<0.001
tkuwaters_2km	-0.284	0.009
relelev_100m	-0.163	0.109

Table 14. The regression models for the momentary maximum temperature range in March 2024.

CORINE-based regression model		
R Square	0.499	
Adjusted R Square	0.475	
Variable	**Standardized Coefficients Beta**	**Significance**
Constant		<0.001
vl_3_5_700m	0.772	<0.001
tkuwaters_2kmsqrt	0.516	<0.001
relelev_300m	0.068	0.458

YKR-based regression model		
R Square	0.466	
Adjusted R Square	0.441	
Variable	**Standardized Coefficients Beta**	**Significance**
Constant		<0.001
rakvae_5x5	0.708	<0.001
tkuwaters_2kmsqrt	0.418	<0.001
relelev_300m	0.060	0.529

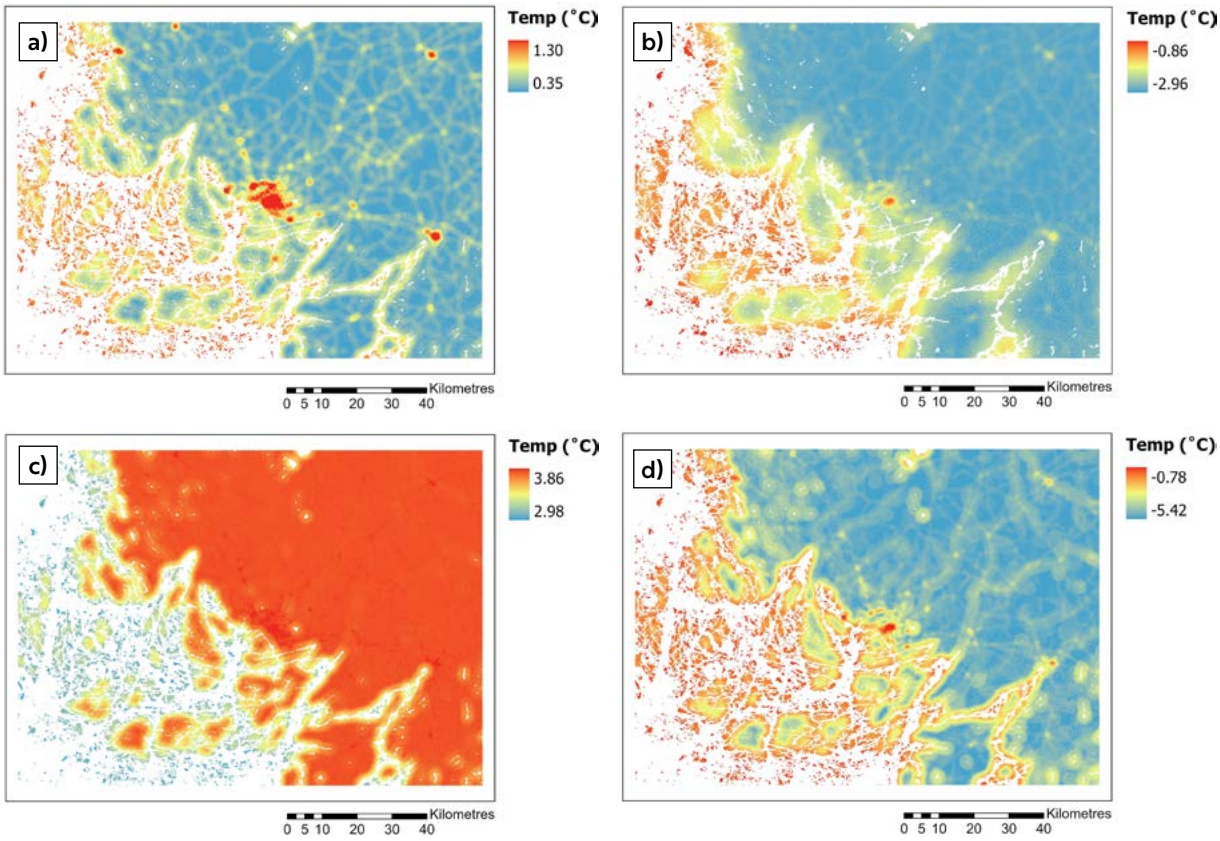

Figure 16. High-resolution (100 m) temperatures based on linear regression model depicting March 2024 a) monthly average temperatures, b) monthly averages of daily minimum temperatures, c) monthly averages of daily maximum temperatures and d) temperatures of momentary maximum temperature range on March 18th, 2024, at 22.30. The abnormally low temperature area in the limestone quarry located in Parainen is marked in black (arrow).

The maximum momentary temperature range in March occurred on the 18th at 22.30 regarding the whole Turku region. During this period an extensive high-pressure zone was located over Turku and southern Finland (Figure 17). The high-pressure zone extends over to eastern Russia while low-pressure zones revolve around Iceland and over the Kara Sea east of Novaya Zemlya. The map is time stamped at 18.00 UTC and the 500 hPa surface pressure height over Turku was 548–552 decametres. Regarding the momentary maximum temperature range in the Student Village, which occurred on the 12th of March at 23.00, Turku was on the north-western edge of a high-pressure ridge with the 500 hPa surface pressure height being 548–552 decametres (Figure 18). Low-pressure centres appeared on the Kara Sea and over the North Atlantic north-west of Ireland. The map was timed at 18.00 UTC. On March 18th at 22.30 the average wind speed was 0.675 m/s and average cloudiness was 8 oktas. In the case of March 12th at 23.00 the average wind speed was 1.1 m/s and average cloudiness 0 oktas.

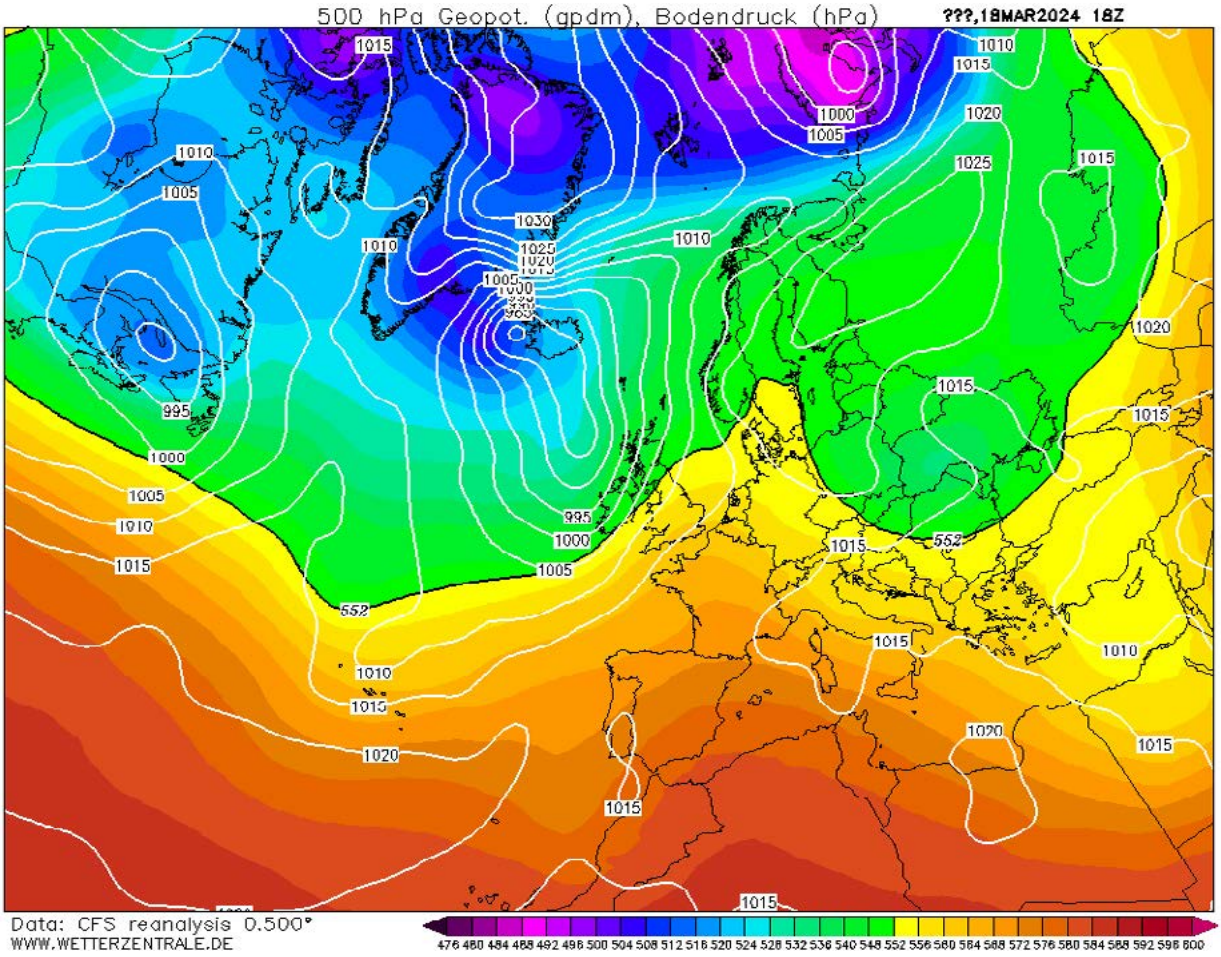

Figure 17. Sea level air pressure (white contours) and height of 500 hectopascal pressure level in decametres (colour ramp) for March 18th at 18.00 UTC. Retrieved from Wetterzentrale (https://www.wetter-zentrale.de/en/reanalysis.php?model=cfsr).

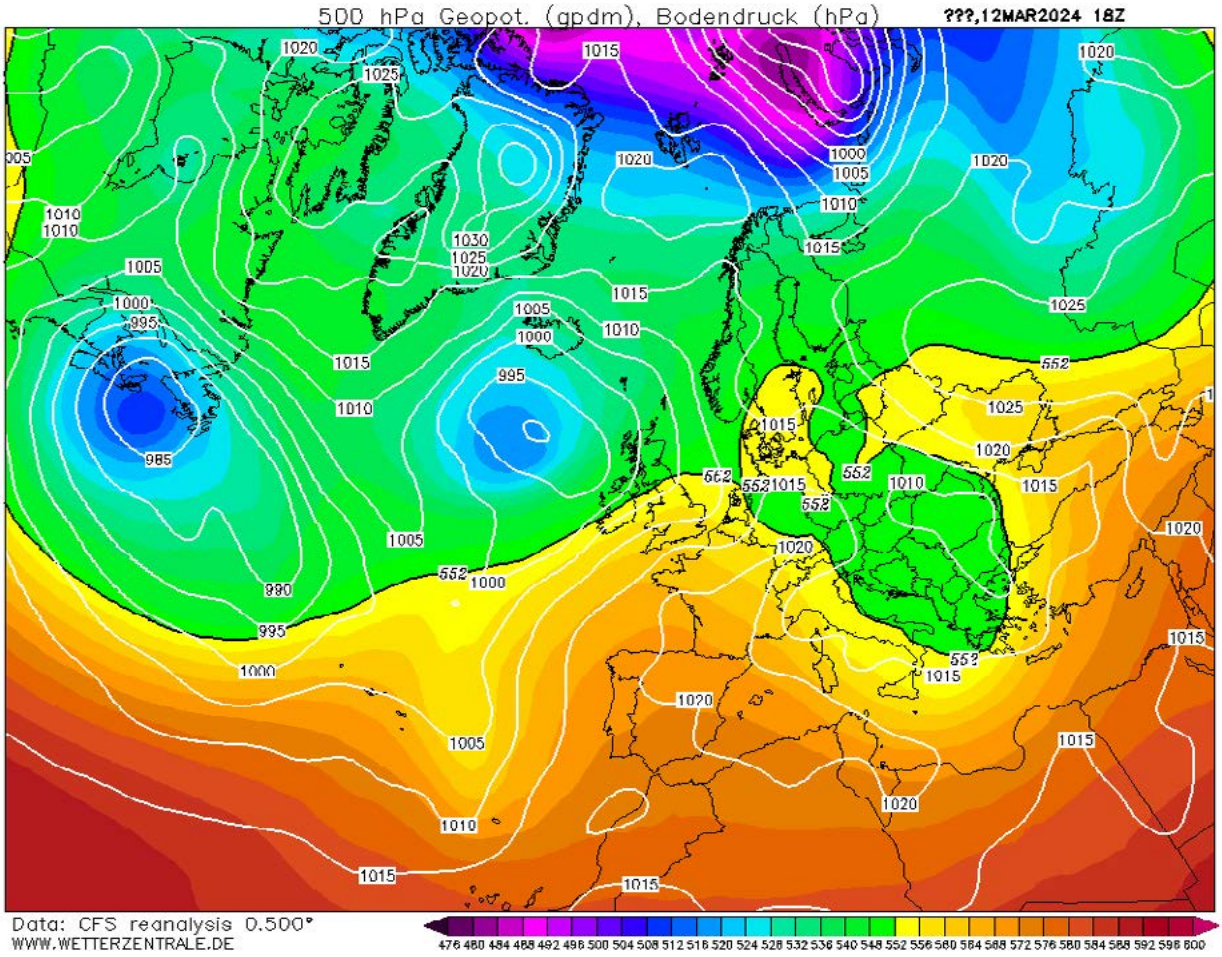

Figure 18. Sea level air pressure (white contours) and height of 500 hectopascal pressure level in decametres (colour ramp) for March 12th at 18.00 UTC. Retrieved from Wetterzentrale (https://www.wetter-zentrale.de/en/reanalysis.php?model=cfsr).

4.1.4 April

For April, the average temperature in 2024 was 3.3 °C. During the 1991–2020 climate reference period the equivalent was 4.1 °C resulting in a 0.8 °C difference (Jokinen et al., 2021).

In April 2024 the lowest and highest average temperatures appeared in Kolkka (3.0 °C) and Kauppatori (4.4 °C) (Figure 19). The highest average of daily minimum temperatures was acquired in Kauppatori as well with the average being 1.4 °C. The lowest average in this case appeared in Niuskala with the average of –0.8 °C. For the equivalent maximums the highest and lowest averages appeared in Kauppatori and Kolkka, similarly to the lowest and highest monthly averages. Kauppatori measured 7.6 °C and Kolkka 6.1 °C. The maximum momentary temperature range in April was 8.2 °C measured between Kuuva and Sikilä between on April 29th at 16.00. Sikilä is a colder site due to its location being on the mainland, while Kuuva, a coastal site, is surrounded by the sea which can have a warming effect during spring time.

The highest average temperature in the Turku Student Village in April was 3.9 °C measured in Pispalantie and Suntiontie, respectively (Figure 20). The lowest average temperature of 3.6 °C was reached in Aurajokiranta. For the monthly average of daily minimum temperatures, the lowest value was also reached in Aurajokiranta with the value of 0.1 °C. The highest value of 0.7 °C was reached in Kirkkotie, Pispalantie and Suntiontie, respectively. In the case of the monthly averages for daily maximum temperatures the warmest sites were Suntiontie, Yo-kylä and Yo-kylä itä with the average of 7.2 °C, respectively. The coldest sites were Aurajokiranta and Kuuvuori kenttä with the average 7.0 °C, respectively. A difference of 5.2 °C was measured between Aurajokiranta and Kuuvuori on April 9th at 23.30. This was the momentary maximum temperature range reached in April. The elevation difference between Aurajokiranta and Kuuvuori is a plausible explanation between the temperature differences.

For the monthly average temperatures, the explanatory power is 0.709 for the CORINE-based regression model and 0.733 for the YKR-based regression model (Table 15). Only the land cover and building floor area and population variables were statistically significant both having a warming effect. The explanatory power for the monthly averages of daily minimums are 0.746 and 0.736 (Table 16). Land cover and building floor area and population had a strong warming effect. The water body variable was statistically significant in the CORINE-based regression model but not in the YKR-based regression model. In the CORINE-based regression model, it had a weaker warming effect. For the maximum temperatures the explanatory powers are 0.535 and 0.556 (Table 17). In the CORINE-based regression model, only the water body variable was statistically significant having a cooling effect. In the YKR-based regression model, the building floor area and population variable had a weak warming effect while water bodies a stronger cooling effect. In the case of the momentary maximum temperature range only the water body variable was statistically significant (Table 18). This effect was cooling in both models. The explanatory powers of the models are 0.714 and 0.717.

The coldest areas in the temperature models in April 2024 are the coast areas while the mainland is warmer (Figure 21). The only exception is averages of daily minimum temperatures model where the coast is warmer than the mainland. In this case

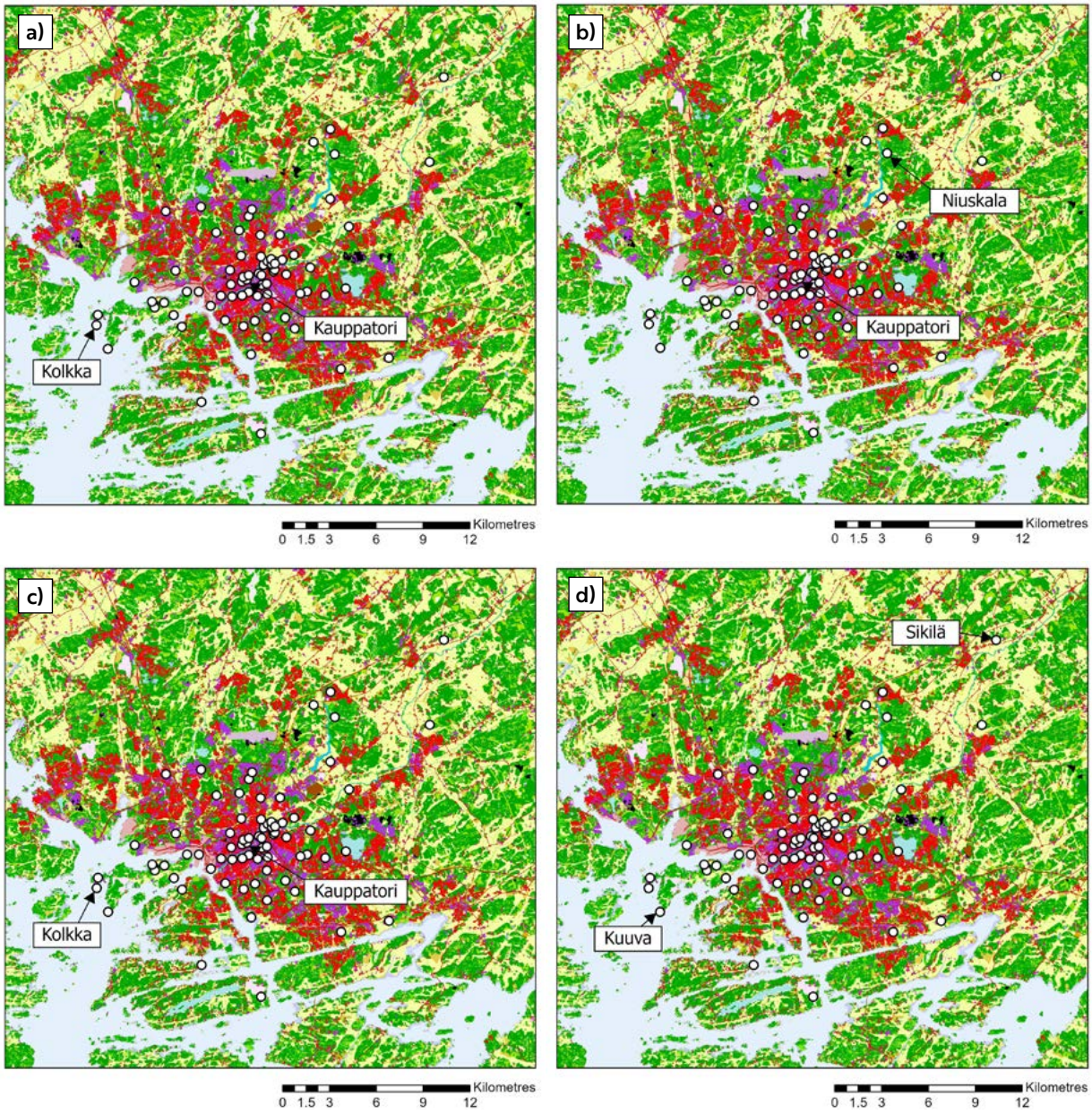

Figure 19. The locations of the logger sites of the highest and lowest a) monthly average temperatures (Kauppatori 4.4 °C, Kolkka 3.0 °C), b) monthly averages of daily minimum temperatures (Kauppatori 1.4 °C, Niuskala –0.8 °C), c) monthly averages of daily maximum temperatures (Kauppatori 7.6 °C, Kolkka 6.1 °C) and d) momentary maximum temperature range on April 29th at 16.00 with the difference of 8.2 °C (Kuuva 15.8 °C, Sikilä 7.6 °C). Background map: CORINE Land Cover 2018. For information on CORINE level 4 classes and respective colours, used in this Figure and subsequent CORINE based Figures, see Suomi et al. 2024, Appendix A.

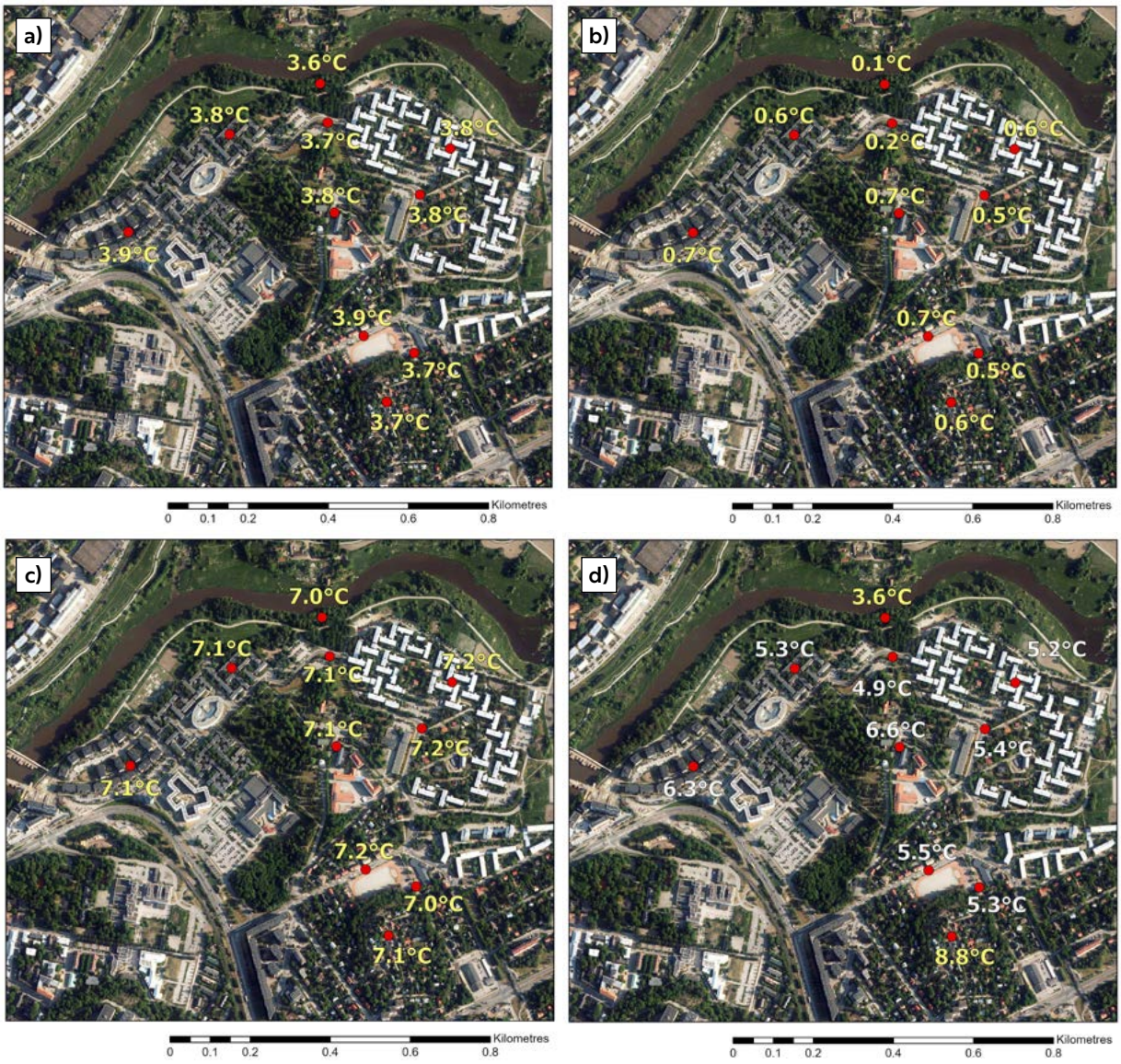

Figure 20. The Student Village logger sites with a) monthly average temperatures, b) monthly averages of daily minimum temperatures, c) monthly averages of daily maximum temperatures and d) the momentary maximum temperature range on April 9th at 23.30 in 2024 with the difference of 5.2 °C between Kuuvuori and Aurajokiranta. For individual logger site names, see Figure 4.

the low-lying sites are the coldest where cold air drainage occurs. The UHI effect is also the clearest in this map when compared to the others. The UHI effect can be somewhat be seen in the average temperatures model appearing slightly warmer than the surrounding areas. In the averages of daily maximum temperatures map and the maximum momentary temperature range map the effect is not as distinctive with the mainland appearing the warmest relatively evenly.

Table 15. The regression models for the monthly average temperatures in April 2024.

CORINE-based regression model		
R Square	0.722	
Adjusted R Square	0.709	
Variable	**Standardized Coefficients Beta**	**Significance**
Constant		<0.001
vl_3_5_700m	0.790	<0.001
tkuwaters_2km	-0.120	0.118
relelev_200m	-0.021	0.764

YKR-based regression model		
R Square	0.745	
Adjusted R Square	0.733	
Variable	**Standardized Coefficients Beta**	**Significance**
Constant		<0.001
rakvae_5x5	0.779	<0.001
tkuwaters_2km	-0.189	0.008
relelev_200m	-0.041	0.537

Table 16. The regression models for the monthly averages of daily minimum temperatures in April 2024.

CORINE-based regression model		
R Square	0.757	
Adjusted R Square	0.746	
Variable	**Standardized Coefficients Beta**	**Significance**
Constant		<0.001
vl_3_5_700m	0.916	<0.001
tkuwaters_1000m	0.314	<0.001
relelev_300m	0.166	0.011

YKR-based regression model		
R Square	0.747	
Adjusted R Square	0.736	
Variable	**Standardized Coefficients Beta**	**Significance**
Constant		0.091
rakvae_5x5	0.875	<0.001
tkuwaters_1000m	0.222	0.002
relelev_300m	0.146	0.029

Table 17. The regression models for the monthly averages of daily maximum temperatures in April 2024.

CORINE-based regression model		
R Square	0.555	
Adjusted R Square	0.535	
Variable	**Standardized Coefficients Beta**	**Significance**
Constant		<0.001
vl_3_5_1000m	0.292	0.005
tkuwaters_2km	-0.539	<0.001
relelev_500m	-0.188	0.034

YKR-based regression model		
R Square	0.576	
Adjusted R Square	0.556	
Variable	**Standardized Coefficients Beta**	**Significance**
Constant		<0.001
rakvae_3x3	0.310	<0.001
tkuwaters_2km	-0.573	<0.001
relelev_500m	-0.181	0.034

Table 18. The regression models for the momentary maximum temperature range in April 2024.

CORINE-based regression model		
R Square	0.727	
Adjusted R Square	0.714	
Variable	**Standardized Coefficients Beta**	**Significance**
Constant		<0.001
vl_3_5_1000m	-0.043	0.575
tkuwaters_5km	-0.872	<0.001
relelev_200m	0.009	0.892

YKR-based regression model		
R Square	0.729	
Adjusted R Square	0.717	
Variable	**Standardized Coefficients Beta**	**Significance**
Constant		<0.001
rakvae_3x3	0.064	0.375
tkuwaters_5km	-0.831	<0.001
relelev_200m	-0.017	0.799

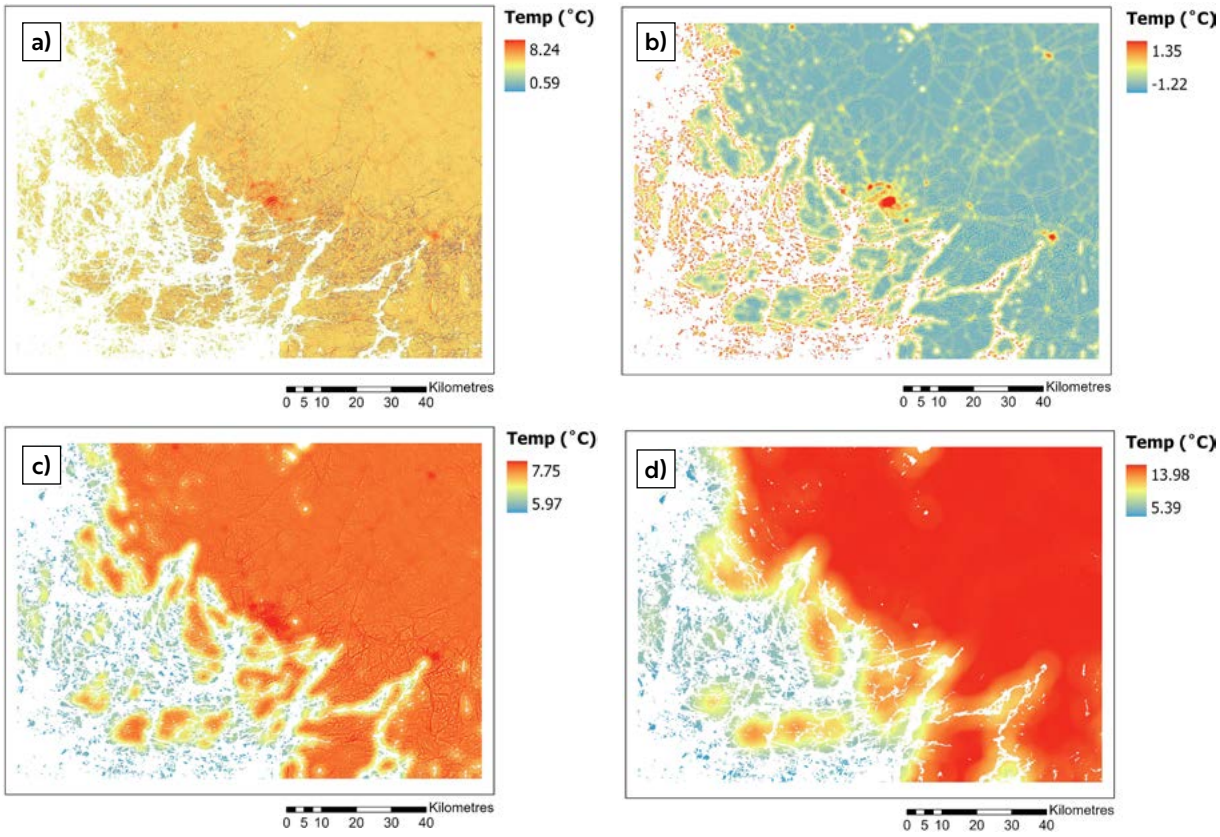

Figure 21. High-resolution (100 m) temperatures based on linear regression model depicting April 2024 a) monthly average temperatures, b) monthly averages of daily minimum temperatures, c) monthly averages of daily maximum temperatures and d) temperatures of momentary maximum temperature range on April 29th, 2024, at 16.00. The abnormally low temperature area in the limestone quarry located in Parainen is marked in black (arrow).

In April Turku was located on the northeastern edge of a high-pressure ridge during the momentary maximum temperature difference regarding the whole Turku region (Figure 22). This occurred on April 29th at 16.00 (map is timed at 12.00 UTC) with the 500 hPa surface pressure height being about 564–568 decametres. Another high-pressure centre is located over the Kola peninsula while a low-pressure centre is over Northern Ireland. In the case of the Student Village the maximum temperature range occurred on the 9th at 23.30. Turku is located on the eastern edge of a low pressure ridge with the centre lying over the Norwegian Sea north-west from the northern Norwegian coast (Figure 23). High-pressure centres appeared close to Novaya Zemlya and over Greenland. In Turku the 500 hPa surface pressure height was at around 560–564 decametres. The map was timed at 00.00 UTC on the 10th of April. During the whole Turku region maximum difference on the 29th at 16.00 the average wind speed was 4.475 m/s and average cloudiness 5.5 oktas. For the Student Village maximum difference on the 9th at 23.30 the average wind speed was 2.175 m/s and average cloudiness 0 oktas during this time.

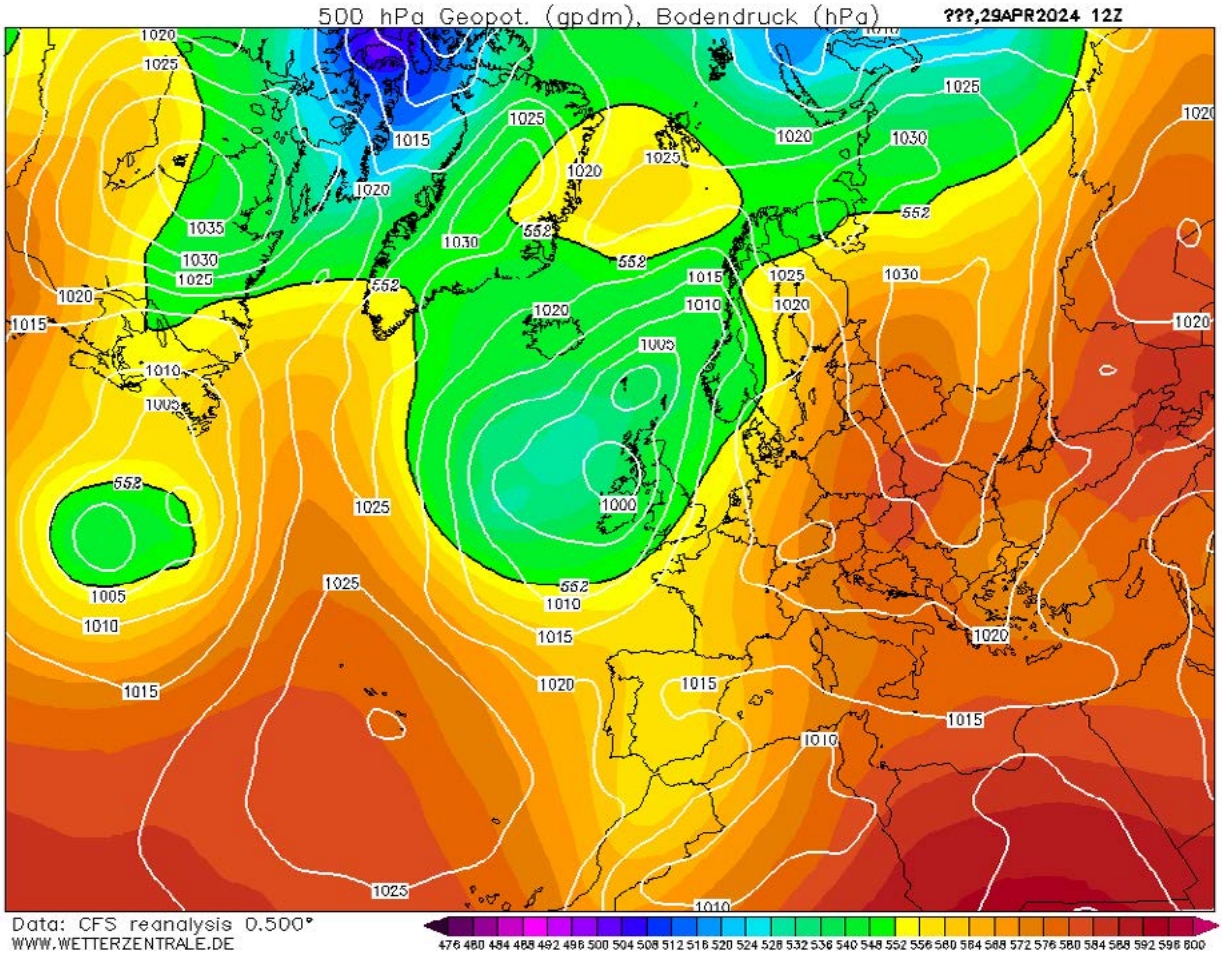

Figure 22. Sea level air pressure (white contours) and height of 500 hectopascal pressure level in decametres (colour ramp) for April 29th at 12.00 UTC. Retrieved from Wetterzentrale (https://www.wetter-zentrale.de/en/reanalysis.php?model=cfsr).

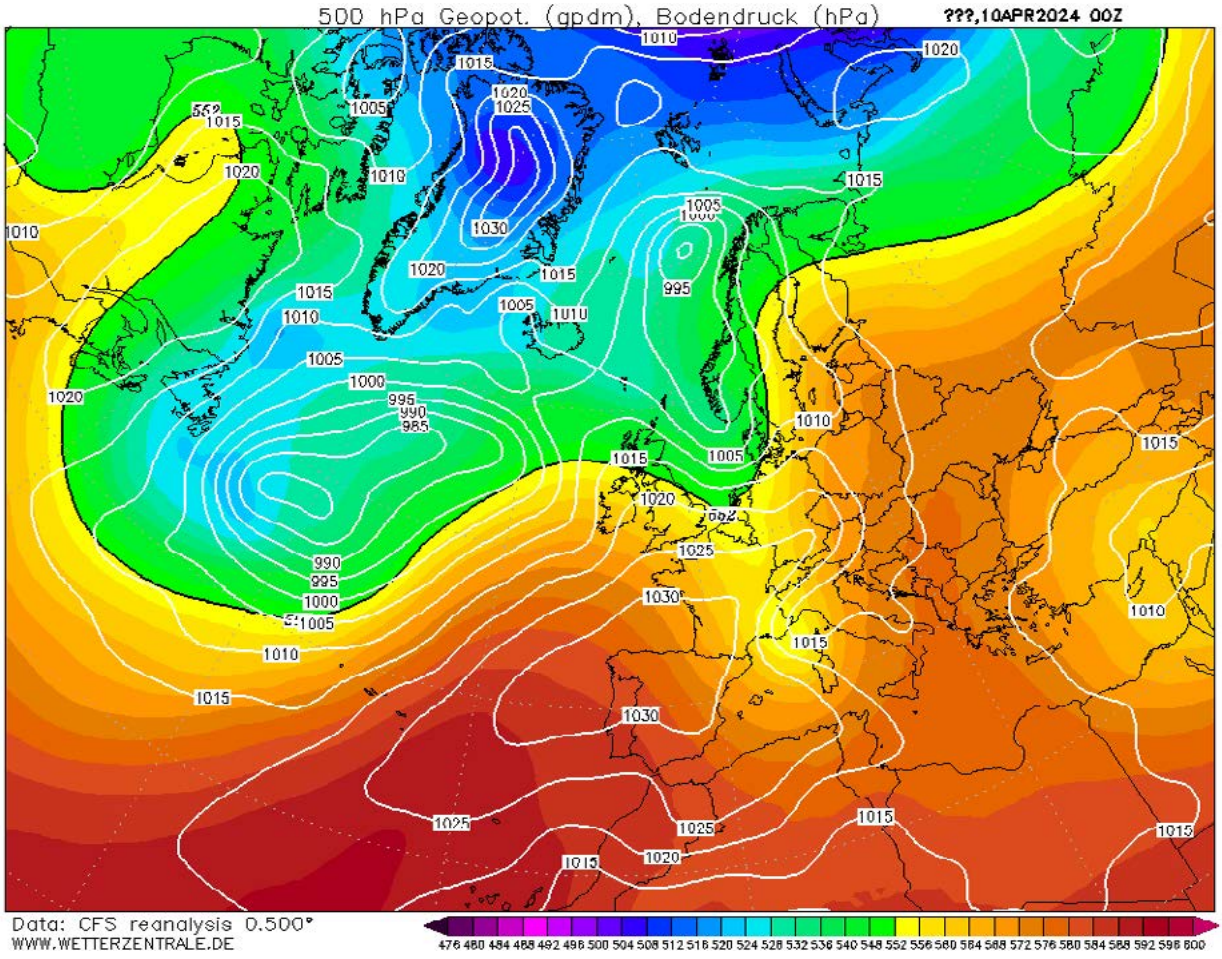

Figure 23. Sea level air pressure (white contours) and height of 500 hectopascal pressure level in decametres (colour ramp) for April 10th at 00.00 UTC. Retrieved from Wetterzentrale (https://www.wetter-zentrale.de/en/reanalysis.php?model=cfsr).

4.1.5 May

In May 2024 the average temperature at the Turku airport was 13.8 °C while during the climate reference period of 1991–2020 it was 10.0 °C. This means that May 2024 was 3.8 °C warmer than what was reported in the 1991–2020 climate reference period (Jokinen et al., 2021).

The highest and lowest monthly average temperatures out of the whole observation network were 15.6 °C in Kauppatori and 13.2 °C in Niuskala (Figure 24). In the case of the monthly averages for daily minimum temperatures the warmest average occurred in Betel with the value 9.7 °C while the coldest average of 4.4 °C occurred in Niuskala. For the monthly averages of daily maximum temperatures, the warmest site was Lieto (21.1 °C) and the coldest site Kuuva (18.4 °C). The maximum momentary temperature range in May was measured on the 29th at 01.00 between Ylijoki and Luostarivuori. The difference between these two sites was 8.9 °C.

For the Student Village sites, the highest average temperature in May was 14.9 °C recorded in Kuuvuori and Yo-kylä itä, respectively (Figure 25). The lowest average temperature was 14.0 °C in Aurajokiranta. With the monthly averages of daily minimum temperatures, the highest average occurred in Kuuvuori with the value of 8.1 °C and the lowest in Aurajokiranta with the value of 6.5 °C, respectively. The highest monthly average of daily maximum temperatures of 20.7 °C occurred in Kuuvuori and in Yo-kylä itä while the lowest of 19.8 °C in Aurajokiranta, similarly to the monthly average temperatures. For the momentary maximum temperature range the difference between Kuuvuori and Aurajokiranta was 4.7 °C on May 28th at 23.30. Similarly to prior months the topography and elevation differences between Aurajokiranta and Kuuvuori can explain the observable temperature differences.

In May the explanatory powers in the monthly average temperature regression models are 0.765 and 0.754 (Table 19). In both CORINE-based and YKR-based regression models the land cover and building floor area and population variables had a warming effect. In the YKR-based model water bodies had a weaker cooling effect. In the minimum temperatures regression model all explanatory variables were statistically significant (Table 20). All had a warming effect with the strongest being land cover and building floor area and population variables and the weakest being elevation. The explanatory powers for the models are 0.692 and 0.673. In the daily maximum temperature regression models the explanatory powers are 0.580 and 0.594 (Table 21). Out of the explanatory variables only the water body variable was statistically significant and had a cooling effect. For the regression models of the momentary maximum temperature range the explanatory powers are 0.623 and 0.664 (Table 22). Out of explanatory variables land cover, building floor area and population and elevation were statistically significant. All had a warming effect with the weakest being with elevation.

For May's temperature models the warmest areas were the mainland in the average temperatures and averages of daily maximum temperatures models while these areas were cooler in the averages of daily minimum temperatures and momentary maximum temperature difference models (Figure 26). In the averages and averages of daily maximums maps the coast and islands are the coldest. In the averages

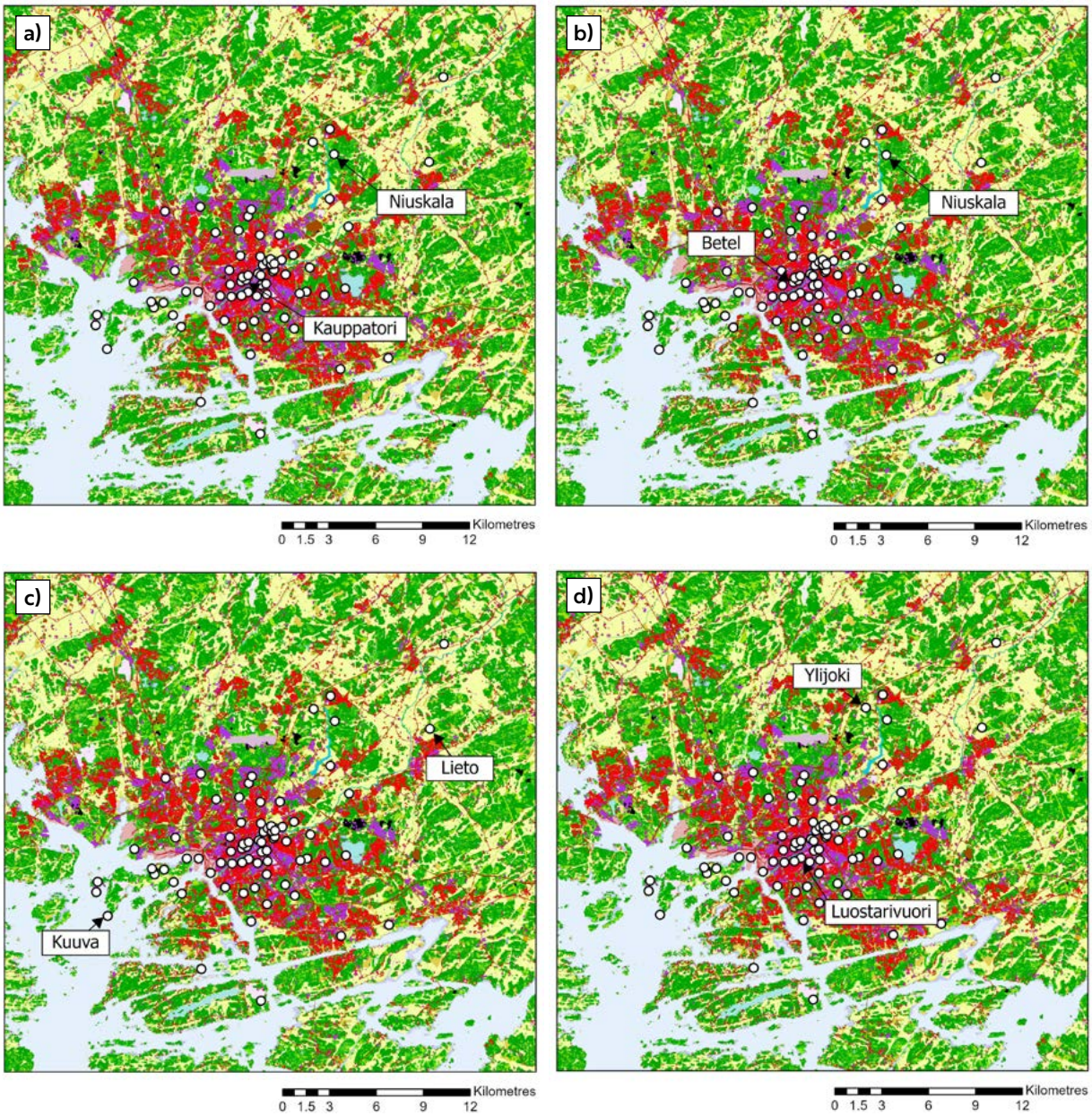

Figure 24. The locations of the logger sites of the highest and lowest a) monthly average temperatures (Kauppatori 15.6 °C, Niuskala 13.2 °C), b) monthly averages of daily minimum temperatures (Betel 9.7 °C, Niuskala 4.4 °C), c) monthly averages of daily maximum temperatures (Lieto 21.1 °C, Kuuva 18.4 °C) and d) momentary maximum temperature range on May 29th at 01.00 with the difference of 8.9 °C (Luostarivuori 19.2 °C, Ylijoki 10.3 °C). Background map: CORINE Land Cover 2018. For information on CORINE level 4 classes and respective colours, used in this Figure and subsequent CORINE based Figures, see Suomi et al. 2024, Appendix A.

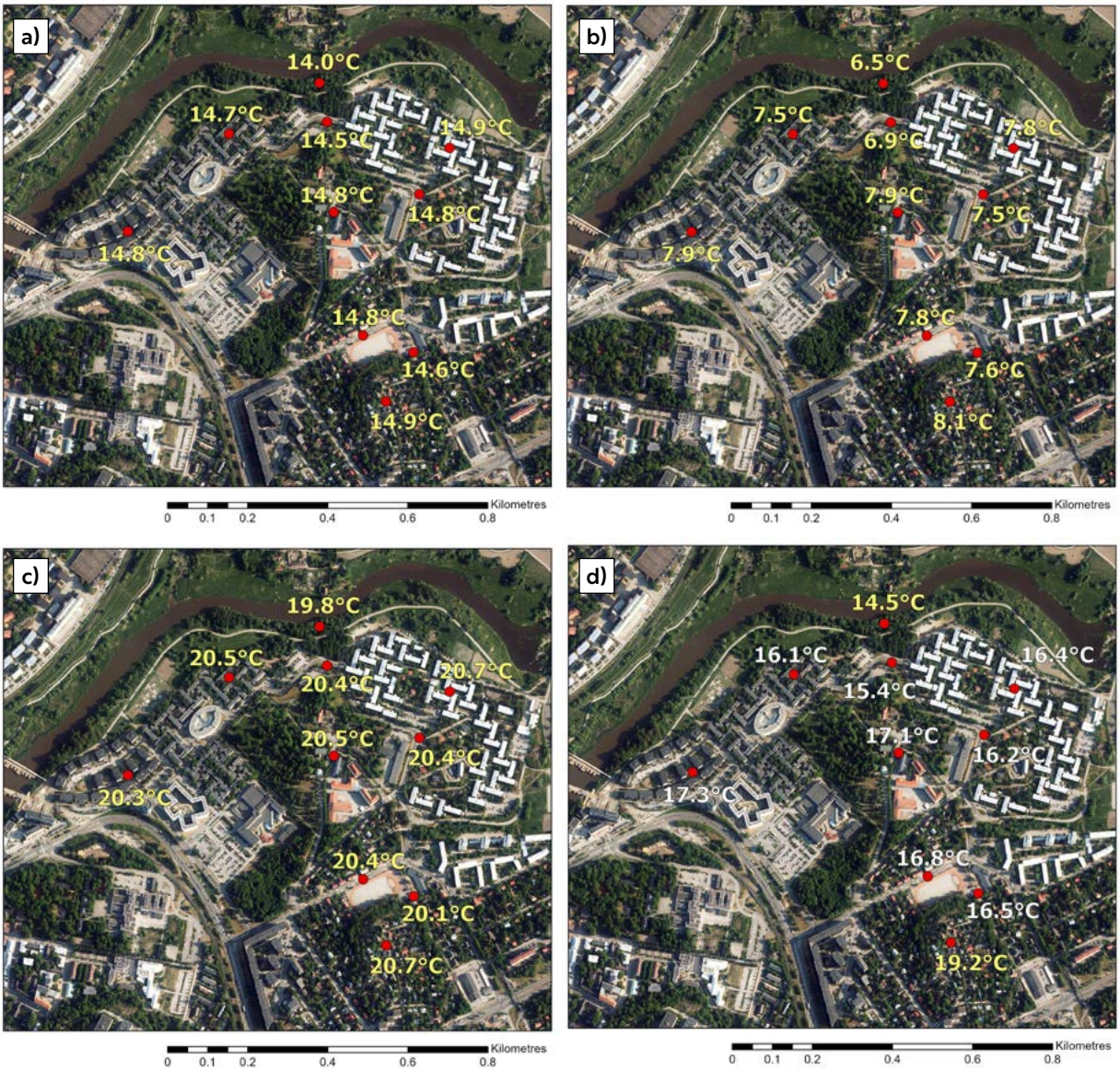

Figure 25. The Student Village logger sites with a) monthly average temperatures, b) monthly averages of daily minimum temperatures, c) monthly averages of daily maximum temperatures and d) the momentary maximum temperature range on May 28th at 23.30 in 2024 with the difference of 4.7 °C between Kuuvuori and Aurajokiranta. For individual logger site names, see Figure 4.

map the UHI effect is clear extending rather far from the Turku city centre to the neighbouring municipalities. The biggest roads and some suburban areas are also distinctive as relatively warm areas. In the maximum temperatures model the UHI is not as distinctive. The UHI can be weakly distinguished from the minimum temperatures and momentary maximum temperature range models although not appearing as clear as in the average temperature model. In these two maps the mainland is a bit

Table 19. The regression models for the monthly average temperatures in May 2024.

CORINE-based regression model		
R Square	0.776	
Adjusted R Square	0.765	
Variable	**Standardized Coefficients Beta**	**Significance**
Constant		<0.001
vl_3_5_700m	0.712	<0.001
tkuwaters_1500m	-0.198	0.005
relelev_300m	0.181	0.004

YKR-based regression model		
R Square	0.765	
Adjusted R Square	0.754	
Variable	**Standardized Coefficients Beta**	**Significance**
Constant		<0.001
rakvae_5x5	0.677	<0.001
tkuwaters_1500m	-0.268	<0.001
relelev_300m	0.167	0.010

Table 20. The regression models for the monthly averages of daily minimum temperatures in May 2024.

CORINE-based regression model		
R Square	0.706	
Adjusted R Square	0.692	
Variable	**Standardized Coefficients Beta**	**Significance**
Constant		<0.001
vl_3_5_700m	0.829	<0.001
tkuwaters_1000m	0.368	<0.001
relelev_300m	0.274	<0.001

YKR-based regression model		
R Square	0.688	
Adjusted R Square	0.673	
Variable	**Standardized Coefficients Beta**	**Significance**
Constant		<0.001
rakvae_5x5	0.784	<0.001
tkuwaters_1000m	0.282	<0.001
relelev_300m	0.258	<0.001

Table 21. The regression models for the monthly averages of daily maximum temperatures in May 2024.

CORINE-based regression model		
R Square	0.599	
Adjusted R Square	0.580	
Variable	**Standardized Coefficients Beta**	**Significance**
Constant		<0.001
vl_3_5_200m	0.031	0.721
tkuwaters_1500m	-0.762	<0.001
relelev_200m	-0.031	0.702

YKR-based regression model		
R Square	0.612	
Adjusted R Square	0.594	
Variable	**Standardized Coefficients Beta**	**Significance**
Constant		<0.001
rakvae_1x1	0.128	0.133
tkuwaters_1500m	-0.737	<0.001
relelev_200m	-0.054	0.501

Table 22. The regression models for the momentary maximum temperature range in May 2024.

CORINE-based regression model		
R Square	0.640	
Adjusted R Square	0.623	
Variable	**Standardized Coefficients Beta**	**Significance**
Constant		<0.001
vl_3_5_100m	0.605	<0.001
tkuwaters_500m	0.213	0.009
relelev_300m	0.458	<0.001

YKR-based regression model		
R Square	0.679	
Adjusted R Square	0.664	
Variable	**Standardized Coefficients Beta**	**Significance**
Constant		<0.001
rakvae_3x3	0.646	<0.001
tkuwaters_500m	0.223	0.004
relelev_300m	0.428	<0.001

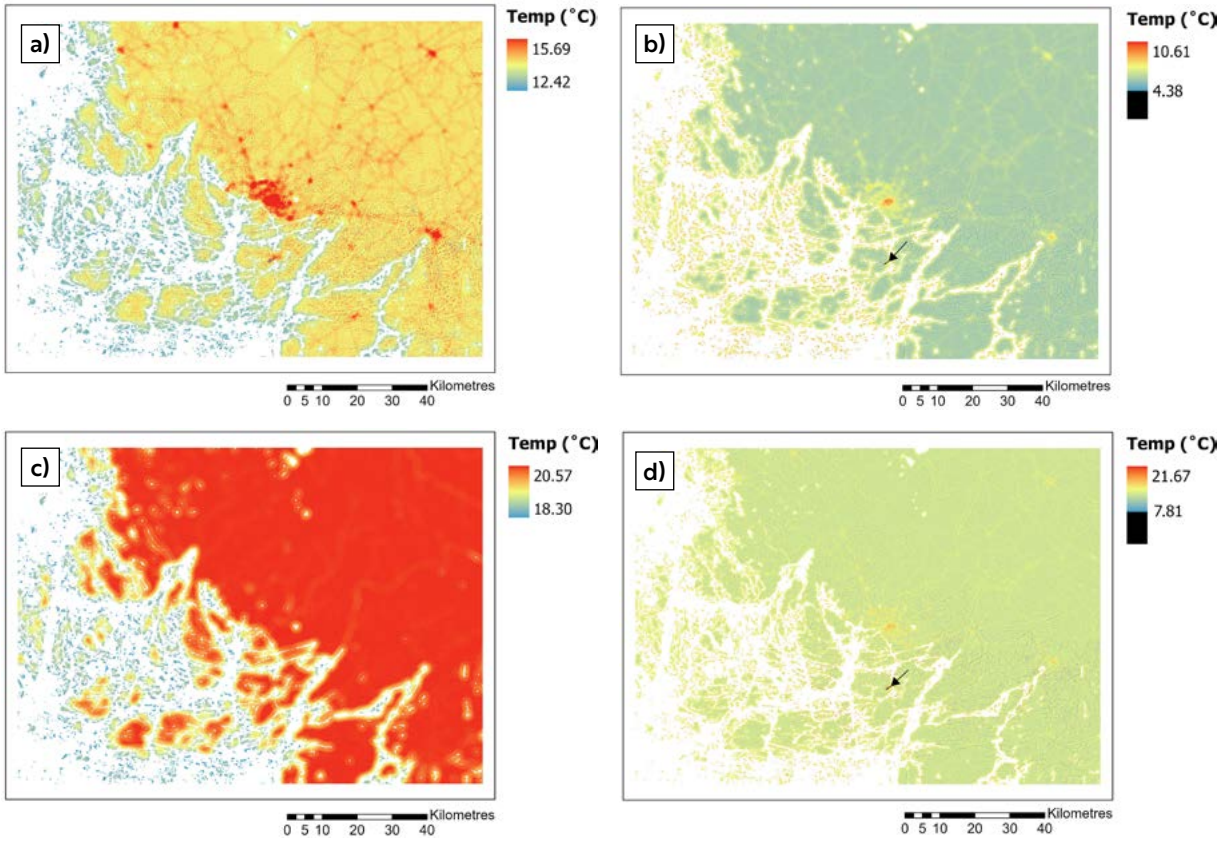

Figure 26. High-resolution (100 m) temperatures based on linear regression model depicting May 2024 a) monthly average temperatures, b) monthly averages of daily minimum temperatures, c) monthly averages of daily maximum temperatures and d) temperatures of momentary maximum temperature range on May 29th, 2024, at 01.00. The abnormally low temperature area in the limestone quarry located in Parainen is marked in black (arrow).

cooler than the coast. The limestone quarry in Parainen also distorts the temperature range in these maps.

The momentary maximum temperature range in May occurred at a similar time between the whole Turku region (May 29th at 01.00) and the Student Village (May 28th at 23.30). During this period Turku was located between a high-pressure and low-pressure centre (Figure 27). The high-pressure centre located north of the Kola peninsula over the Barents Sea while the low-pressure centre was over the British Isles. The map was timed at 00.00 UTC on the 29th with the 500 hPa surface pressure height being about 568–572 decametres over Turku during this time. The average wind speed on May 29th at 01.00 was 0.325 m/s while the average cloudiness was 0 oktas. On the 28th at 23.30, i.e. at the time of maximum range for the Student Village, average wind speed was 0.25 m/s and average cloudiness 0 oktas.

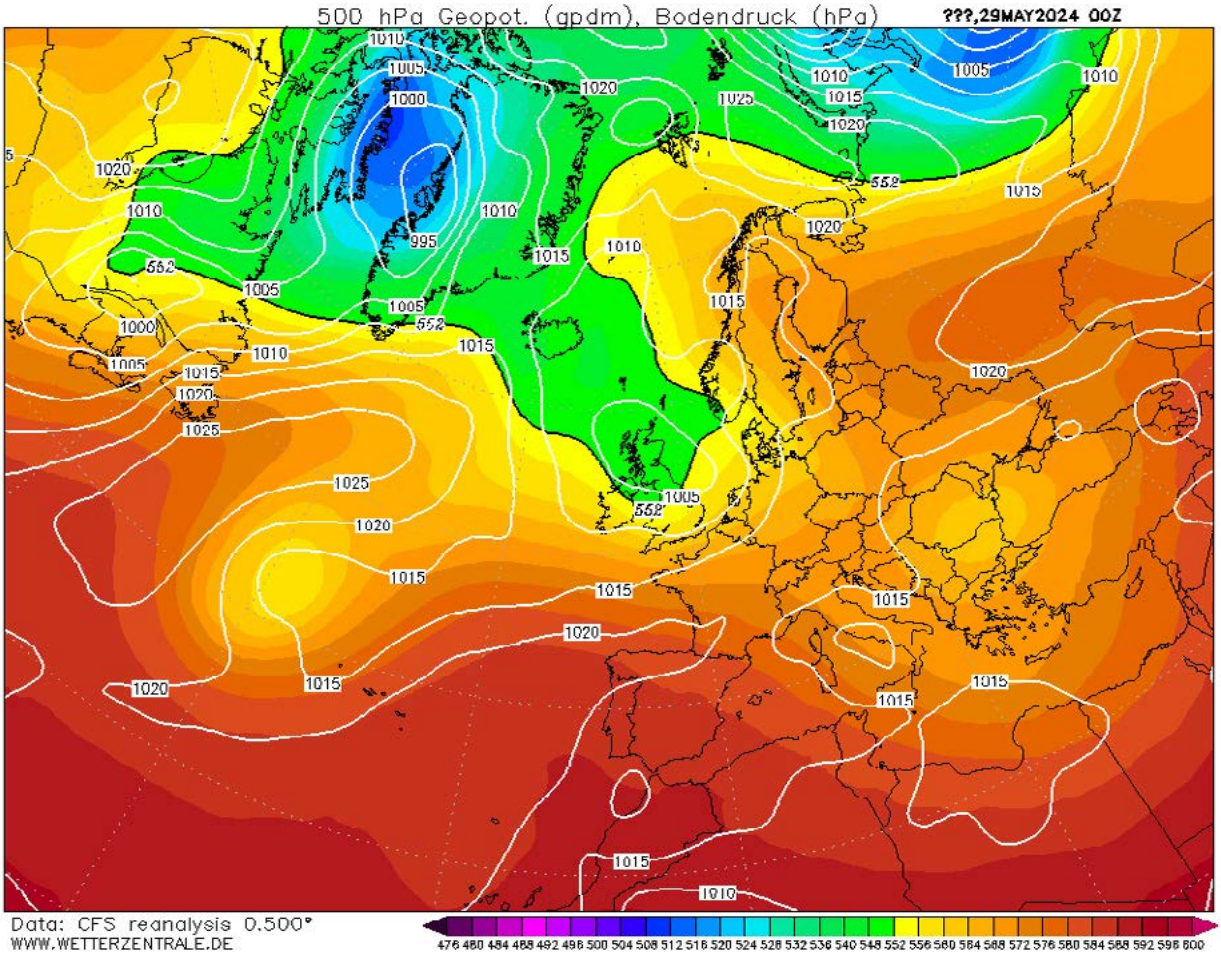

Figure 27. Sea level air pressure (white contours) and height of 500 hectopascal pressure level in decametres (colour ramp) for May 29th at 00.00 UTC. Retrieved from Wetterzentrale (https://www.wetter-zentrale.de/en/reanalysis.php?model=cfsr).

4.1.6 June

At the FMI weather station located at Turku Airport, the average temperature in June 2024 was 16.1 °C, which is 1.7 °C warmer than the average June temperature for the 1991–2020 climate reference period (Jokinen et al., 2021).

In June 2024 the highest and lowest monthly average temperatures were measured in Puutori (17.6 °C) and Niuskala (15.1 °C) (Figure 28). In the case of the monthly averages for daily minimum temperatures the lowest average temperature of 9.2 °C was measured in Niuskala and the highest of 13.8 °C in Kauppatori. For the maximums the highest average appeared in Piispankatu with the average being 21.2 °C while the lowest average of 19.5 °C appeared in the Hiiriluoto, manner observation site. The highest momentary temperature difference in June was 10.0 °C on the 12th at 18.00. This was measured between the Nummi and Lieto logger sites.

In June the lowest monthly average temperature was 16.3 °C in Aurajokiranta while the highest was 17.1 °C in Pispalantie and Yo-kylä itä, respectively (Figure 29). For the monthly averages of daily minimum temperatures, the highest average of 12.5 °C was reached in Kuuvuori while the lowest of 11.3 °C was reached in Aurajokiranta, respectively. In the case of the monthly averages of daily maximum temperatures the highest value of 21.2 °C occurred in Yo-kylä itä while the lowest of 20.3 °C in Aurajokiranta, respectively. During the momentary maximum temperature range on the 28th of June at 05.00 the coldest site was Aurajokiranta and the warmest site was Suntiontie. The temperature difference between these sites was 3.6 °C during this time. In this case a possible explanation for the temperature difference between Aurajokiranta and Suntiontie is that Aurajokiranta is a low-lying site next to the River Aura on a river bank which tends to be colder often while the Suntiontie logger is close to traffic which can warm the air.

In the monthly average temperature regression models land cover, building floor area and population and water bodies were statistically significant out of the explanatory variables (Table 23). All had a warming effect with water bodies having the weakest effect. The explanatory powers of the models are 0.615 and 0.631. For the monthly averages of daily minimum temperatures, the explanatory powers of the models are 0.610 and 0.709 (Table 24). In the CORINE-based regression model all explanatory variables were statistically significant and had a warming effect. The land cover variable's effect was the strongest while elevation had the weakest. In the YKR-based model water bodies and the building floor area and population variable were statistically significant. Out of these the building floor area and population variable was stronger. For the average daily maximum temperatures, the explanatory powers are 0.302 and 0.389 (Table 25). Here only the water body variable was statistically significant having a cooling effect. In the regression models for the maximum momentary temperature range the explanatory powers are 0.223 and 0.140 (Table 26). In this case the land cover and the building floor area and population variables both had a warming effect.

In all the temperature model cases the coastal areas were the warmest compared to the mainland except for the averages of daily maximum temperatures model in June (Figure 30). In the averages of daily maximum temperatures map the coast is the coolest area with the mainland appearing evenly the warmest. The UHI effect appears clearly in the average temperature map and also in the momentary max-

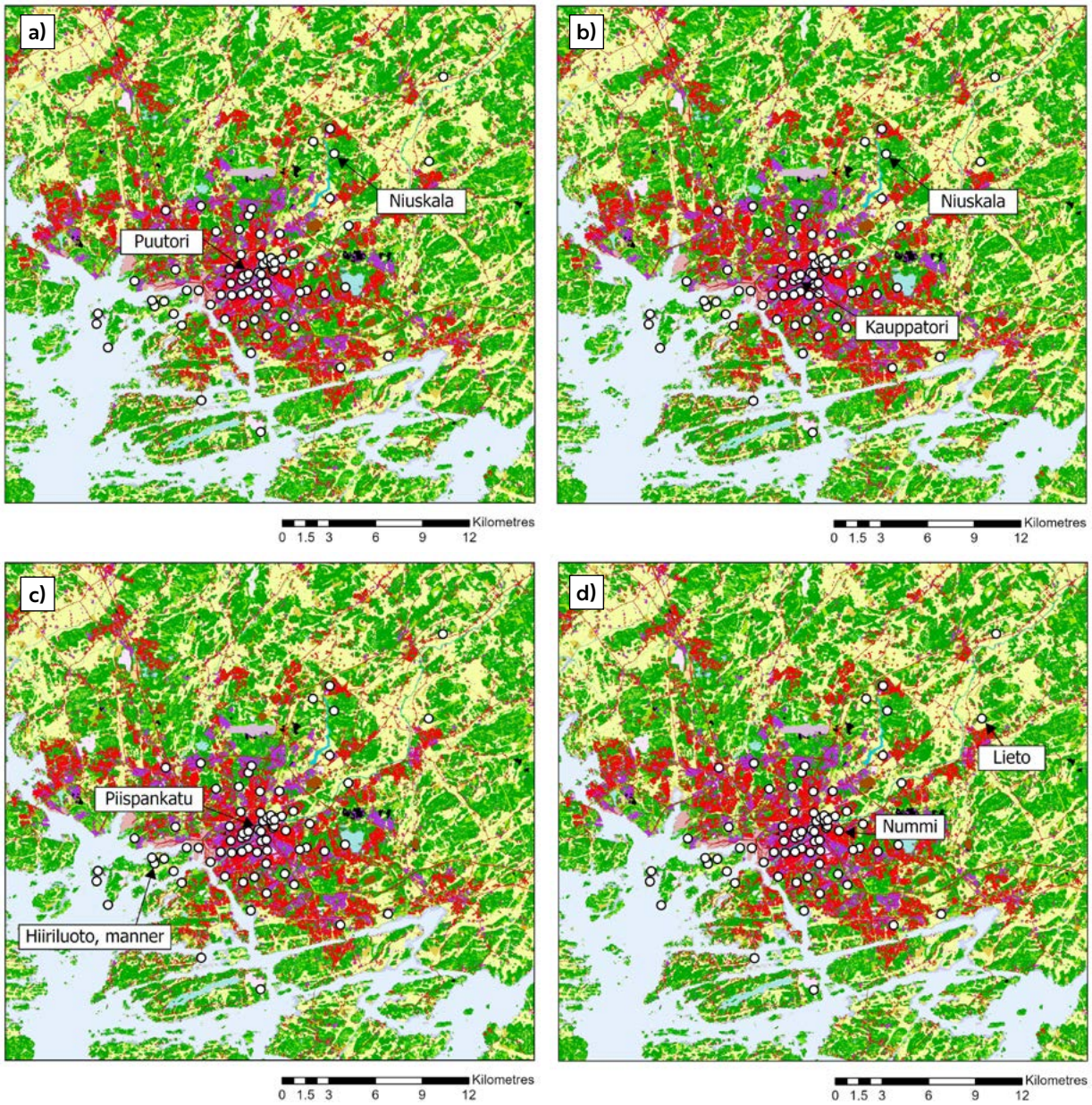

Figure 28. The locations of the logger sites of the highest and lowest a) monthly average temperatures (Puutori 17.6 °C, Niuskala 15.1 °C), b) monthly averages of daily minimum temperatures (Kauppatori 13.8 °C, Niuskala 9.2 °C), c) monthly averages of daily maximum temperatures (Piispankatu 21.2 °C, Hiiriluoto, manner 19.5 °C) and d) momentary maximum temperature range on June 12th at 18.00 with the difference of 10.0 °C (Nummi 18.9 °C, Lieto 8.9 °C). Background map: CORINE Land Cover 2018. For information on CORINE level 4 classes and respective colours, used in this Figure and subsequent CORINE based Figures, see Suomi et al. 2024, Appendix A.

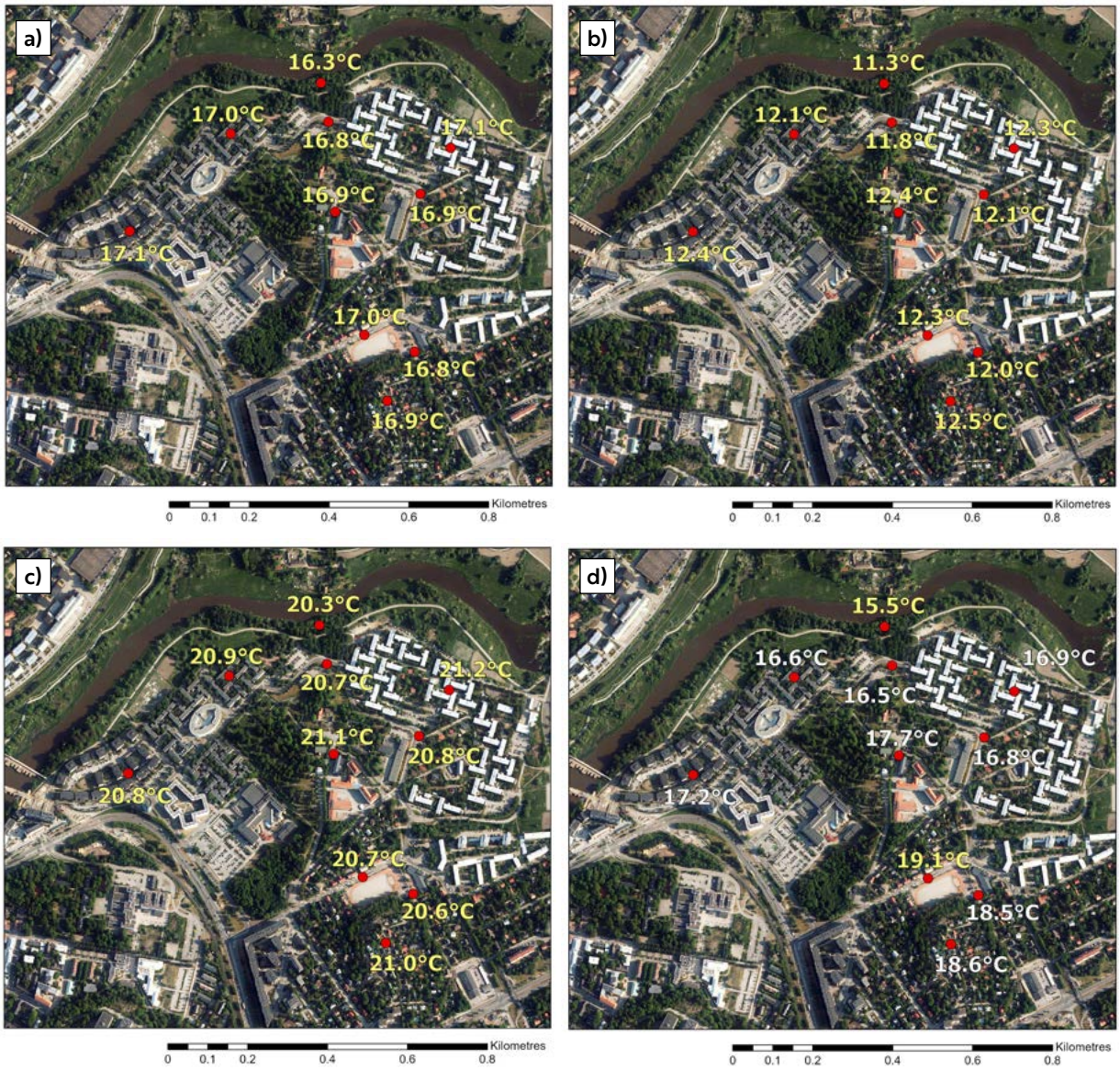

Figure 29. The Student Village logger sites with a) monthly average temperatures, b) monthly averages of daily minimum temperatures, c) monthly averages of daily maximum temperatures and d) the momentary maximum temperature range on June 28th at 05.00 in 2024 with the difference of 3.6 °C between Suntiontie and Aurajokiranta. For individual logger site names, see Figure 4.

imum temperature range map. Major roads also appear warmer than surrounding areas in these maps. In the average temperatures and averages of daily minimums models the coldest areas are the low-lying sites. With the minimums model the Parainen quarry distorts the temperature range and has been marked in black into the model. The lowest temperature outside of the quarry was 9.37 °C in the model.

During the maximum momentary temperature difference on June 12th at 18.00 a weak low-pressure centre was located over Turku

Table 23. The regression models for the monthly average temperatures in June 2024.

CORINE-based regression model		
R Square	0.632	
Adjusted R Square	0.615	
Variable	**Standardized Coefficients Beta**	**Significance**
Constant		<0.001
vl_3_5_400m	0.820	<0.001
tkuwaters_1500m	0.304	<0.001
relelev_300m	0.192	0.016

YKR-based regression model		
R Square	0.647	
Adjusted R Square	0.631	
Variable	**Standardized Coefficients Beta**	**Significance**
Constant		<0.001
rakvae_5x5	0.840	<0.001
tkuwaters_1500m	0.290	<0.001
relelev_300m	0.109	0.163

Table 24. The regression models for the monthly averages of daily minimum temperatures in June 2024.

CORINE-based regression model		
R Square	0.628	
Adjusted R Square	0.610	
Variable	**Standardized Coefficients Beta**	**Significance**
Constant		<0.001
vl_3_5_100m	0.690	<0.001
tkuwaters_2km	0.522	<0.001
relelev_500m	0.282	<0.001

YKR-based regression model		
R Square	0.722	
Adjusted R Square	0.709	
Variable	**Standardized Coefficients Beta**	**Significance**
Constant		<0.001
rakvae_5x5	0.788	<0.001
tkuwaters_2km	0.582	<0.001
relelev_500m	0.215	0.002

Table 25. The regression models for the monthly averages of daily maximum temperatures in June 2024.

CORINE-based regression model		
R Square	0.334	
Adjusted R Square	0.302	
Variable	**Standardized Coefficients Beta**	**Significance**
Constant		<0.001
vl_3_5_500m	-0.007	0.949
tkuwaters_1500m	-0.567	<0.001
relelev_200m	0.091	0.380

YKR-based regression model		
R Square	0.416	
Adjusted R Square	0.389	
Variable	**Standardized Coefficients Beta**	**Significance**
Constant		<0.001
rakvae_3x3	0.316	0.004
tkuwaters_1500m	-0.452	<0.001
relelev_200m	0.021	0.836

Table 26. The regression models for the momentary maximum temperature range in June 2024.

CORINE-based regression model		
R Square	0.258	
Adjusted R Square	0.223	
Variable	**Standardized Coefficients Beta**	**Significance**
Constant		<0.001
vl_3_5_700m	0.586	<0.001
tkuwaters_2kmsqrt	0.332	0.009
relelev_100m	-0.016	0.886

YKR-based regression model		
R Square	0.179	
Adjusted R Square	0.140	
Variable	**Standardized Coefficients Beta**	**Significance**
Constant		<0.001
rakvae_5x5	0.458	<0.001
tkuwaters_2kmsqrt	0.228	0.070
relelev_100m	0.001	0.990

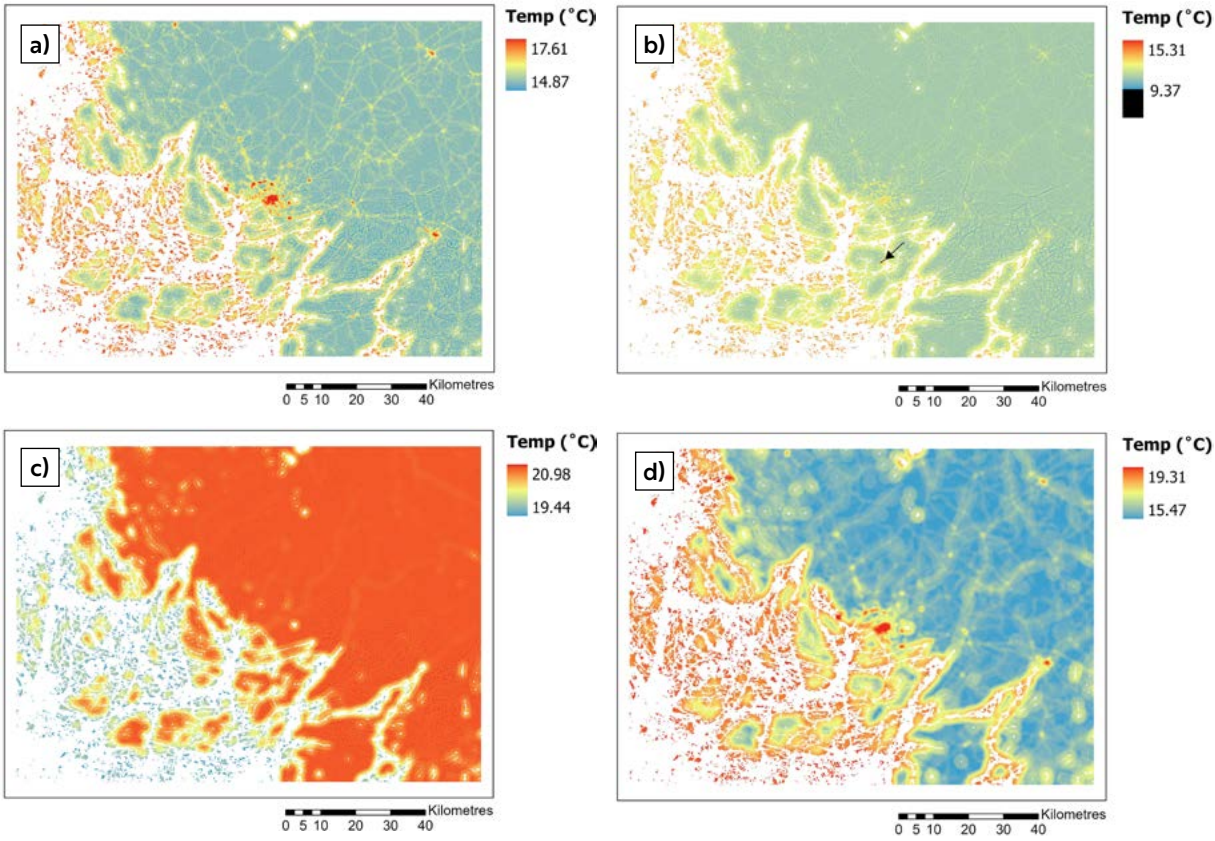

Figure 30. High-resolution (100 m) temperatures based on linear regression model depicting June 2024 a) monthly average temperatures, b) monthly averages of daily minimum temperatures, c) monthly averages of daily maximum temperatures and d) temperatures of momentary maximum temperature range on June 12th, 2024, at 18.00. The abnormally low temperature area in the limestone quarry located in Parainen is marked in black (arrow).

(map is timed at 18.00 UTC) (Figure 31). During this time the 500 hPa surface pressure height was about 548–552 decametres over the Turku region and the rest of Finland. A low-pressure centre appeared west of Iceland on the North Atlantic Ocean. In the case of the Student Village the maximum range occurred on the 28th at 05.00 (map is timed at 00.00 UTC) with Turku located on the western edge of a weaker high-pressure ridge (Figure 32). This weaker high-pressure ridge extended over eastern Europe. A low-pressure ridge appeared north of the British Isles. The 500 hPa surface pressure height over Turku was 576–580 decametres. During the momentary maximum temperature range for the whole Turku region on the 12th at 18.00 the average wind speed was 3.625 m/s and average cloudiness 0 oktas. For the Student Villages momentary maximum difference on the 28th at 05.00 the average wind speed was 1.325 m/s and average cloudiness 0 oktas.

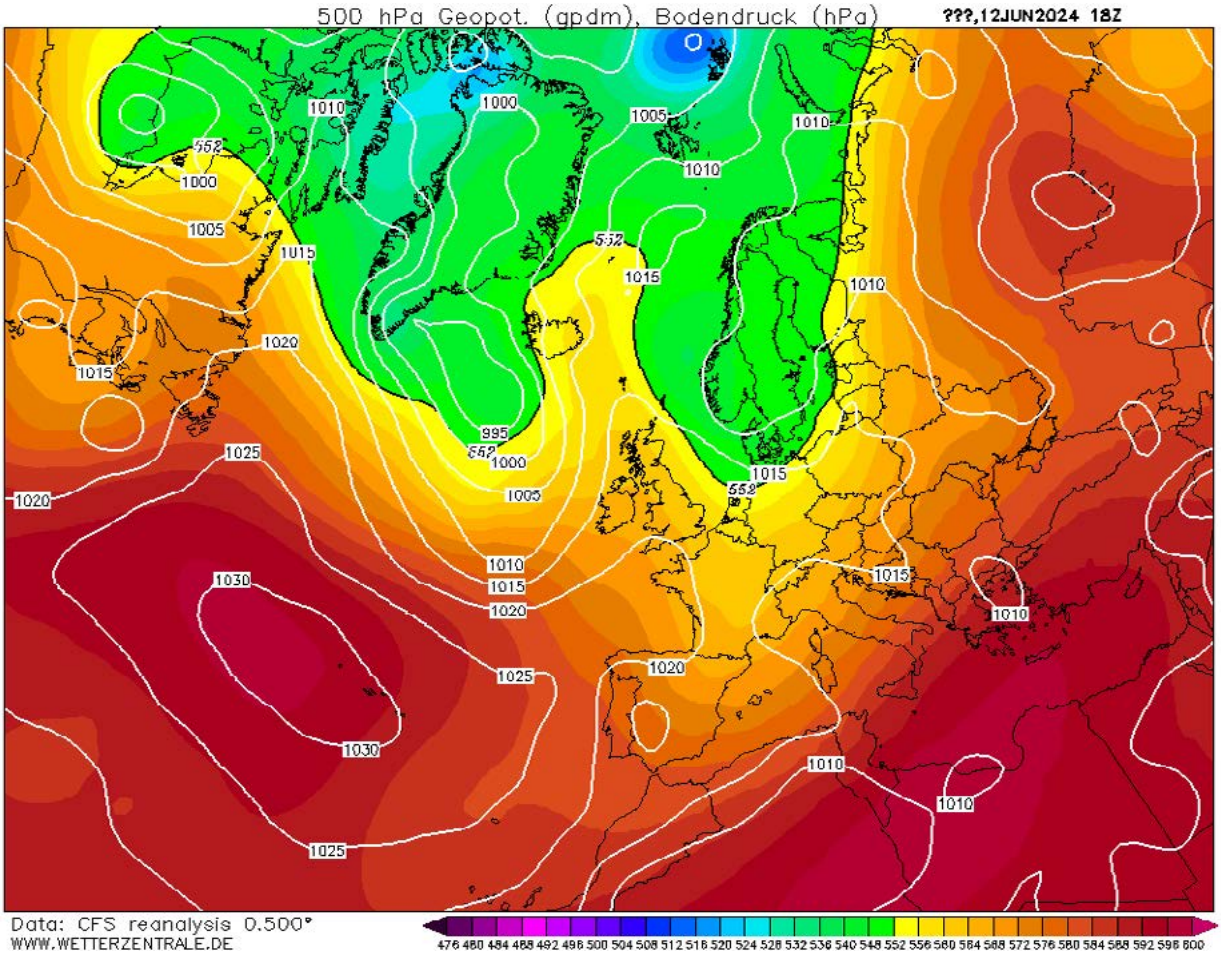

Figure 31. Sea level air pressure (white contours) and height of 500 hectopascal pressure level in decametres (colour ramp) for June 12th at 18.00 UTC. Retrieved from Wetterzentrale (https://www.wetter-zentrale.de/en/reanalysis.php?model=cfsr).

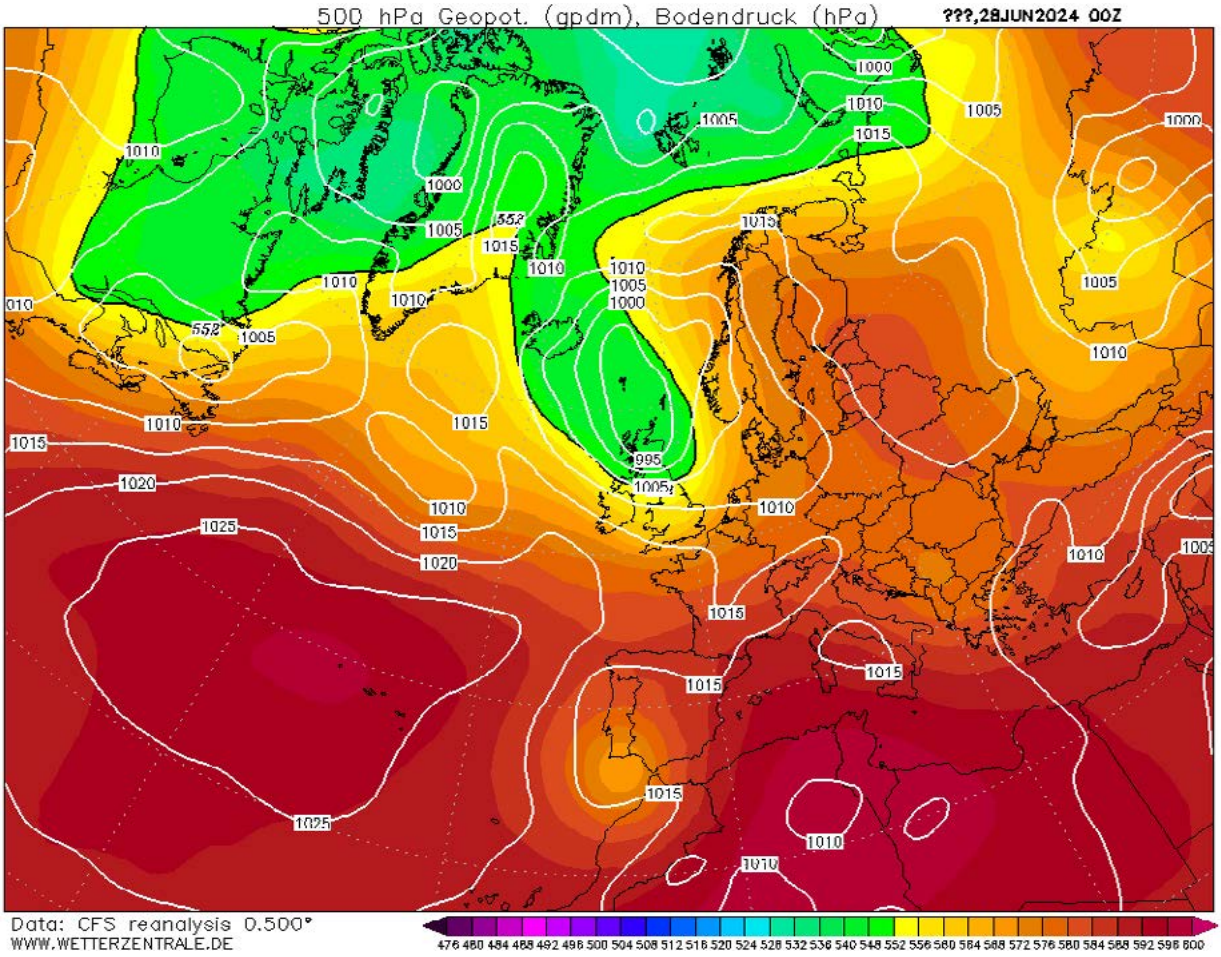

Figure 32. Sea level air pressure (white contours) and height of 500 hectopascal pressure level in decametres (colour ramp) for June 28th at 00.00 UTC. Retrieved from Wetterzentrale (https://www.wetter-zentrale.de/en/reanalysis.php?model=cfsr).

4.1.7 July

The average temperature in July 2024 recorded 18.2 °C at the Turku airport observation site which was 0.7 °C warmer than during the climate reference period in 1991–2020 (Jokinen et al., 2021).

In July 2024 the highest average temperature was acquired in Kauppatori with the value being 19.4 °C (Figure 33). The lowest average of 17.3 °C was acquired in Niuskala. These same sites applied for the monthly averages of daily minimum and maximum temperatures with Kauppatori being the warmest site and Niuskala the coldest. In the minimums case Kauppatori measured 16.4 °C and Niuskala measured 13.4 °C while with maximums the averages were 22.8 °C (Kauppatori) and 20.9 °C (Niuskala). The momentary maximum temperature range was 7.3 °C on July 10th at 03.00. This difference occurred between Kuuva and Sikilä. Kuuva is influenced by the warming effect of the sea while Sikilä is located further on the mainland.

The highest average temperature in July for the Student Village was 19.0 °C and measured in Pispalantie and Yo-kylä itä observation sites and the lowest average temperature was 18.3 °C measured in Aurajokiranta, respectively (Figure 34). For the monthly averages of daily minimum temperatures, the warmest site was Pispalantie with a value of 15.8 °C while the coldest site was Aurajokiranta with a value of 15.0 °C, respectively. For the monthly averages of daily maximum temperatures, the highest average of 22.5 °C was measured in Kuuvuori and Yo-kylä itä while the lowest average of 21.8 °C in Aurajokiranta, respectively. The momentary maximum temperature range occurred between Aurajokiranta and Pispalantie with the difference between these loggers being 2.6 °C. This happened on July 16th at 22.00. Aurajokiranta is a low-lying site on the river bank while Pispalantie is close to a highly trafficked road which can cause the temperature difference.

The explanatory powers in the linear regression models for the monthly average temperatures are 0.571 and 0.548 (Table 27). In the CORINE-based regression model both land cover and water bodies had a warming effect with land cover being stronger. In the YKR-based regression model the explanatory variable for the building floor area and population had a warming effect. In the case of monthly averages for daily minimum temperatures land cover, building floor area and population and water bodies were statistically significant (Table 28). All had a warming effect with land cover and the building floor area and population variable having a stronger one. The explanatory powers are 0.643 in the CORINE-based regression model and 0.660 in the YKR-based regression model. For the monthly averages of maximums only land cover and building floor area and population variables were statistically significant having a warming effect in both models (Table 29). The explanatory powers are 0.355 and 0.348. In the case of the momentary maximum temperature range in July the explanatory powers are 0.628 and 0.689 (Table 30). In the CORINE-based regression model all variables had a warming effect with the strongest ones being land cover and water body. These two variables were the strongest in the YKR-based regression model as well although elevation was not statistically significant.

Similarly to the previous month in the averages of daily maximum temperatures model the coast is the coolest and mainland the warmest area while in the other three models it is the other way around (Figure 35). Low-lying sites appear to be

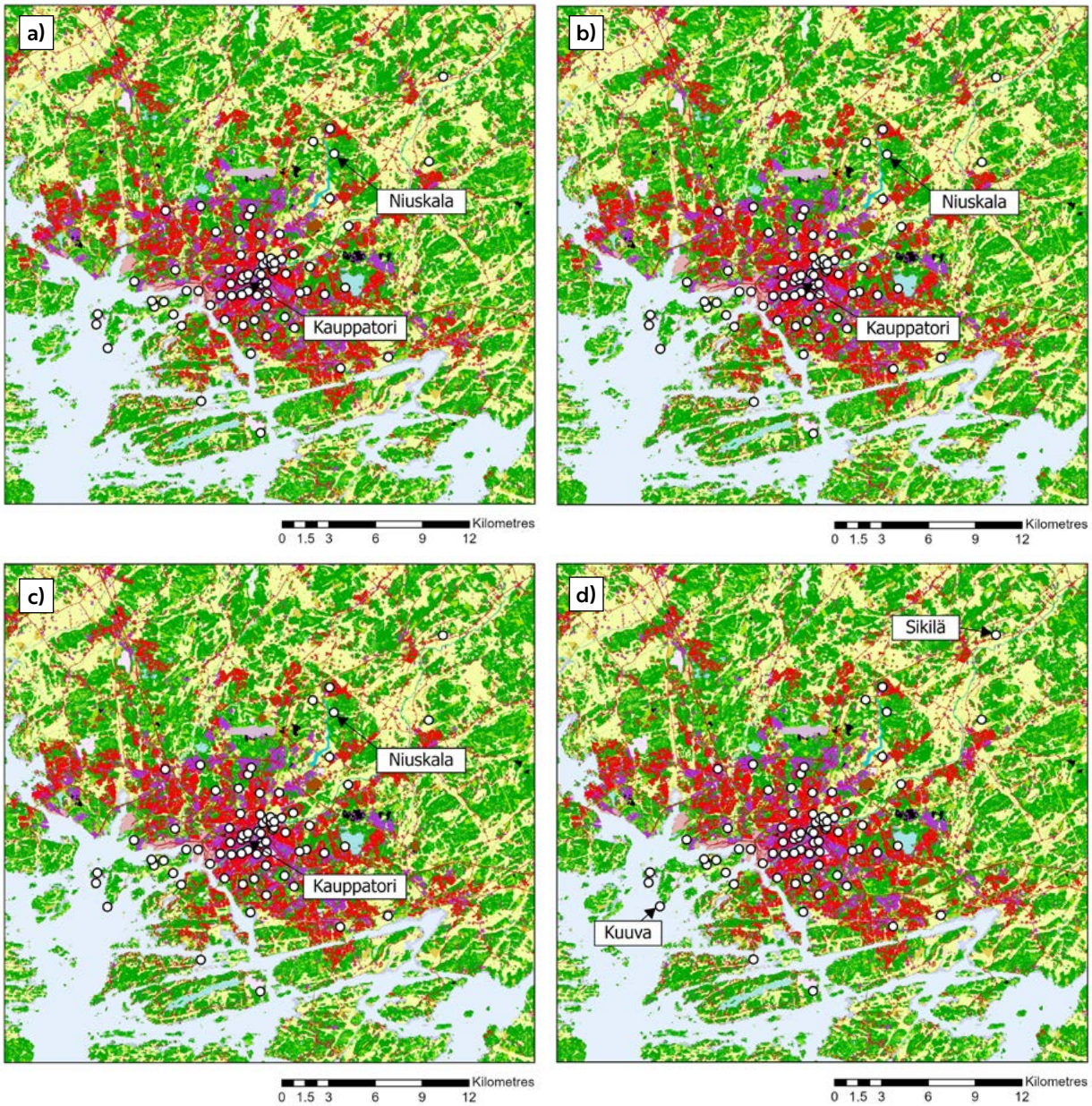

Figure 33. The locations of the logger sites of the highest and lowest a) monthly average temperatures (Kauppatori 19.4 °C, Niuskala 17.3 °C), b) monthly averages of daily minimum temperatures (Kauppatori 16.4 °C, Niuskala 13.4 °C), c) monthly averages of daily maximum temperatures (Kauppatori 22.8 °C, Niuskala 20.9 °C) and d) momentary maximum temperature range on July 10th at 03.00 with the difference of 7.3 °C (Kuuva 16.3 °C, Sikilä 9.0 °C). Background map: CORINE Land Cover 2018. For information on CORINE level 4 classes and respective colours, used in this Figure and subsequent CORINE based Figures, see Suomi et al. 2024, Appendix A.

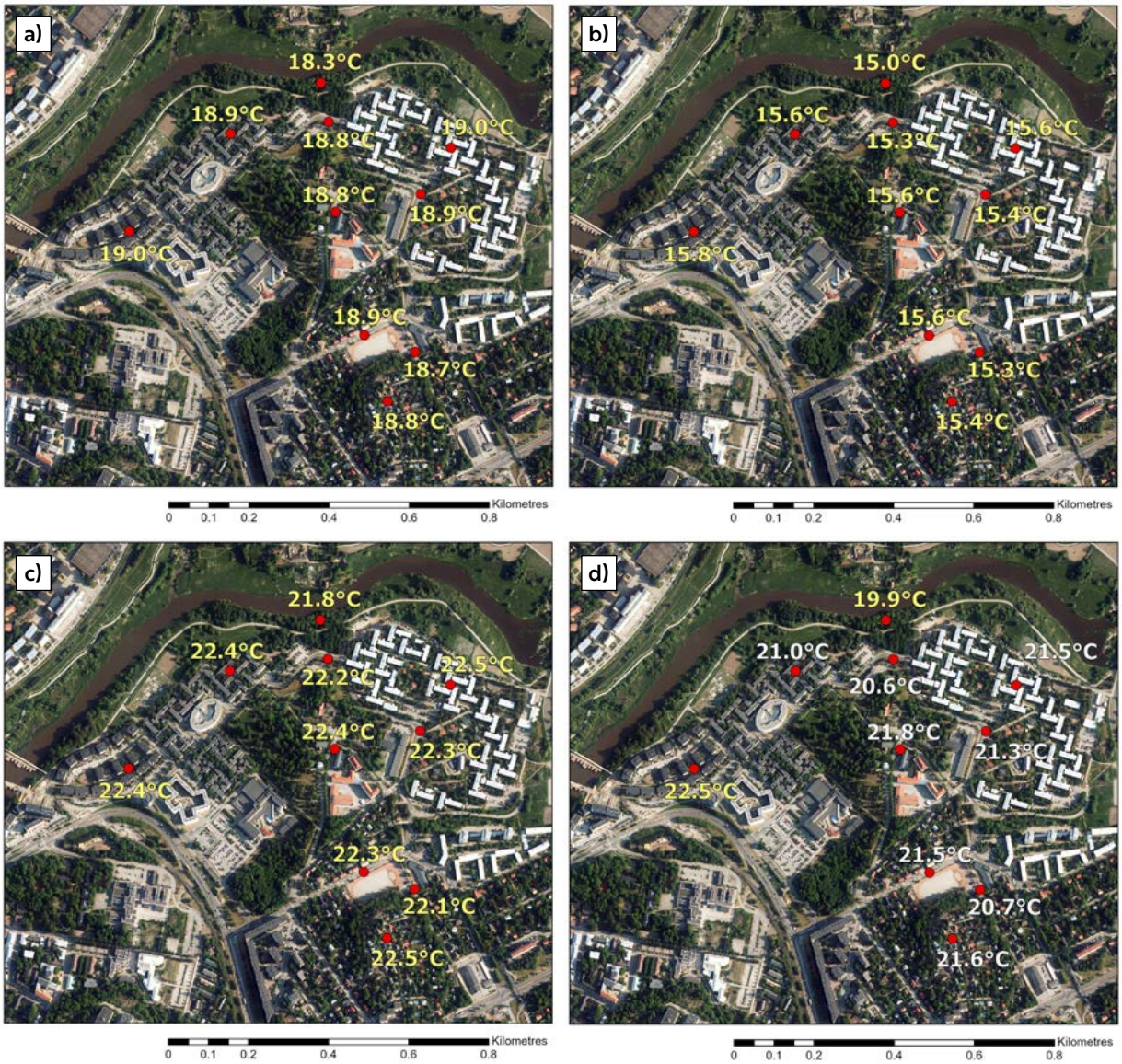

Figure 34. The Student Village logger sites with a) monthly average temperatures, b) monthly averages of daily minimum temperatures, c) monthly averages of daily maximum temperatures and d) the momentary maximum temperature range on July 16th at 22.00 in 2024 with the difference of 2.6 °C between Pispalantie and Aurajokiranta. For individual logger site names, see Figure 4.

the coldest in the average temperatures, averages of daily minimums and momentary maximum temperature range models. The UHI around Turku city centre is distinguishable in nearly all cases but it most visible in the average temperatures model and the averages of daily maximum temperatures model. Neighbouring municipalities also appear warmer in these two maps. The distorting effect of the limestone quarry in Parainen appeared in the averages of daily minimum temper-

Table 27. The regression models for the monthly average temperatures in July 2024.

CORINE-based regression model		
R Square	0.590	
Adjusted R Square	0.571	
Variable	**Standardized Coefficients Beta**	**Significance**
Constant		<0.001
v1_3_5_400m	0.800	<0.001
tkuwaters_500m	0.351	<0.001
relelev_300m	0.119	0.147

YKR-based regression model		
R Square	0.568	
Adjusted R Square	0.548	
Variable	**Standardized Coefficients Beta**	**Significance**
Constant		<0.001
rakvae_5x5	0.782	<0.001
tkuwaters_500m	0.296	0.001
relelev_300m	0.047	0.582

Table 28. The regression models for the monthly averages of daily minimum temperatures in July 2024.

CORINE-based regression model		
R Square	0.659	
Adjusted R Square	0.643	
Variable	**Standardized Coefficients Beta**	**Significance**
Constant		<0.001
v1_3_5_400m	0.778	<0.001
tkuwaters_2km	0.599	<0.001
relelev_500m	0.215	0.005

YKR-based regression model		
R Square	0.675	
Adjusted R Square	0.660	
Variable	**Standardized Coefficients Beta**	**Significance**
Constant		<0.001
rakvae_5x5	0.796	<0.001
tkuwaters_2km	0.588	<0.001
relelev_500m	0.134	0.072

Table 29. The regression models for the monthly averages of daily maximum temperatures in July 2024.

CORINE-based regression model		
R Square	0.384	
Adjusted R Square	0.355	
Variable	**Standardized Coefficients Beta**	**Significance**
Constant		<0.001
v1_3_5_700m	0.445	<0.001
tkuwaters_2kmsqrt	-0.273	0.019
relelev_200m	-0.043	0.673

YKR-based regression model		
R Square	0.377	
Adjusted R Square	0.348	
Variable	**Standardized Coefficients Beta**	**Significance**
Constant		<0.001
rakvae_3x3	0.402	<0.001
tkuwaters_2kmsqrt	-0.348	0.002
relelev_200m	-0.034	0.739

Table 30. The regression models for the momentary maximum temperature range in July 2024.

CORINE-based regression model		
R Square	0.645	
Adjusted R Square	0.628	
Variable	**Standardized Coefficients Beta**	**Significance**
Constant		<0.001
v1_3_5_100m	0.630	<0.001
tkuwaters_2km	0.629	<0.001
relelev_300m	0.279	<0.001

YKR-based regression model		
R Square	0.703	
Adjusted R Square	0.689	
Variable	**Standardized Coefficients Beta**	**Significance**
Constant		<0.001
rakvae_5x5	0.706	<0.001
tkuwaters_2km	0.675	<0.001
relelev_300m	0.217	0.003

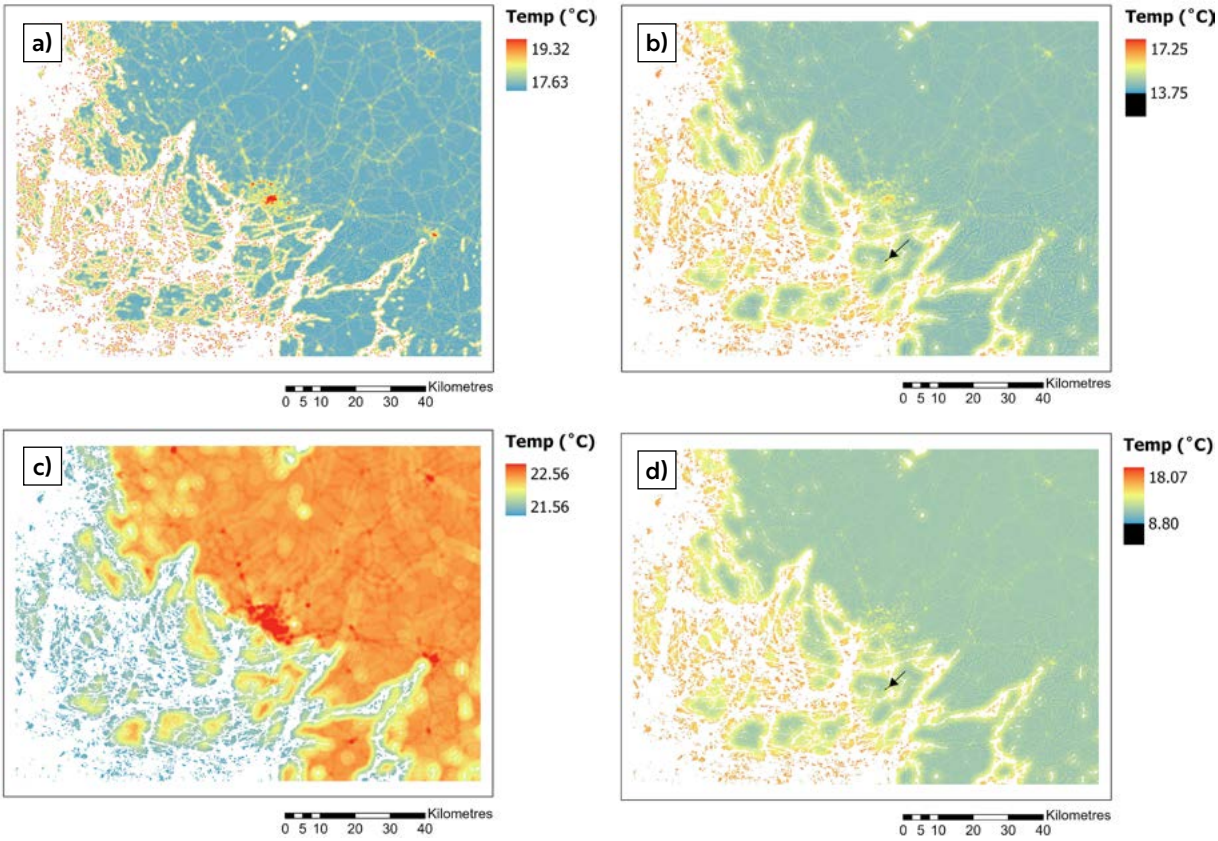

Figure 35. High-resolution (100 m) temperatures based on linear regression model depicting July 2024 a) monthly average temperatures, b) monthly averages of daily minimum temperatures, c) monthly averages of daily maximum temperatures and d) temperatures of momentary maximum temperature range on July 10th, 2024, at 03.00. The abnormally low temperature area in the limestone quarry located in Parainen is marked in black (arrow).

atures model and the momentary maximum temperature range model. The temperatures in the quarry have been marked in black and the location of the quarry is indicated by a black arrow.

In July during the maximum momentary temperature range on the 10th regarding the whole Turku region Turku was located on the northern edge of a high-pressure ridge (Figure 36). The 500 hPa surface pressure hight was about 568–572 decametres in Turku and low-pressure centres appeared north of Svalbard and a weaker one over the British Isles. The map was timed at 00.00 UTC. During the Student Village's maximum range on the 16th an extensive high pressure ridge appeared over Greenland extending to the Barents Sea and eastern Russia (Figure 37). A low-pressure centre appeared over the North Atlantic southwest from Iceland. The 500 hPa surface pressure height over Turku was 572–576 decametres and the map was timed at 18.00 UTC. On July 10th at 03.00 the average wind speed was 1.625 m/s and average cloudiness 0 oktas whereas on the 16th at 22.00 they measured 1.65 m/s and 7 oktas.

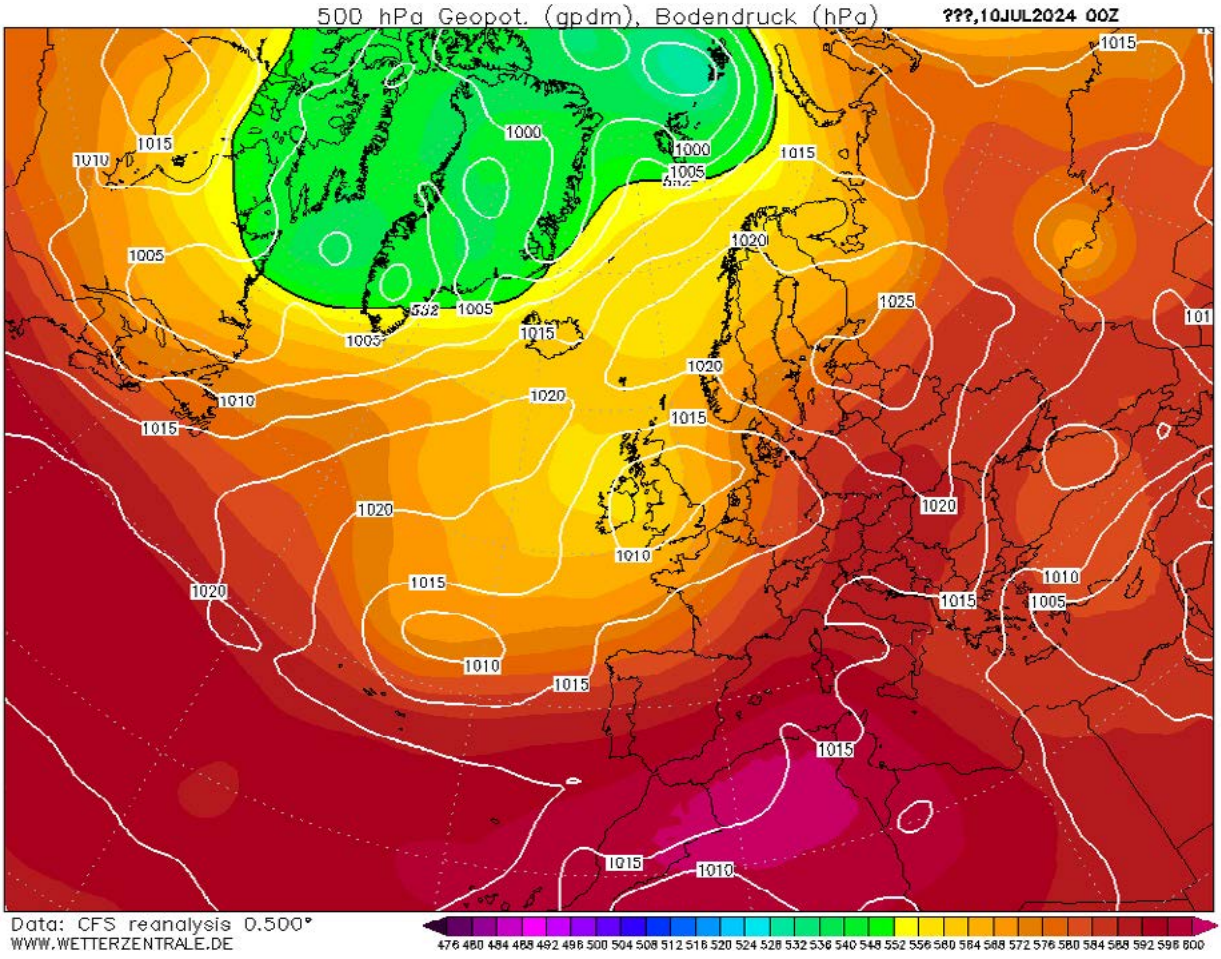

Figure 36. Sea level air pressure (white contours) and height of 500 hectopascal pressure level in decametres (colour ramp) for July 10th at 00.00 UTC. Retrieved from Wetterzentrale (**https://www.wetter-zentrale.de/en/reanalysis.php?model=cfsr**).

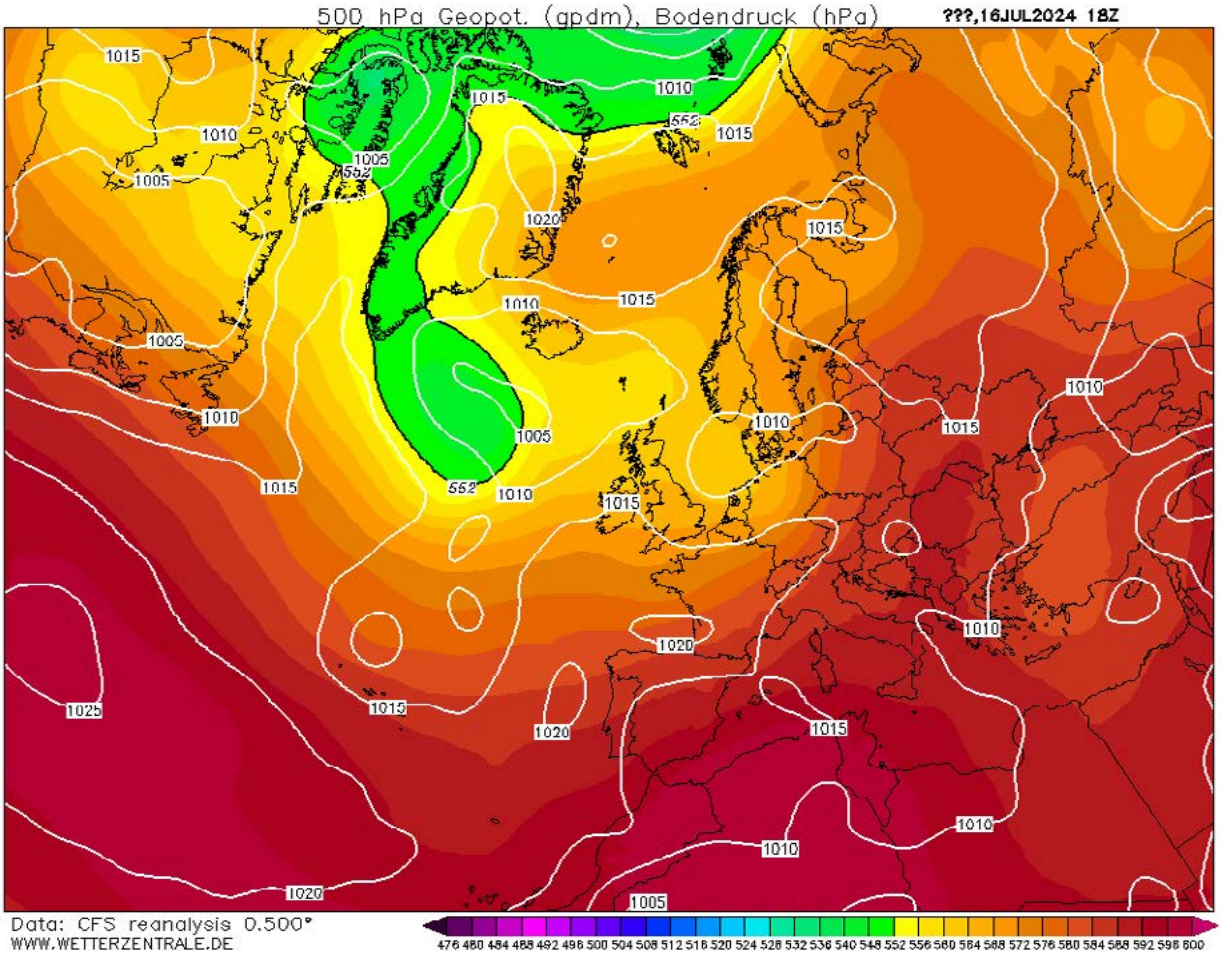

Figure 37. Sea level air pressure (white contours) and height of 500 hectopascal pressure level in decametres (colour ramp) for July 16th at 18.00 UTC. Retrieved from Wetterzentrale (https://www.wetter-zentrale.de/en/reanalysis.php?model=cfsr).

4.1.8 August

For August the average temperature in the 1991–2020 climate reference period was 16.2 °C (Jokinen et al., 2021). In 2024 the average temperature of 17.2 °C was recorded resulting in a 1.0 °C difference.

Regarding the complete observation network the highest and lowest average temperatures in July were measured in Kauppatori (18.7 °C) and Niuskala (16.2 °C) (Figure 38). For the averages of daily minimum temperatures, the highest average of 15.5 °C was obtained in Kuuva while the lowest average of 11.3 °C appeared in Sikilä. For the averages of daily maximums Piispankatu (22.3 °C) and Niuskala (20.6 °C) were the sites where the highest and lowest values appeared. In August the momentary maximum temperature difference occurred on the 18th at 05.00 between Kolkka and Sikilä. The difference was 8.6 °C.

The Turku Student Village average temperatures were highest in Pispalantie (18.1 °C) and lowest in Aurajokiranta (17.2 °C) in August, respectively (Figure 39). In the case of the monthly averages of daily minimum temperatures the coldest site was still Aurajokiranta with a value of 12.9 °C while the warmest site this time was Kuuvuori with a value of 14.1 °C, respectively. For the monthly averages of daily maximum temperatures Aurajokiranta was the coldest site with an average of 20.9 °C while the warmest sites were Kuuvuori and Yo-kylä itä with values of 22.1 °C, respectively. For the momentary maximum temperature range the occurrence was on the 18th of August at 06.00 with the difference being 4.3 °C between Aurajokiranta and Kuuvuori. Elevation differences can possibly explain this temperature difference.

In August of 2024 the explanatory powers of the regression models completed for monthly average temperatures are 0.600 and 0.595 (Table 31). In these models, land cover, building floor area and population and water bodies were statistically significant and had a warming effect. The warmest effect was with the land cover and building floor area and population. For the minimums the explanatory powers of the models are 0.640 and 0.662 (Table 32). In the CORINE-based regression model all variables were statistically significant with the strongest effect being with land cover. In the YKR-based regression model elevation was not statistically significant. Here the building floor area and population explanatory variable also was the strongest. Water bodies also had a relatively strong effect in both models. For the maximum temperatures the explanatory powers are 0.206 and 0.303 (Table 33). In the CORINE-based regression model water bodies had a cooling effect while none of the explanatory variables were statistically significant in the YKR-based regression model. In the momentary maximum temperature range models all variables had a warming effect with the strongest occurring with water bodies (Table 34). The explanatory powers here are 0.640 and 0.737.

The warmest areas in the temperature models in August 2024 were the coast and the archipelago (Figure 40). The mainland appeared as the coolest area with the low-lying sites being clearly the coldest areas in the maximum temperatures and momentary maximum temperature difference models. The model on average daily maximum temperatures was deviant from the other three models with the coast area being the coldest and the mainland the warmest similarly to the temperature models in June and July. The UHI effect was distinguishable only in the average tempera-

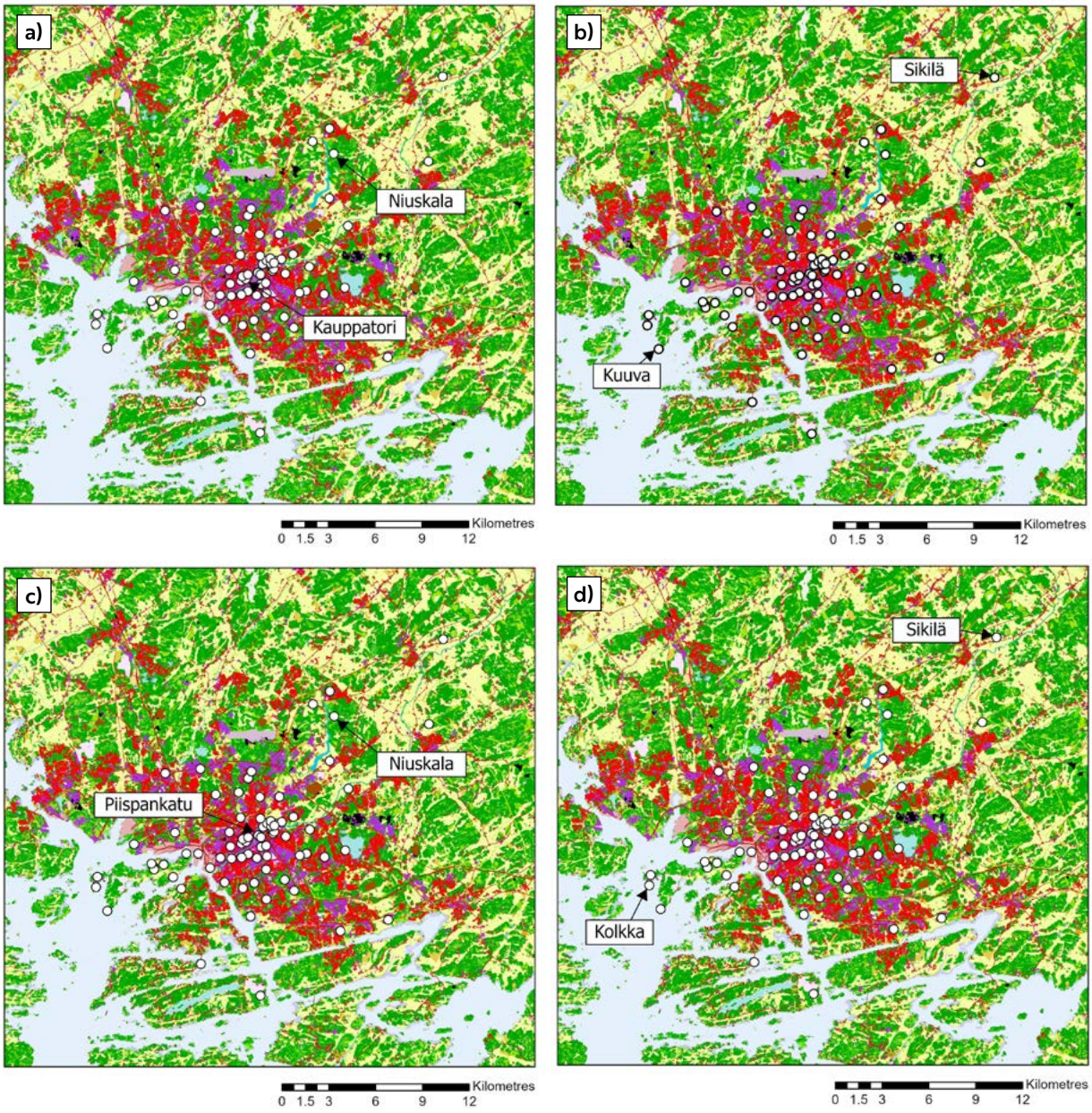

Figure 38. The locations of the logger sites of the highest and lowest a) monthly average temperatures (Kauppatori 18.7 °C, Niuskala 16.2 °C), b) monthly averages of daily minimum temperatures (Kuuva 15.5 °C, Sikilä 11.3 °C), c) monthly averages of daily maximum temperatures (Piispankatu 22.3 °C, Niuskala 20.6 °C) and d) momentary maximum temperature range on August 18th at 05.00 with the difference of 8.6 °C (Kolkka 16.0 °C, Sikilä 7.4 °C). Background map: CORINE Land Cover 2018. For information on CORINE level 4 classes and respective colours, used in this Figure and subsequent CORINE based Figures, see Suomi et al. 2024, Appendix A.

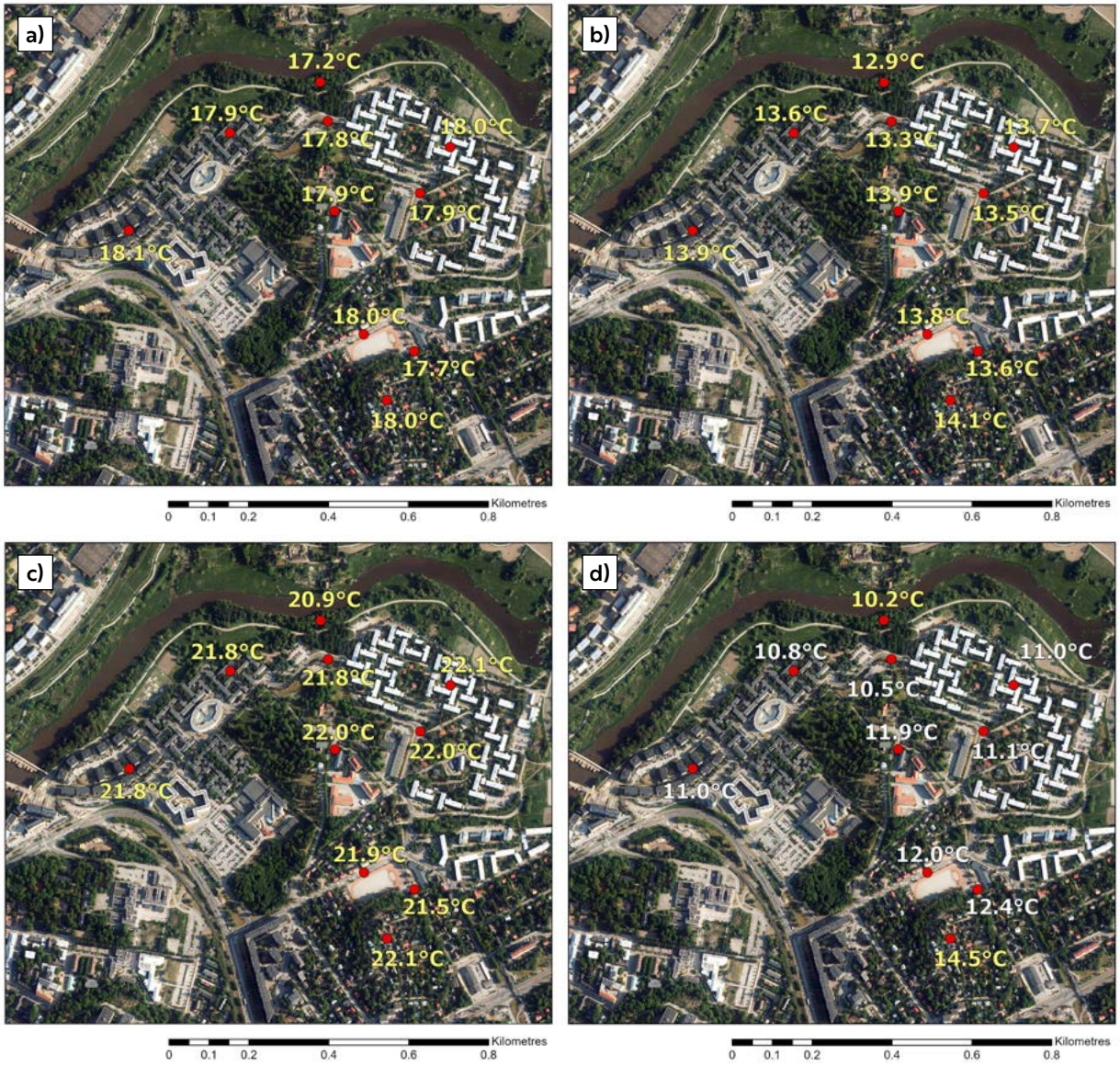

Figure 39. The Student Village logger sites with a) monthly average temperatures, b) monthly averages of daily minimum temperatures, c) monthly averages of daily maximum temperatures and d) the momentary maximum temperature range on August 18th at 06.00 in 2024 with the difference of 4.3 °C between Kuuvuori and Aurajokiranta. For individual logger site names, see Figure 4.

tures model with bigger roads appearing also warmer. The Parainen quarry distorted the temperature ranges in the minimum temperatures model and the momentary maximum difference model. The lowest temperatures outside of the quarry were 11.48 °C (minimum temperatures) and 6.69 °C (momentary maximum range).

Regarding the maximum momentary temperature range for the whole Turku region on

Table 31. The regression models for the monthly average temperatures in August 2024.

CORINE-based regression model		
R Square	0.618	
Adjusted R Square	0.600	
Variable	**Standardized Coefficients Beta**	**Significance**
Constant		<0.001
vl_3_5_400m	0.764	<0.001
tkuwaters_500m	0.489	<0.001
relelev_300m	0.197	0.014

YKR-based regression model		
R Square	0.613	
Adjusted R Square	0.595	
Variable	**Standardized Coefficients Beta**	**Significance**
Constant		<0.001
rakvae_5x5	0.758	<0.001
tkuwaters_500m	0.441	<0.001
relelev_300m	0.126	0.124

Table 32. The regression models for the monthly averages of daily minimum temperatures in August 2024.

CORINE-based regression model		
R Square	0.657	
Adjusted R Square	0.640	
Variable	**Standardized Coefficients Beta**	**Significance**
Constant		<0.001
vl_3_5_100m	0.657	<0.001
tkuwaters_2km	0.628	<0.001
relelev_500m	0.270	<0.001

YKR-based regression model		
R Square	0.677	
Adjusted R Square	0.662	
Variable	**Standardized Coefficients Beta**	**Significance**
Constant		<0.001
rakvae_3x3	0.675	<0.001
tkuwaters_2km	0.625	<0.001
relelev_500m	0.242	0.001

Table 33. The regression models for the monthly averages of daily maximum temperatures in August 2024.

CORINE-based regression model		
R Square	0.242	
Adjusted R Square	0.206	
Variable	**Standardized Coefficients Beta**	**Significance**
Constant		<0.001
vl_3_5_300m	0.042	0.708
tkuwaters_2kmsqrt	-0.477	<0.001
relelev_300m	0.086	0.438

YKR-based regression model		
R Square	0.334	
Adjusted R Square	0.303	
Variable	**Standardized Coefficients Beta**	**Significance**
Constant		<0.001
rakvae_3x3	0.335	0.004
tkuwaters_2kmsqrt	-0.364	0.001
relelev_300m	0.016	0.881

Table 34. The regression models for the momentary maximum temperature range in August 2024.

CORINE-based regression model		
R Square	0.656	
Adjusted R Square	0.640	
Variable	**Standardized Coefficients Beta**	**Significance**
Constant		<0.001
vl_3_5_100m	0.561	<0.001
tkuwaters_2km	0.633	<0.001
relelev_500m	0.357	<0.001

YKR-based regression model		
R Square	0.749	
Adjusted R Square	0.737	
Variable	**Standardized Coefficients Beta**	**Significance**
Constant		<0.001
rakvae_5x5	0.671	<0.001
tkuwaters_2km	0.693	<0.001
relelev_500m	0.296	<0.001

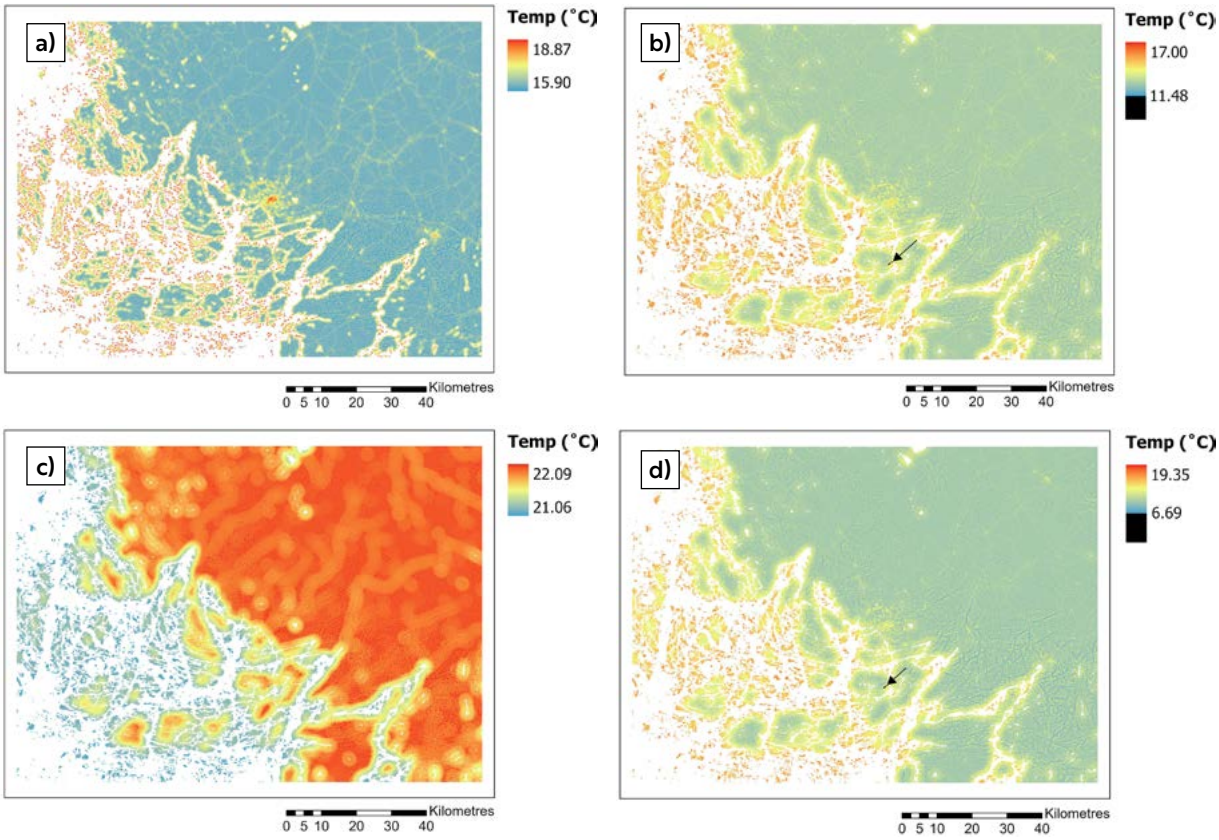

Figure 40. High-resolution (100 m) temperatures based on linear regression model depicting August 2024 a) monthly average temperatures, b) monthly averages of daily minimum temperatures, c) monthly averages of daily maximum temperatures and d) temperatures of momentary maximum temperature range on August 18th, 2024, at 05.00. The abnormally low temperature area in the limestone quarry located in Parainen is marked in black (arrow).

the 18th, during this time Turku was located on the south-eastern edge of a low-pressure ridge (Figure 41). The centre of the low-pressure ridge was over the Norwegian Sea east of the Icelandic coast. The surface pressure height in Turku during this period was 564–568 decametres. The map is timed at 00.00 UTC. Regarding the momentary maximum difference of the Student Village which occurred on the same day but later on as the whole Turku region, the situations were similar due to the minimal time difference (Figure 42). The surface pressure height stayed the same over Turku and the low-pressure centre east of the Icelandic coast remained. The map was timed at 06.00 UTC. During August 18th at 05.00 the average wind speed measured 1.9 m/s and average cloudiness 0 oktas. An hour later at 06.00 during the momentary maximum temperature range of the Student Village the average wind speed was 1.225 m/s and average cloudiness was 0 oktas.

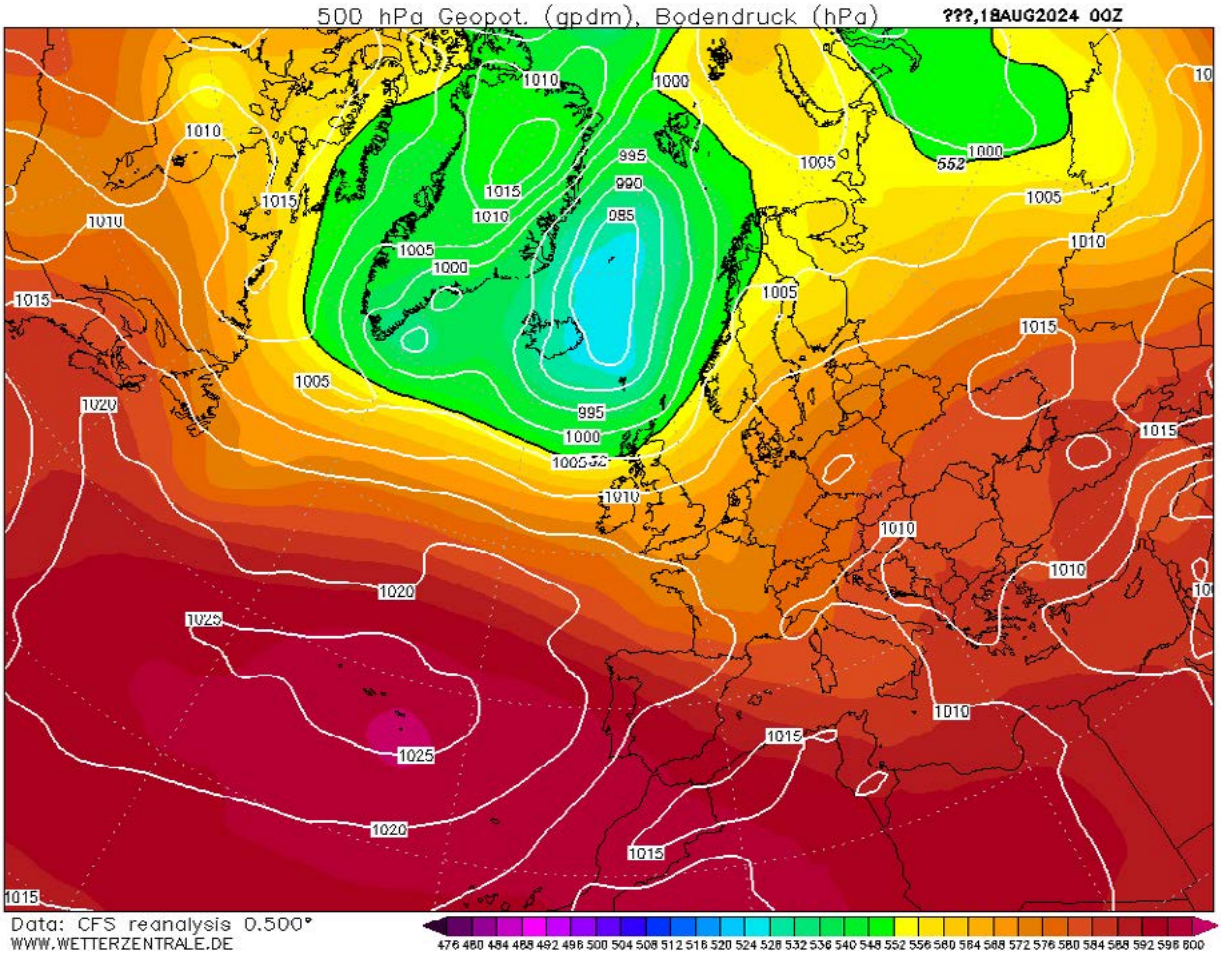

Figure 41. Sea level air pressure (white contours) and height of 500 hectopascal pressure level in decametres (colour ramp) for August 18th at 00.00 UTC. Retrieved from Wetterzentrale (https://www.wetter-zentrale.de/en/reanalysis.php?model=cfsr).

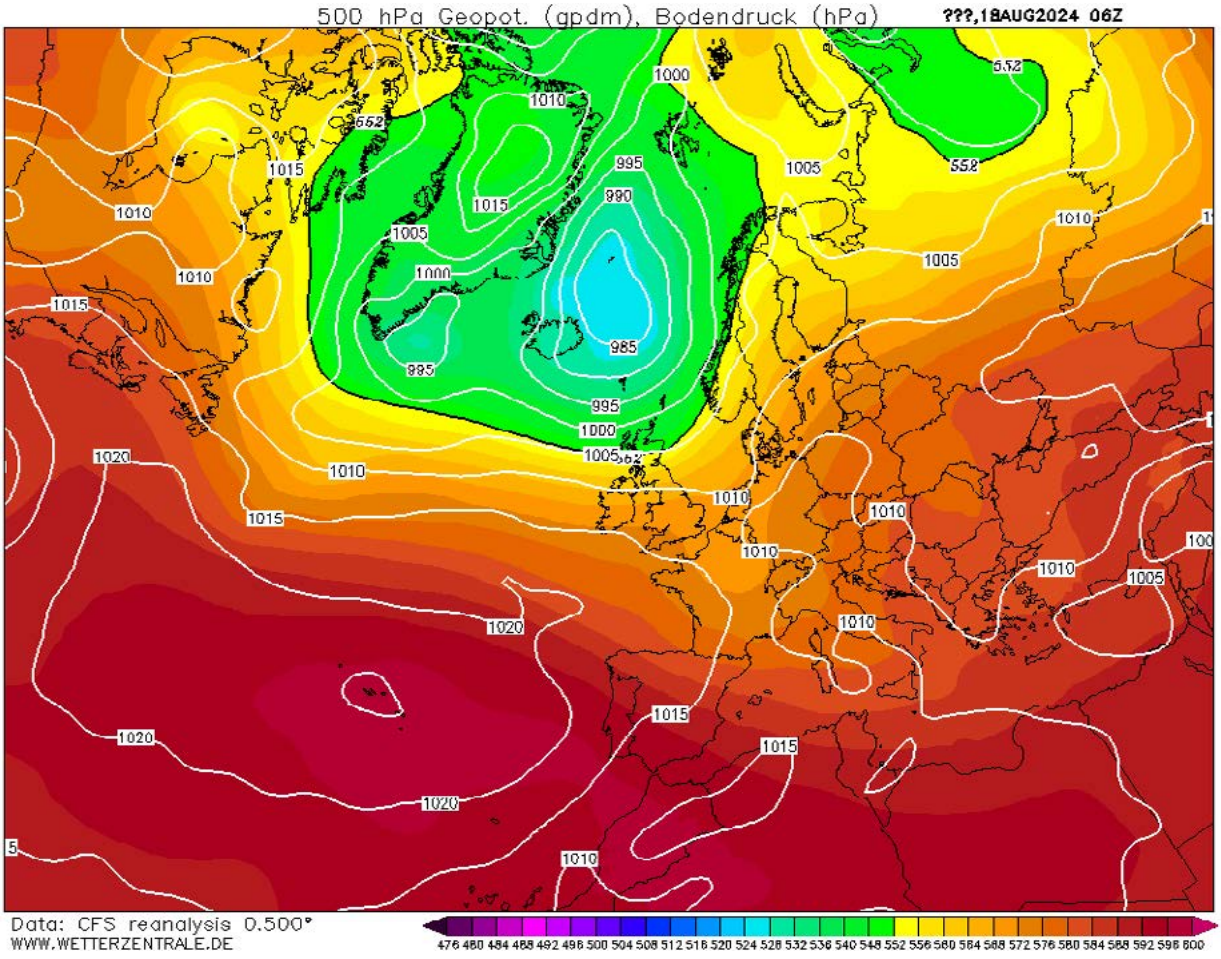

Figure 42. Sea level air pressure (white contours) and height of 500 hectopascal pressure level in decametres (colour ramp) for August 18th at 06.00 UTC. Retrieved from Wetterzentrale (**https://www.wetter-zentrale.de/en/reanalysis.php?model=cfsr**).

4.1.9 September

In September 2024, the average temperature at the Turku airport was 13.5 °C which was 2.2 °C warmer than the average temperature recorded for September in the 1991–2020 climate reference period (Jokinen et al., 2021).

The highest and lowest average temperatures in September were 15.2 °C measured in Kauppatori and 12.8 °C measured in Niuskala (Figure 43). In the case of averages of daily minimum temperatures, the coldest site was Ylijoki (8.0 °C) and the warmest site was Kuuva (12.1 °C). For the averages of maximum temperatures, the warmest average temperature of 18.9 °C was measured in Kauppatori and the coldest average temperature of 17.2 °C in Hiiriluoto, manner. The maximum momentary temperature range was measured between Lieto and Kolkka on the 30th at 08.00. The difference during this time was 10.8 °C.

For the Student Village observation sites Kuuvuori was the warmest in September regarding the monthly average temperatures recording a value of 14.5 °C (Figure 44). The coldest site was Aurajokiranta with a value of 13.5 °C. In the monthly averages for daily minimum temperatures the highest and lowest temperature sites remained the same. Aurajokiranta measured 9.1 °C and Kuuvuori 10.4 °C, respectively. For the monthly averages of daily maximum temperatures Aurajokiranta reached the lowest value at 17.4 °C and the highest value of 18.6 °C occurred in Kuuvuori, Suntiontie and Yo-kylä sites, respectively. The momentary maximum temperature range reached a value of 5.5 °C on September 30th at 09.30. Exceptionally Yo-kylä länsi was the coldest site instead of Aurajokiranta while the warmest was Kuuvuori.

The linear regression models for monthly average temperatures had explanatory powers of 0.651 and 0.619 in September (Table 35). All variables had a warming effect in the CORINE-based regression model with land cover having the strongest effect. Elevation however was not statistically significant in the YKR-based regression model, but here the building floor area and population variable was the strongest. The explanatory powers for the monthly averages of daily minimum temperatures are 0.636 and 0.698 (Table 36). All explanatory variables were statistically significant in both models. In the CORINE-based regression model water bodies had the strongest effect while in the YKR-based regression model the building floor area and population variable had the strongest effect. All variables had a warming effect with elevation being the weakest. In the case of the maximum temperatures none of the explanatory variables were statistically significant in either model (Table 37). The explanatory powers here are 0.067 and 0.196. All variables, however, were statistically significant in the momentary maximum temperature range regression models (Table 38). In both cases water bodies had clearly the strongest effect. The weakest effect in the CORINE-based regression model was with the land cover variable while in the YKR-based regression model it was with elevation. The explanatory powers for these models are 0.647 and 0.701.

The temperature models in September look rather similar to the models in August (Figure 45). Similarly to the summer months the coast and the islands are the warmest compared to the mainland which is the coolest except for the averages of daily maximum temperatures model where the mainland is the warmest and the coast the coolest. The UHI is distinc-

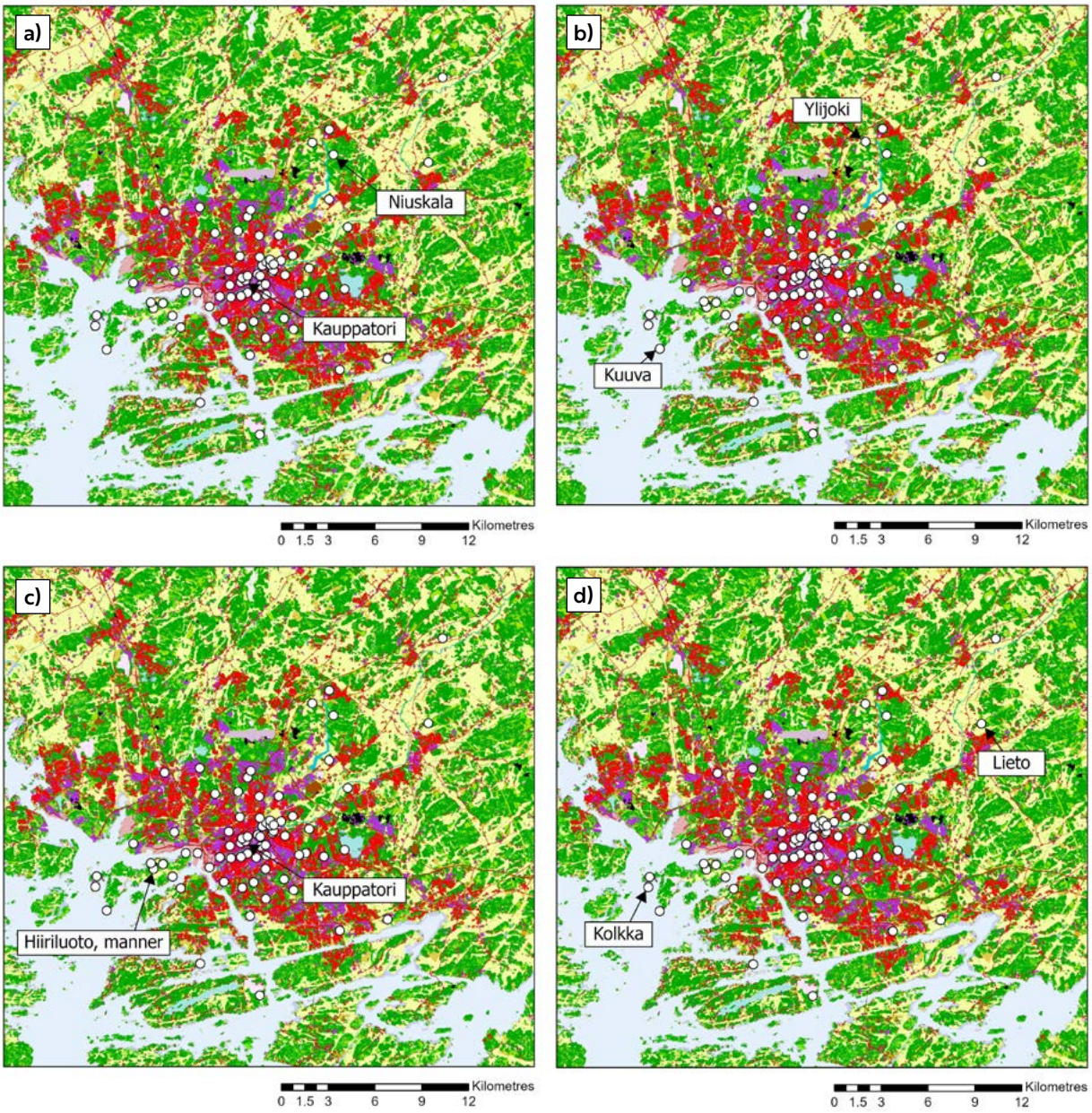

Figure 43. The locations of the logger sites of the highest and lowest a) monthly average temperatures (Kauppatori 15.2 °C, Niuskala 12.8 °C), b) monthly averages of daily minimum temperatures (Kuuva 12.1 °C, Ylijoki 8.0 °C), c) monthly averages of daily maximum temperatures (Kauppatori 18.9 °C, Hiiriluoto, manner 17.2 °C) and d) momentary maximum temperature range on September 30th at 08.00 with the difference of 10.8 °C (Kolkka 9.5 °C, Lieto –1.3 °C). Background map: CORINE Land Cover 2018. For information on CORINE level 4 classes and respective colours, used in this Figure and subsequent CORINE based Figures, see Suomi et al. 2024, Appendix A.

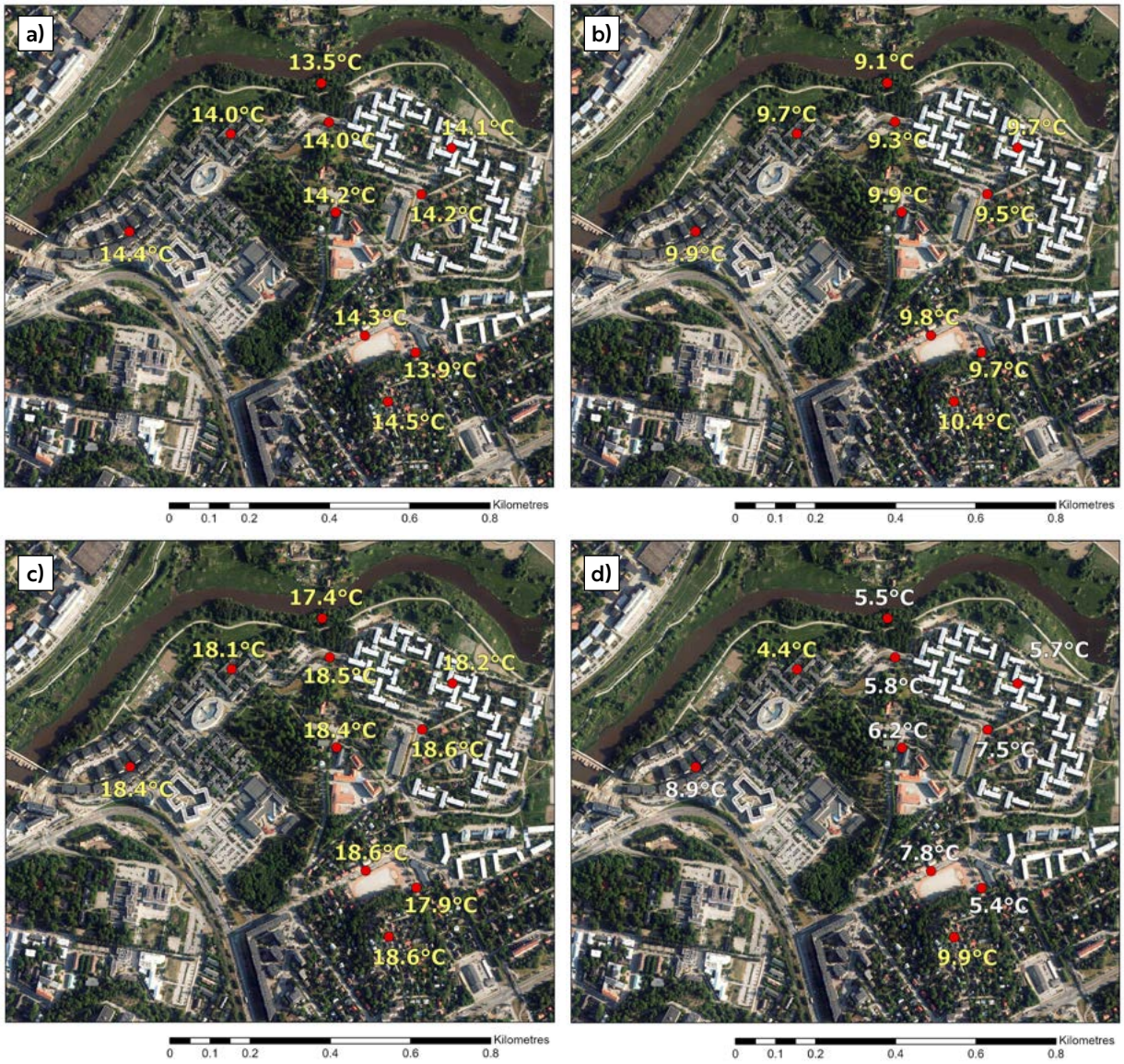

Figure 44. The Student Village logger sites with a) monthly average temperatures, b) monthly averages of daily minimum temperatures, c) monthly averages of daily maximum temperatures and d) the momentary maximum temperature range on September 30th at 09.30 in 2024 with the difference of 5.5 °C between Kuuvuori and Yo-kylä länsi. For individual logger site names, see Figure 4.

tive in the average temperatures model with the Turku city centre appearing warmer than surrounding areas. In the models where the coast is the warmest the coldest areas on the mainland are low-lying sites. Both in the averages of daily minimum temperatures model and the momentary maximum temperature range model the Parainen limestone quarry influenced the temperature ranges (marked in black).

In September there was a high-pressure centre over Turku and the most south-

Table 35. The regression models for the monthly average temperatures in September 2024.

CORINE-based regression model		
R Square	0.666	
Adjusted R Square	0.651	
Variable	**Standardized Coefficients Beta**	**Significance**
Constant		<0.001
v1_3_5_400m	0.725	<0.001
tkuwaters_500m	0.545	<0.001
relelev_300m	0.296	<0.001

YKR-based regression model		
R Square	0.636	
Adjusted R Square	0.619	
Variable	**Standardized Coefficients Beta**	**Significance**
Constant		<0.001
rakvae_3x3	0.687	<0.001
tkuwaters_500m	0.479	<0.001
relelev_300m	0.258	0.001

Table 36. The regression models for the monthly averages of daily minimum temperatures in September 2024.

CORINE-based regression model		
R Square	0.652	
Adjusted R Square	0.636	
Variable	**Standardized Coefficients Beta**	**Significance**
Constant		<0.001
v1_3_5_100m	0.594	<0.001
tkuwaters_2km	0.622	<0.001
relelev_500m	0.335	<0.001

YKR-based regression model		
R Square	0.712	
Adjusted R Square	0.698	
Variable	**Standardized Coefficients Beta**	**Significance**
Constant		<0.001
rakvae_3x3	0.652	<0.001
tkuwaters_2km	0.634	<0.001
relelev_500m	0.301	<0.001

Table 37. The regression models for the monthly averages of daily maximum temperatures in September 2024.

CORINE-based regression model		
R Square	0.109	
Adjusted R Square	0.067	
Variable	**Standardized Coefficients Beta**	**Significance**
Constant		<0.001
v1_3_5_300m	0.073	0.543
tkuwaters_2kmsqrt	-0.306	0.013
relelev_100m	0.047	0.692

YKR-based regression model		
R Square	0.232	
Adjusted R Square	0.196	
Variable	**Standardized Coefficients Beta**	**Significance**
Constant		<0.001
rakvae_3x3	0.391	0.002
tkuwaters_2kmsqrt	-0.184	0.122
relelev_100m	-0.033	0.770

Table 38. The regression models for the momentary maximum temperature range in September 2024.

CORINE-based regression model		
R Square	0.662	
Adjusted R Square	0.647	
Variable	**Standardized Coefficients Beta**	**Significance**
Constant		0.088
v1_3_5_100m	0.306	<0.001
tkuwaters_2km	0.729	<0.001
relelev_300m	0.388	<0.001

YKR-based regression model		
R Square	0.714	
Adjusted R Square	0.701	
Variable	**Standardized Coefficients Beta**	**Significance**
Constant		0.081
rakvae_3x3	0.396	<0.001
tkuwaters_2km	0.757	<0.001
relelev_300m	0.357	<0.001

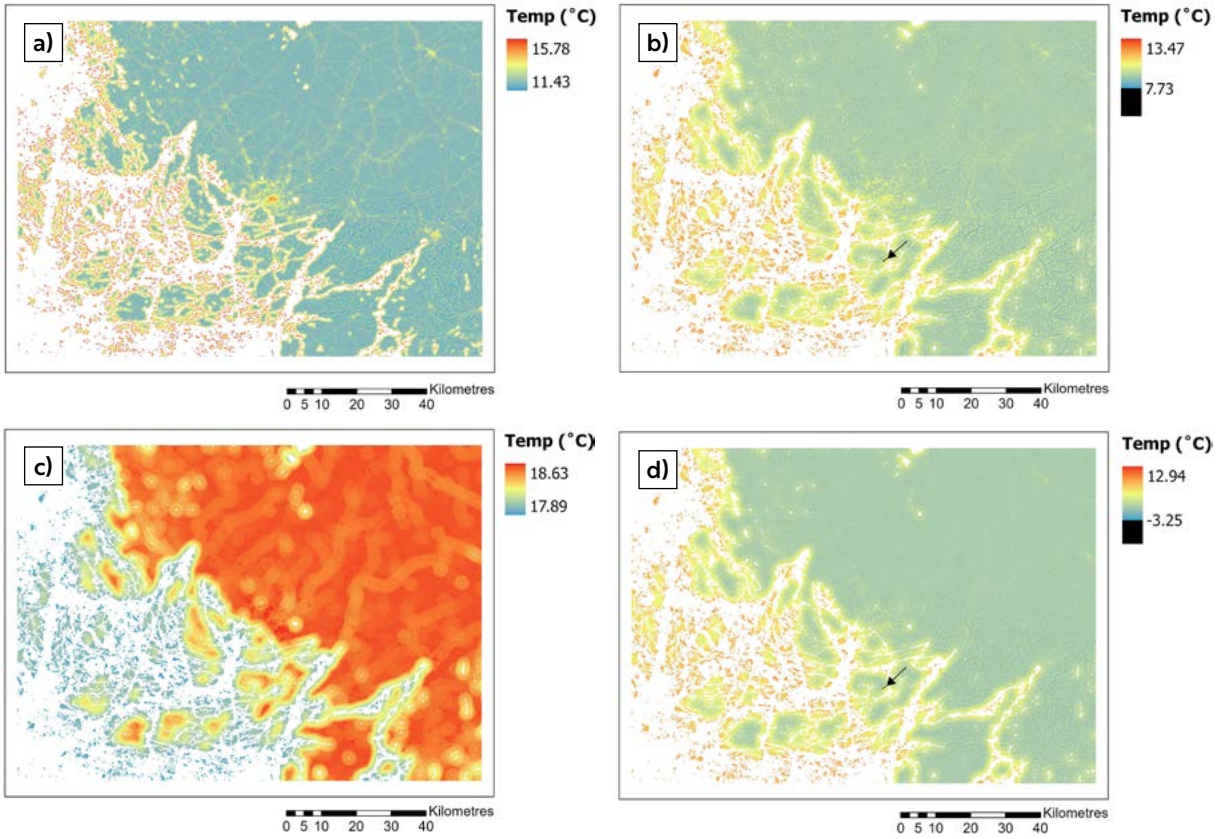

Figure 45. High-resolution (100 m) temperatures based on linear regression model depicting September 2024 a) monthly average temperatures, b) monthly averages of daily minimum temperatures, c) monthly averages of daily maximum temperatures and d) temperatures of momentary maximum temperature range on September 30th, 2024, at 08.00. The abnormally low temperature area in the limestone quarry located in Parainen is marked in black (arrow).

ern parts of Finland during the momentary maximum temperature ranges of the whole Turku region and the Student Village on the 30th (Figure 46). The 500 hPa surface pressure height in Turku was 556–560 decametres and the map was timed at 06.00 UTC. Three low-pressure centres surround northern Europe with the centres located over Novaya Zemlya, east of Iceland on the Norwegian Sea and over the British Isles. An extensive high-pressure zone appears over southern Russia and Kazakhstan. On September 30th at 08.00 the average wind speed was 0.275 m/s and average cloudiness was 0 oktas. One and a half hours later at 09.30, i.e. at the time of maximum range for the Student Village, the average wind speed was 0.75 m/s and average cloudiness 0 oktas.

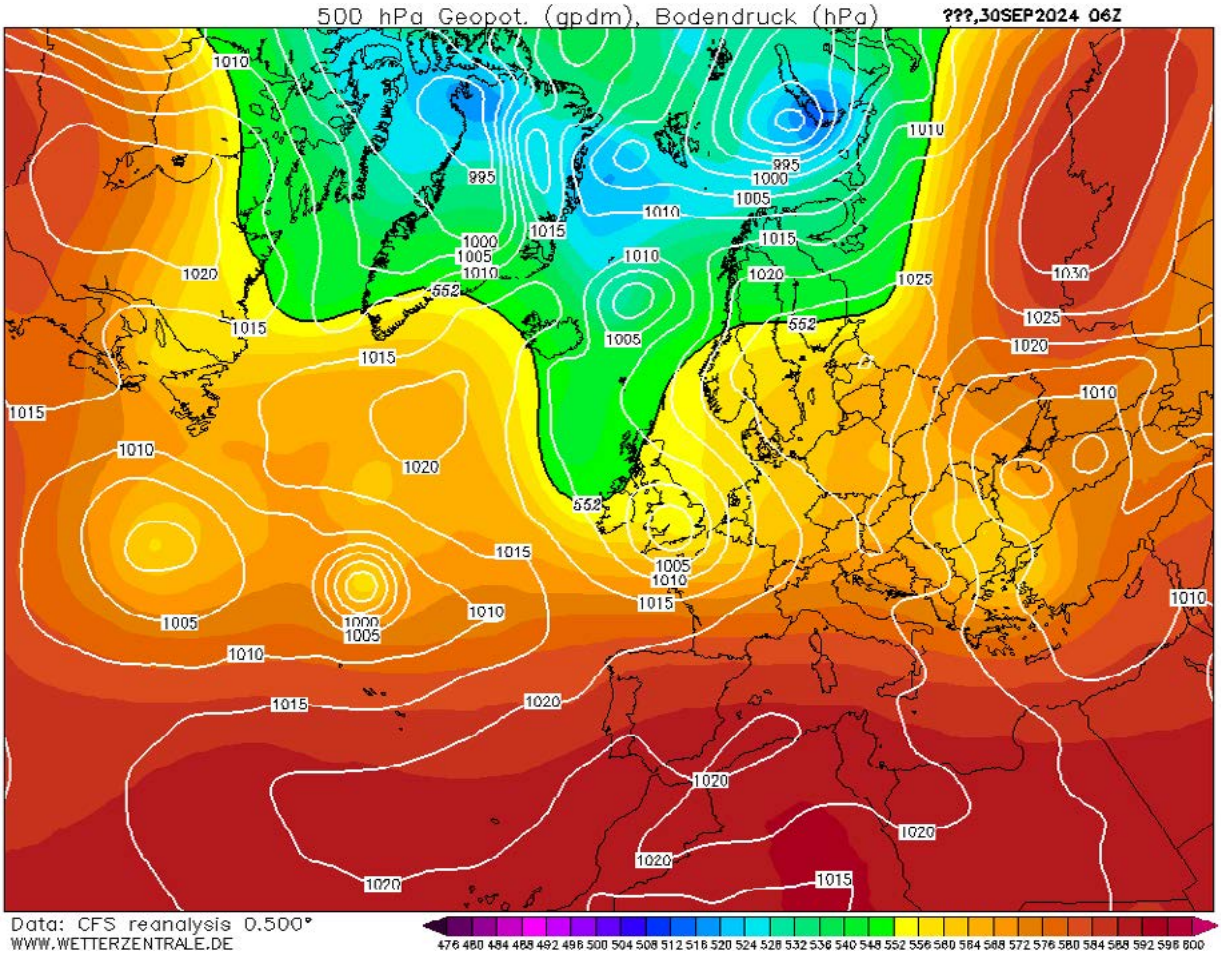

Figure 46. Sea level air pressure (white contours) and height of 500 hectopascal pressure level in decametres (colour ramp) for September 18th at 06.00 UTC. Retrieved from Wetterzentrale (https://www.wetter-zentrale.de/en/reanalysis.php?model=cfsr).

4.1.10 October

The average temperature in October 2024 was 8.0 °C at the Turku airport. In the climate reference period of 1991–2020 the average temperature for October was 5.5 °C meaning that there was a 2.5 °C difference between these two values (Jokinen et al., 2021).

For the monthly average temperatures in October, the highest average was reached in Kuuva (9.7 °C) and the lowest in Niuskala (7.3 °C) (Figure 47). Regarding the averages of daily minimum temperatures, the coldest site was Niuskala with the average being 3.4 °C while the warmest site was Kolkka with 7.5 °C. In the case of the averages of daily maximums the warmest site was Kauppatori in the city centre with an average of 12.3 °C while the coldest site was Ylijoki with an average of 11.2 °C. For the maximum momentary temperature range the difference of 11.0 °C was measured between Kuuva and Ylijoki on October 16th at 08.30.

The warmest average temperature in the Student Village in October occurred in two sites: Kuuvuori and Pispalantie with the value of 8.7 °C, respectively (Figure 48). The coldest average temperature was 8.1 °C in Aurajokiranta. The monthly averages of daily minimum temperatures reached its lowest value in Aurajokiranta with an average of 4.7 °C and its highest value in Kuuvuori with an average of 6.2 °C, respectively. For the equivalent maximum temperatures, the highest value of 11.9 °C occurred in Suntiontie while the lowest value of 11.5 °C occurred in Aurajokiranta and Kuuvuori kenttä, respectively. The temperature difference during the momentary maximum temperature range on the 16th of October at 08.30 was exceptionally high. The difference of 7.2 °C occurred between Aurajokiranta and Kuuvuori. Elevation differences typically could explain the temperature difference with colder air flowing towards the low-lying river bank where the Aurajokiranta site is located.

The explanatory powers for the regression models formed for the monthly average temperatures are 0.664 in the case of the CORINE-based regression model and 0.658 for the YKR-based regression model (Table 39). Out of the explanatory variables land cover, building floor area and population and water bodies were statistically significant. All had a warming effect with the water body variable being the strongest. In the case of minimum temperatures all variables were statistically significant (Table 40). All had a warming effect with the strongest being with water bodies and weakest with elevation. Here the explanatory powers are 0.670 and 0.734. For the maximum temperatures the explanatory powers in the regression models are 0.314 and 0.292 (Table 41). All except elevation were statistically significant and had a warming effect. Out of these the water body variable had the weaker effect. Similarly, elevation was not statistically significant in the momentary maximum temperature range regression models (Table 42). The explanatory powers are 0.564 and 0.550 with the statistically significant variables having a warming effect. Water bodies clearly had the strongest effect in both cases.

In October 2024 the coastal areas and the archipelago was the warmest area in all of the temperature model cases (Figure 49). Colder areas appeared on the mainland with low-lying sites highlighted especially in all models except average temperatures. The quarry in Parainen affected the temperature ranges in the monthly averag-

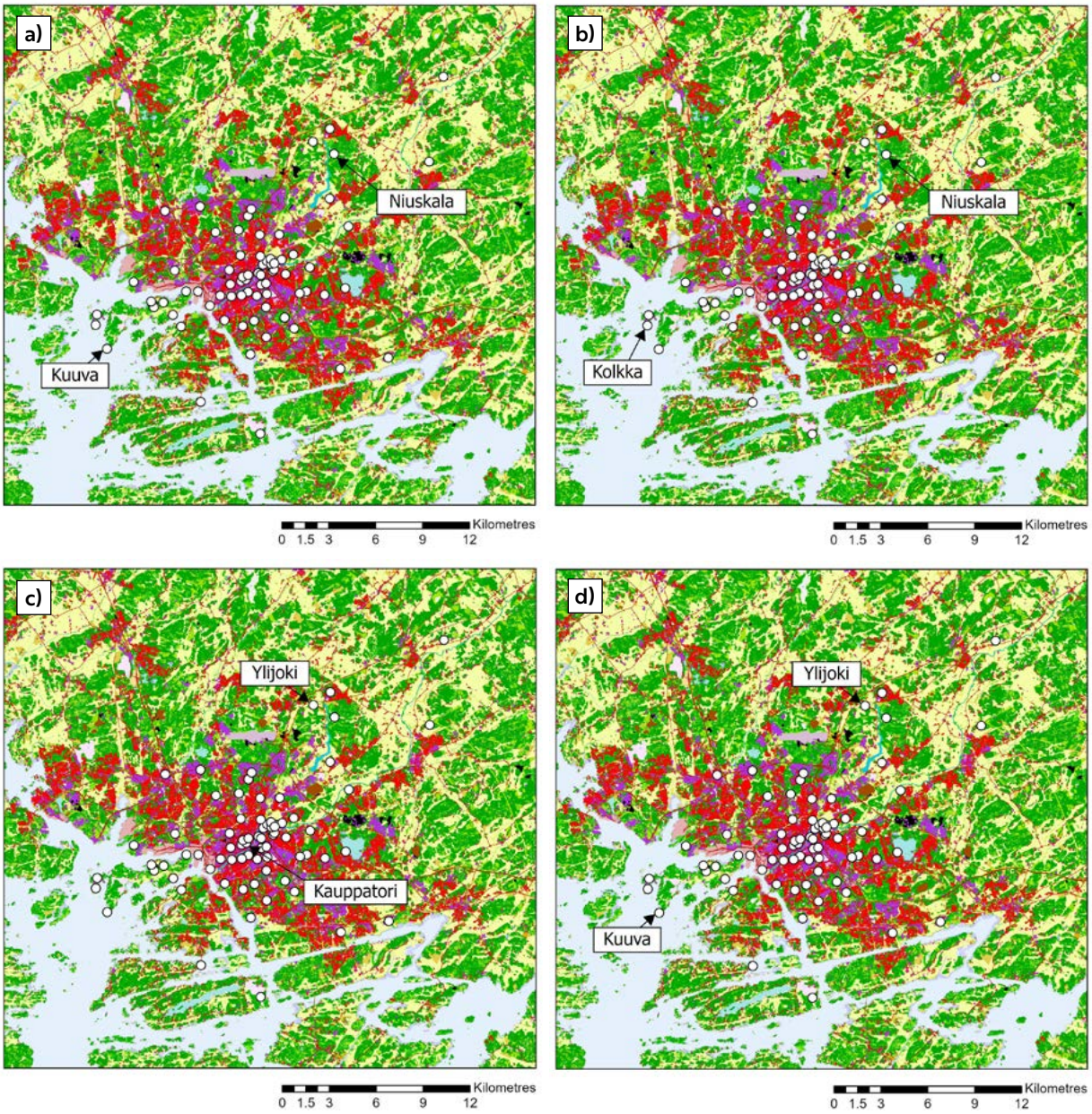

Figure 47. The locations of the logger sites of the highest and lowest a) monthly average temperatures (Kuuva 9.7 °C, Niuskala 7.3 °C), b) monthly averages of daily minimum temperatures (Kolkka 7.5 °C, Niuskala 3.4 °C), c) monthly averages of daily maximum temperatures (Kauppatori 12.3 °C, Ylijoki 11.2 °C) and d) momentary maximum temperature range on October 16th at 08.30 with the difference of 11.0 °C (Kuuva 9.0 °C, Ylijoki –2.0 °C). Background map: CORINE Land Cover 2018. For information on CORINE level 4 classes and respective colours, used in this Figure and subsequent CORINE based Figures, see Suomi et al. 2024, Appendix A.

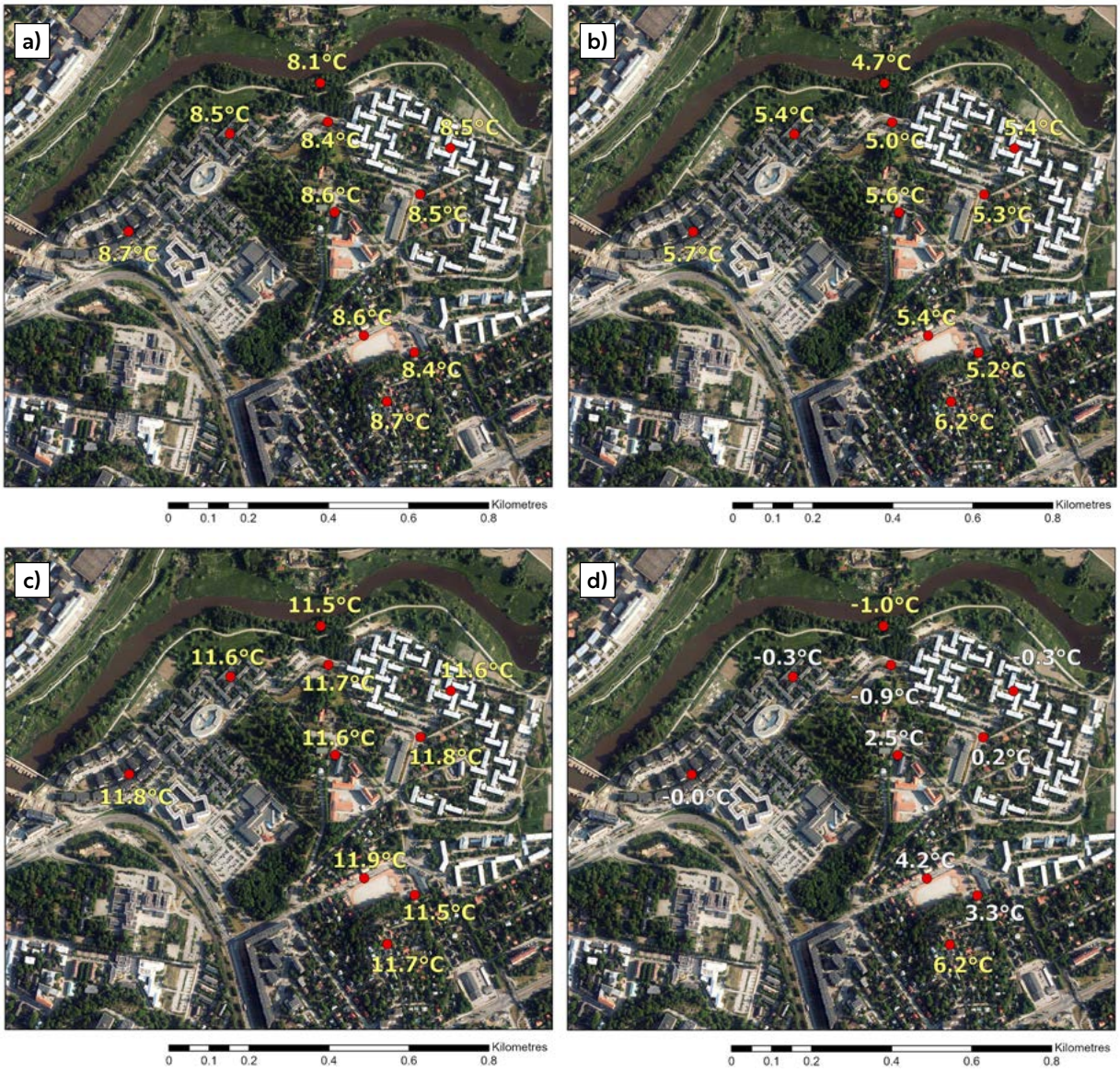

Figure 48. The Student Village logger sites with a) monthly average temperatures, b) monthly averages of daily minimum temperatures, c) monthly averages of daily maximum temperatures and d) the momentary maximum temperature range on October 16th at 08.30 in 2024 with the difference of 7.2 °C between Kuuvuori and Aurajokiranta. For individual logger site names, see Figure 4.

es of daily minimum temperatures model and the momentary maximum temperature range model. The UHI effect stands out clearly in the average temperatures map and the averages of daily maximum temperatures map.

During the momentary maximum temperature ranges of the whole Turku area and the Student Village on the 16th of October there was a high-pressure ridge over the Turku area and southern Finland (Figure 50). The 500 hPa surface pressure height over Tur-

Table 39. The regression models for the monthly average temperatures in October 2024.

CORINE-based regression model		
R Square	0.679	
Adjusted R Square	0.664	
Variable	**Standardized Coefficients Beta**	**Significance**
Constant		<0.001
vl_3_5_400m	0.643	<0.001
tkuwaters_2kmsqrt	0.796	<0.001
relelev_300m	0.172	0.020

YKR-based regression model		
R Square	0.673	
Adjusted R Square	0.658	
Variable	**Standardized Coefficients Beta**	**Significance**
Constant		<0.001
rakvae_3x3	0.626	<0.001
tkuwaters_2kmsqrt	0.747	<0.001
relelev_300m	0.136	0.069

Table 40. The regression models for the monthly averages of daily minimum temperatures in October 2024.

CORINE-based regression model		
R Square	0.685	
Adjusted R Square	0.670	
Variable	**Standardized Coefficients Beta**	**Significance**
Constant		<0.001
vl_3_5_100m	0.561	<0.001
tkuwaters_2km	0.712	<0.001
relelev_500m	0.303	<0.001

YKR-based regression model		
R Square	0.746	
Adjusted R Square	0.734	
Variable	**Standardized Coefficients Beta**	**Significance**
Constant		<0.001
rakvae_3x3	0.623	<0.001
tkuwaters_2km	0.727	<0.001
relelev_500m	0.270	<0.001

Table 41. The regression models for the monthly averages of daily maximum temperatures in October 2024.

CORINE-based regression model		
R Square	0.345	
Adjusted R Square	0.314	
Variable	**Standardized Coefficients Beta**	**Significance**
Constant		<0.001
vl_3_5_400m	0.588	<0.001
tkuwaters_700m	0.478	<0.001
relelev_500m	-0.157	0.128

YKR-based regression model		
R Square	0.324	
Adjusted R Square	0.292	
Variable	**Standardized Coefficients Beta**	**Significance**
Constant		<0.001
rakvae_3x3	0.551	<0.001
tkuwaters_700m	0.416	<0.001
relelev_500m	-0.195	0.067

Table 42. The regression models for the momentary maximum temperature range in October 2024.

CORINE-based regression model		
R Square	0.584	
Adjusted R Square	0.564	
Variable	**Standardized Coefficients Beta**	**Significance**
Constant		0.521
vl_3_5_100m	0.378	<0.001
tkuwaters_2kmsqrt	0.737	<0.001
relelev_500m	0.242	0.004

YKR-based regression model		
R Square	0.570	
Adjusted R Square	0.550	
Variable	**Standardized Coefficients Beta**	**Significance**
Constant		0.591
rakvae_1x1	0.350	<0.001
tkuwaters_2kmsqrt	0.700	<0.001
relelev_500m	0.224	0.010

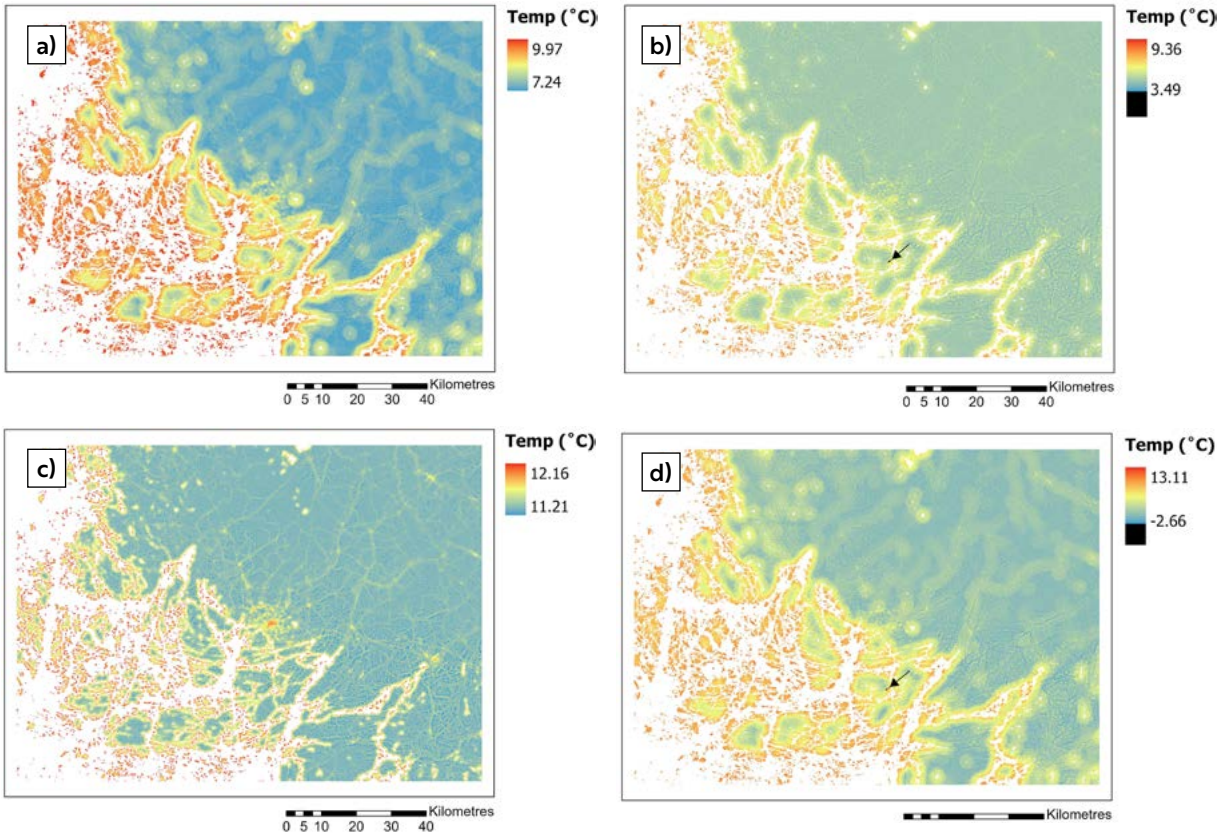

Figure 49. High-resolution (100 m) temperatures based on linear regression model depicting October 2024 a) monthly average temperatures, b) monthly averages of daily minimum temperatures, c) monthly averages of daily maximum temperatures and d) temperatures of momentary maximum temperature range on October 16th, 2024, at 08.30. The abnormally low temperature area in the limestone quarry located in Parainen is marked in black (arrow).

ku was 560–564 decametres with the centre of the high-pressure zone located over Poland and Belarus. Low-pressure ridges appeared around Svalbard, Greenland and over Iceland extending south over the North Atlantic. The map is timed at 06.00 UTC. During the maximum momentary temperature range on October 16th at 08.30 the average wind speed was 2.575 m/s and average cloudiness was 0.25 oktas.

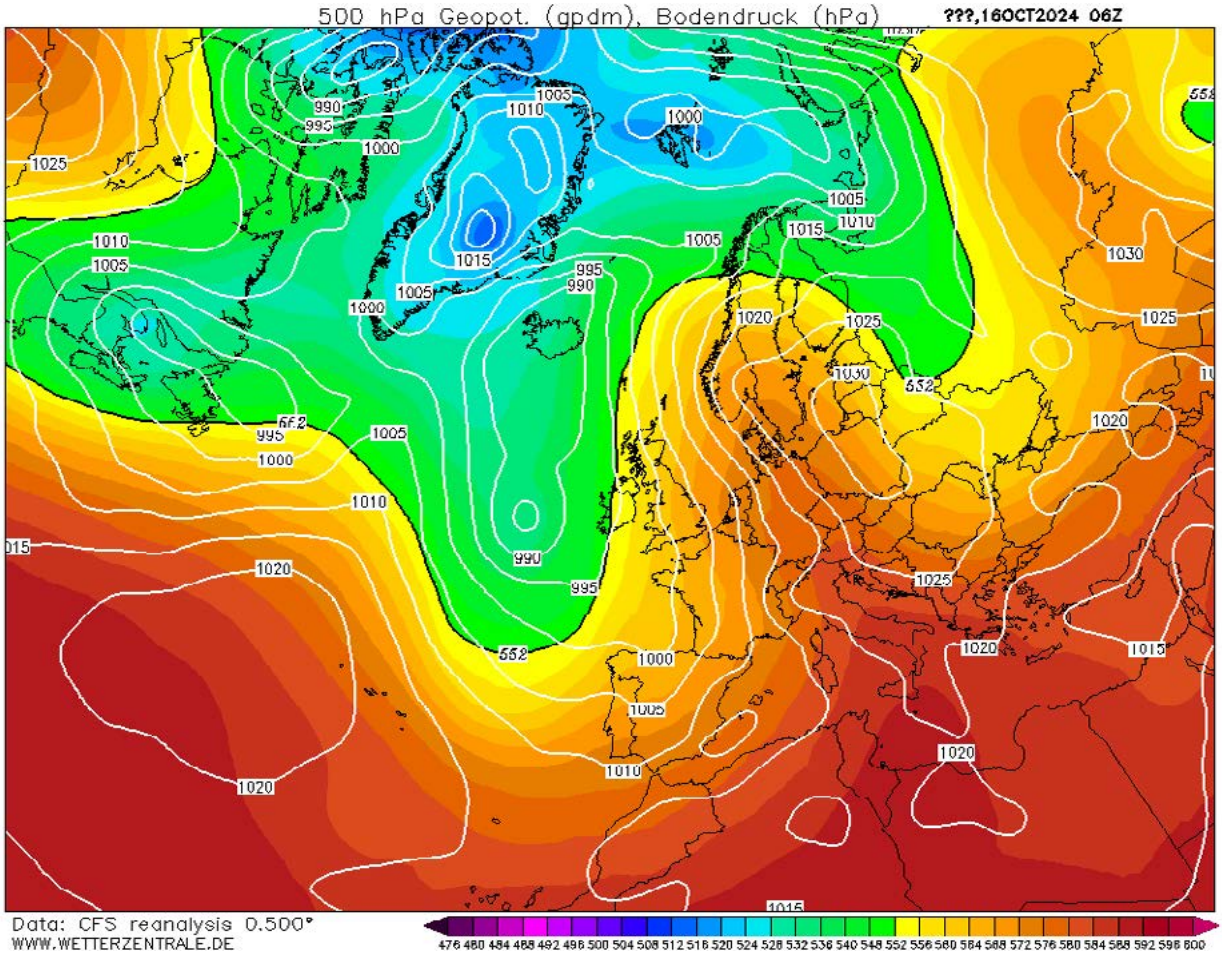

Figure 50. Sea level air pressure (white contours) and height of 500 hectopascal pressure level in decametres (colour ramp) for October 16th at 06.00 UTC. Retrieved from Wetterzentrale (https://www.wetter-zentrale.de/en/reanalysis.php?model=cfsr).

4.1.11 November

The average temperature in November 2024 recorded 3.2 °C at the Turku airport observation site which was 1.7 °C warmer than during the climate reference period in 1991–2020 (Jokinen et al., 2021).

In November the average temperature highest and lowest values were recorded in Kolkka (4.6 °C) and Niuskala (2.7 °C) (Figure 51). These same sites recorded the highest and lowest averages of daily minimum temperatures as well. Kolkka measured 2.9 °C while Niuskala 0.1 °C. In the case of the maximums the coldest site Niuskala recorded 4.8 °C and the warmest site Kauppatori measured 6.3 °C. Regarding the momentary maximum temperature difference the difference of 12.3 °C was measured between the Kuuva and Sikilä logger sites. This difference occurred on November 24th at 11.00.

In November the highest average temperature in the Student Village was 4.0 °C at Pispalantie while the lowest was 3.6 °C at Aurajokiranta, respectively (Figure 52). For the monthly averages of daily minimum temperatures, the lowest value of 1.4 °C was reached in Aurajokiranta while the highest of 2.0 °C in Kuuvuori, respectively. In the case of the monthly averages of daily maximum temperatures the lowest average of 5.5 °C occurred again at Aurajokiranta while the highest average of 5.8 °C appeared in Suntiontie, respectively. The momentary maximum temperature range value remained high with the difference being 7.9 °C between Aurajokiranta and Kuuvuori. This occurred on November 24th at 11.30. Here the elevation difference between these sites is a possible reason for the momentary temperature difference.

In November 2024 the regression models for the monthly average temperatures have explanatory powers of 0.582 and 0.667 (Table 43). All explanatory variables except elevation were statistically significant. Land cover, building floor area and population and water bodies all had a warming effect but the water body variable was the strongest. For the minimums the explanatory powers are 0.644 and 0.750 (Table 44). Again, all but elevation had a warming effect. Water bodies had the strongest effect in the CORINE-based regression model but in the YKR-based regression model the building floor area and population variable was the strongest. In the case of maximum temperatures elevation was not statistically significant (Table 45). Explanatory powers for both models are 0.462 and 0.503. All variables had a warming effect with the water body variable being the strongest. All variables however, had a warming effect in the case of the momentary maximum temperature range (Table 46). The explanatory powers are 0.631 and 0.590 in these models with water bodies clearly having the strongest warming effect and elevation the weakest.

Similarly to October all coastal areas were warmer than the mainland in November's temperature models (Figure 53). Major roads are distinguishable as warmer parts in all except the maximum momentary temperature range model. The UHI effect is mostly visible in the average temperatures and minimum temperatures models although a slight warmth is visible in the maximums model as well. Low-lying sites are the coldest areas in the minimums and momentary maximum temperature range models while in the other two the cold areas extend more evenly. The Parainen limestone quarry distorted the temperature range in the momentary maximum temperature range model.

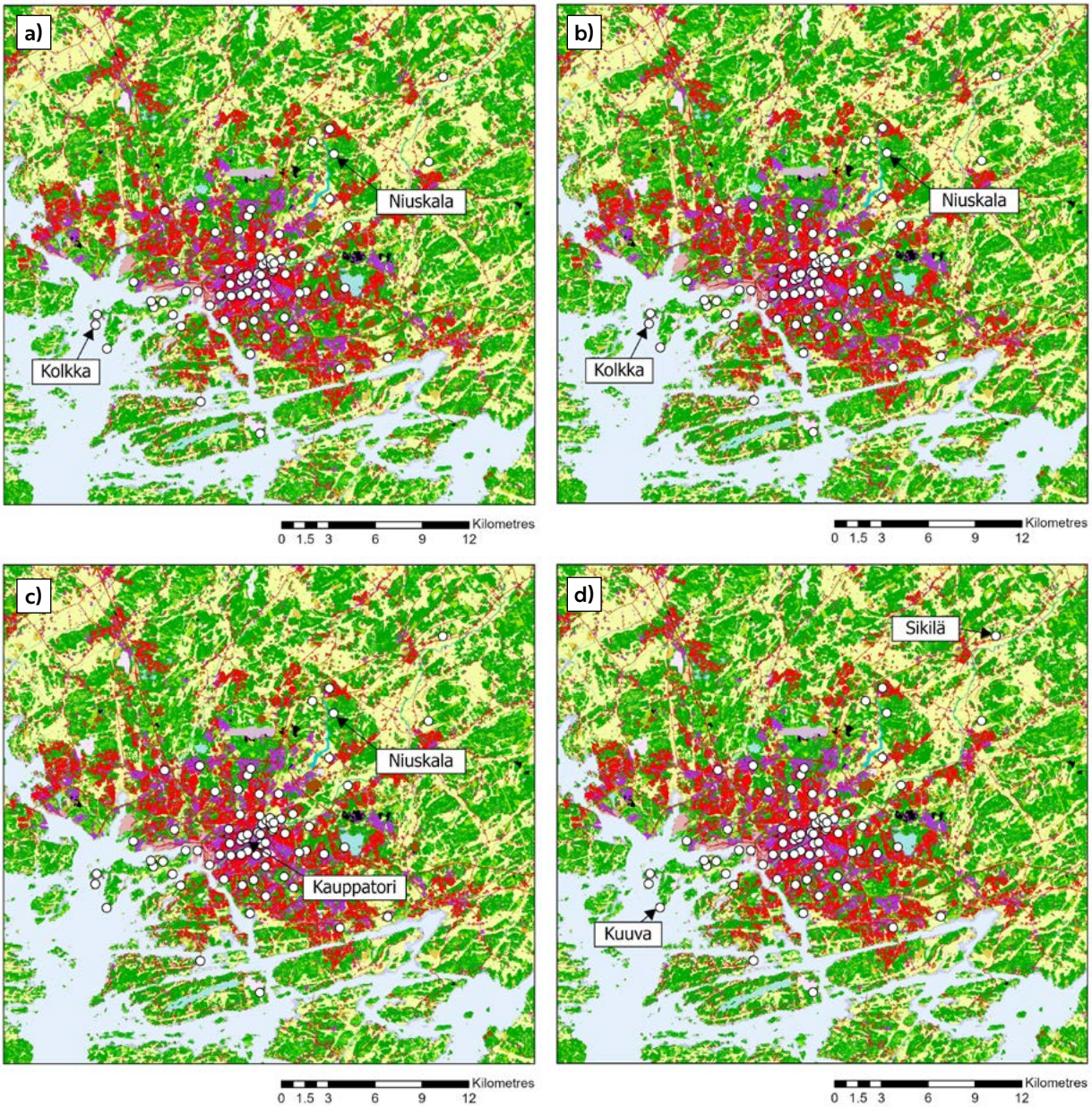

Figure 51. The locations of the logger sites of the highest and lowest a) monthly average temperatures (Kolkka 4.6 °C, Niuskala 2.7 °C), b) monthly averages of daily minimum temperatures (Kolkka 2.9 °C, Niuskala 0.1 °C), c) monthly averages of daily maximum temperatures (Kauppatori 6.3 °C, Niuskala 4.8 °C) and d) momentary maximum temperature range on November 24th at 11.00 with the difference of 12.3 °C (Kuuva 3.5 °C, Sikilä –8.8 °C). Background map: CORINE Land Cover 2018. For information on CORINE level 4 classes and respective colours, used in this Figure and subsequent CORINE based Figures, see Suomi et al. 2024, Appendix A.

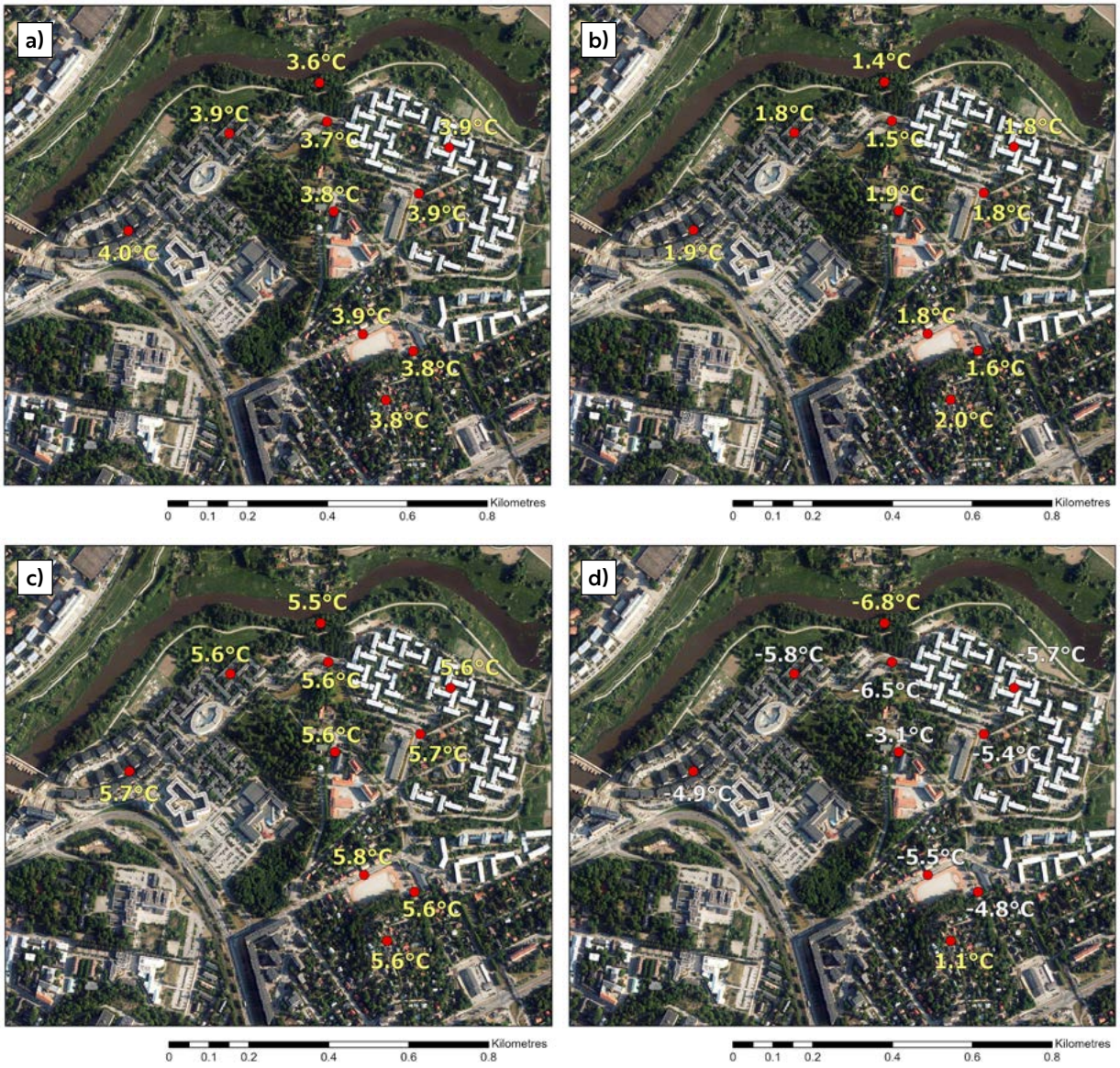

Figure 52. The Student Village logger sites with a) monthly average temperatures, b) monthly averages of daily minimum temperatures, c) monthly averages of daily maximum temperatures and d) the momentary maximum temperature range on November 24th at 11.30 in 2024 with the difference of 7.9 °C between Kuuvuori and Aurajokiranta. For individual logger site names, see Figure 4.

In November 2024 Turku was located on the southern edge of a low-pressure ridge during the maximum momentary temperature range of the whole Turku region on the 24th (map is timed at 06.00 UTC) (Figure 54). The centre of this low-pressure zone located on the Barents Sea just north of Finland. Another low-pressure centre laid north-west of the British Isles on the North Atlantic. High-pressure zones appeared in southern Europe over Bulgaria

Table 43. The regression models for the monthly average temperatures in November 2024.

CORINE-based regression model		
R Square	0.601	
Adjusted R Square	0.582	
Variable	**Standardized Coefficients Beta**	**Significance**
Constant		<0.001
v1_3_5_400m	0.644	<0.001
tkuwaters_2kmsqrt	0.780	<0.001
relelev_100m	0.029	0.722

YKR-based regression model		
R Square	0.682	
Adjusted R Square	0.667	
Variable	**Standardized Coefficients Beta**	**Significance**
Constant		<0.001
rakvae_5x5	0.724	<0.001
tkuwaters_2kmsqrt	0.789	<0.001
relelev_100m	-0.038	0.607

Table 44. The regression models for the monthly averages of daily minimum temperatures in November 2024.

CORINE-based regression model		
R Square	0.660	
Adjusted R Square	0.644	
Variable	**Standardized Coefficients Beta**	**Significance**
Constant		<0.001
v1_3_5_400m	0.666	<0.001
tkuwaters_2kmsqrt	0.726	<0.001
relelev_500m	0.230	0.003

YKR-based regression model		
R Square	0.761	
Adjusted R Square	0.750	
Variable	**Standardized Coefficients Beta**	**Significance**
Constant		<0.001
rakvae_5x5	0.761	<0.001
tkuwaters_2kmsqrt	0.750	<0.001
relelev_500m	0.143	0.027

Table 45. The regression models for the monthly averages of daily maximum temperatures in November 2024.

CORINE-based regression model		
R Square	0.486	
Adjusted R Square	0.462	
Variable	**Standardized Coefficients Beta**	**Significance**
Constant		<0.001
v1_3_5_400m	0.586	<0.001
tkuwaters_700m	0.697	<0.001
relelev_500m	-0.099	0.276

YKR-based regression model		
R Square	0.525	
Adjusted R Square	0.503	
Variable	**Standardized Coefficients Beta**	**Significance**
Constant		<0.001
rakvae_5x5	0.620	<0.001
tkuwaters_700m	0.675	<0.001
relelev_500m	-0.165	0.066

Table 46. The regression models for the momentary maximum temperature range in November 2024.

CORINE-based regression model		
R Square	0.648	
Adjusted R Square	0.631	
Variable	**Standardized Coefficients Beta**	**Significance**
Constant		<0.001
v1_3_5_100m	0.378	<0.001
tkuwaters_5km	0.759	<0.001
relelev_500m	0.292	<0.001

YKR-based regression model		
R Square	0.608	
Adjusted R Square	0.590	
Variable	**Standardized Coefficients Beta**	**Significance**
Constant		<0.001
rakvae_1x1	0.303	<0.001
tkuwaters_5km	0.704	<0.001
relelev_500m	0.287	<0.001

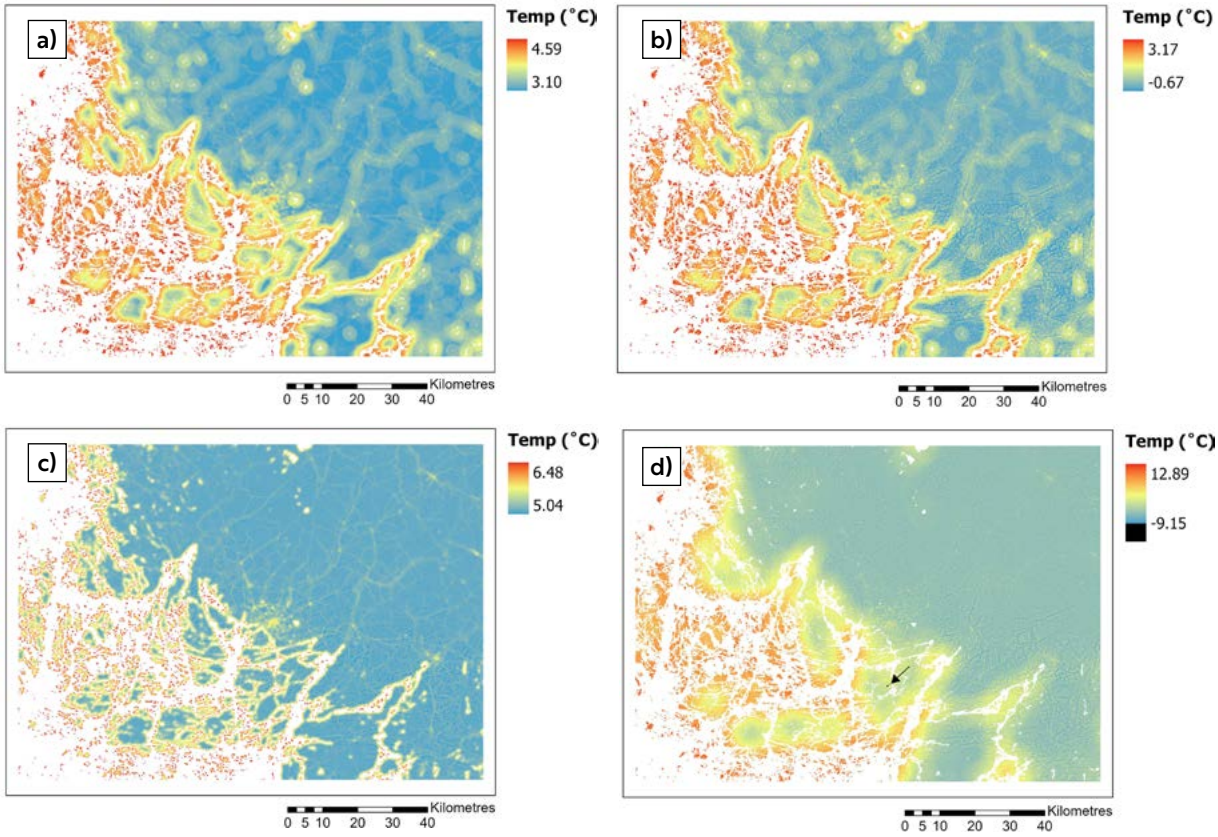

Figure 53. High-resolution (100 m) temperatures based on linear regression model depicting November 2024 a) monthly average temperatures, b) monthly averages of daily minimum temperatures, c) monthly averages of daily maximum temperatures and d) temperatures of momentary maximum temperature range on November 24th, 2024, at 11.00. The abnormally low temperature area in the limestone quarry located in Parainen is marked in black (arrow).

and in northern Kazakhstan. The 500 hPa surface pressure height in Turku was 528–532 decametres. For the maximum range in the Student Village on the 24th a bit later on (map is timed at 12.00 UTC) the situation appears similar due to the minimal time difference between the maps (Figure 55). The low-pressure and high-pressure centres remain but the 500 hPa surface pressure height had risen to 536–540 decametres. In November during the maximum difference for the whole Turku region on the 24th at 11.00 the average wind speed measured 2.125 m/s and average cloudiness 0 oktas. Half an hour later at 11.30 the average wind speed was 1.85 m/s and average cloudiness 0 oktas.

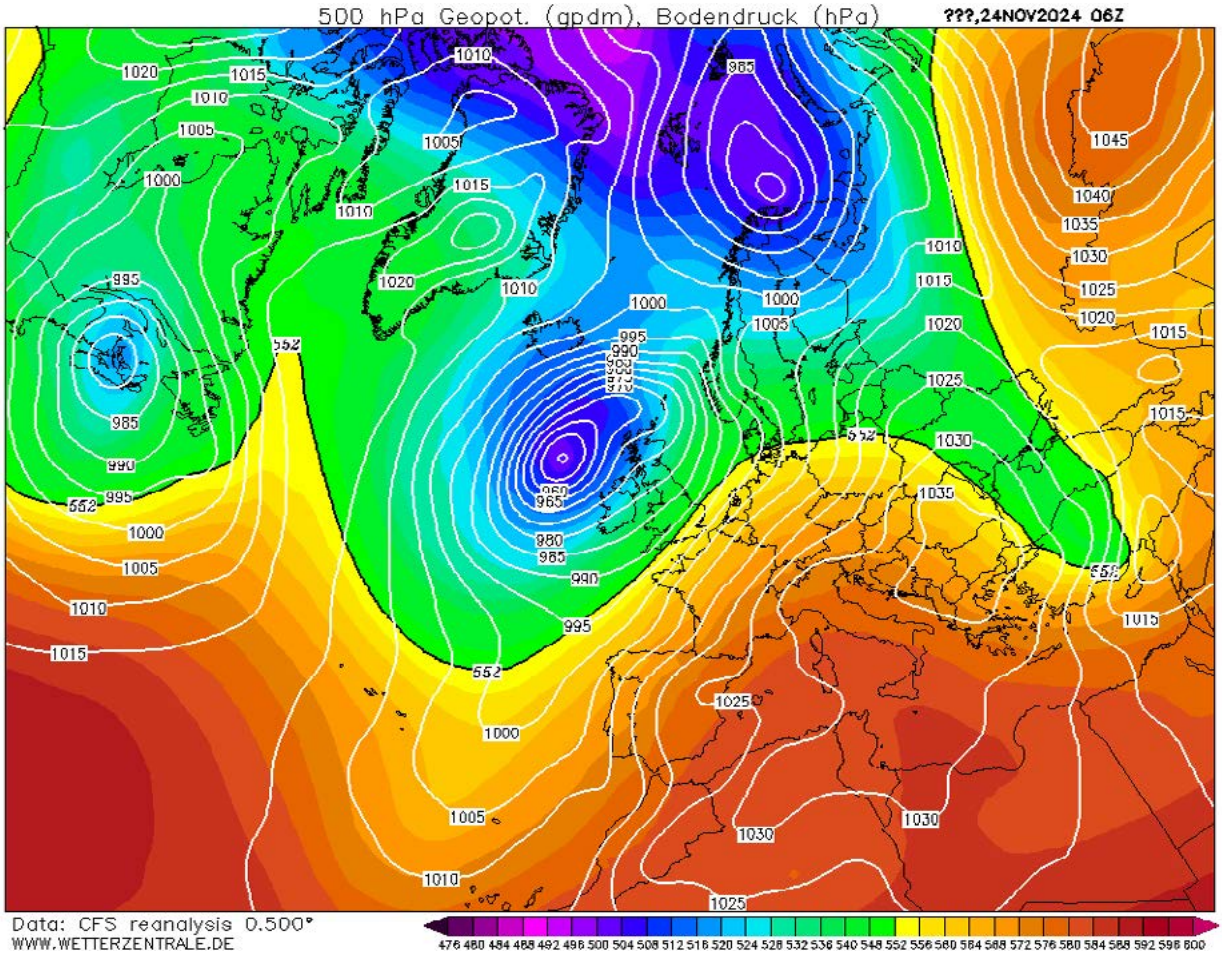

Figure 54. Sea level air pressure (white contours) and height of 500 hectopascal pressure level in decametres (colour ramp) for November 24th at 06.00 UTC. Retrieved from Wetterzentrale (https://www.wetter-zentrale.de/en/reanalysis.php?model=cfsr).

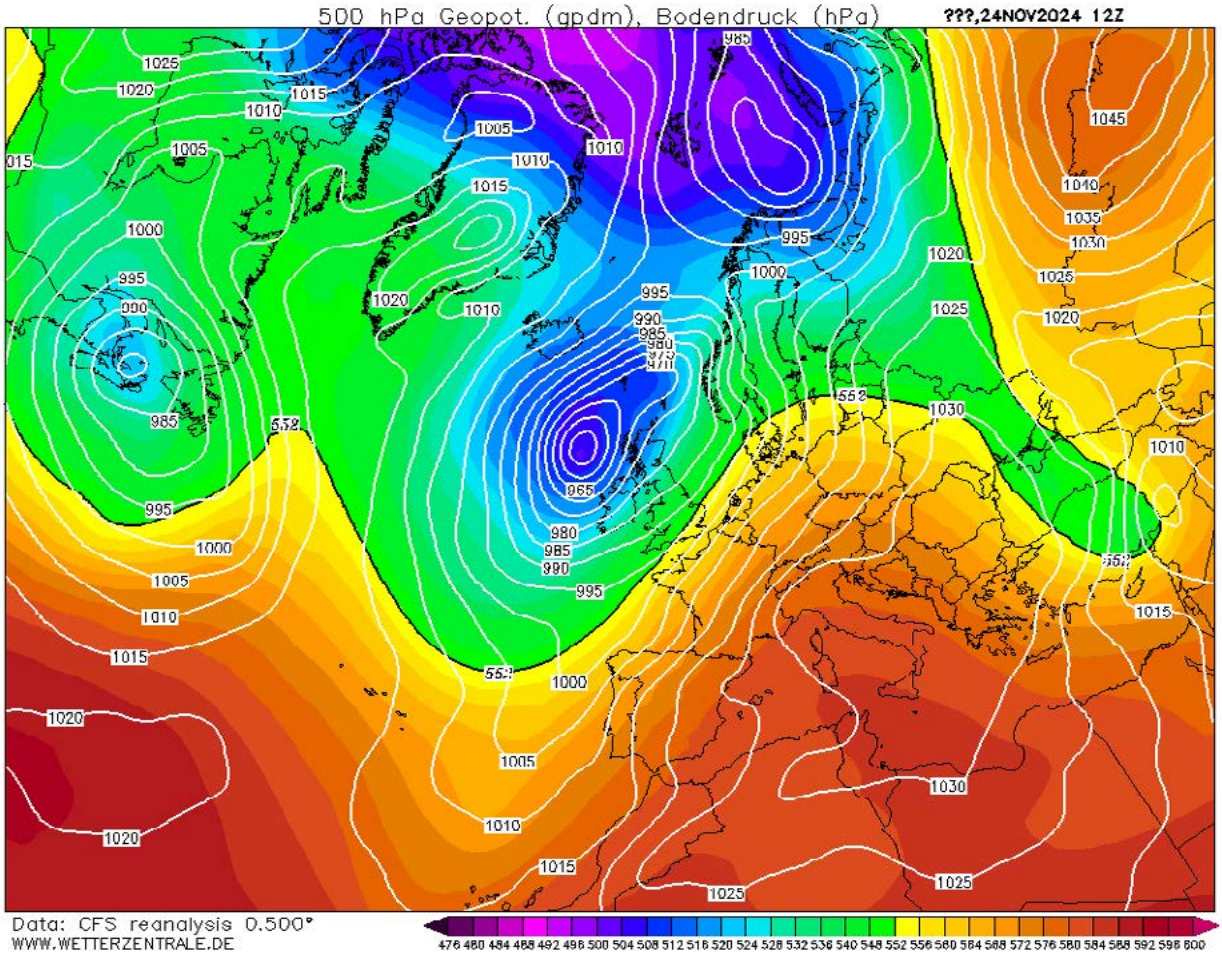

Figure 55. Sea level air pressure (white contours) and height of 500 hectopascal pressure level in decametres (colour ramp) for November 24th at 12.00 UTC. Retrieved from Wetterzentrale (https://www.wetter-zentrale.de/en/reanalysis.php?model=cfsr).

4.1.12 December

For December the average temperature recorded in the Turku airport observation site in 2024 was 0.2 °C which was 1.7 °C warmer than what was reported in the 1991–2020 climate reference period (Jokinen et al., 2021).

Regarding the TURCLIM observation network the highest average temperature in December was recorded in Kauppatori with the average temperature being 1.7 °C while the lowest average temperature was recorded in Niuskala with –0.3 °C (Figure 56). The highest and lowest monthly averages of daily minimum temperatures sites were Kolkka and Sikilä with Kolkka measuring –0.7 °C and Sikilä –3.0 °C. For the averages of daily maximum temperatures, the warmest site was Kauppatori (3.6 °C) and the coldest Niuskala (2.0 °C). The momentary maximum temperature range occurred in December on the 13th at 05.00 between Kolkka and Ylijoki observation sites. The difference during this time between these sites was 9.1 °C.

In the case of the Turku Student village temperatures the highest average temperature in December occurred in Pispalantie with the average being 1.0 °C (Figure 57). The lowest average of 0.7 °C was measured in Aurajokiranta and Kuikkulankatu, respectively. In the case of monthly averages of daily minimum temperatures, the lowest value remained in Aurajokiranta with the average being –2.1 °C but the highest value of –1.7 °C occurred in three sites: Kuuvuori, Pispalantie and Yo-kylä länsi. For the monthly averages of daily maximum temperatures, the highest value remained solely in Pispalantie with an average of 3.1 °C, while the lowest values appeared in Aurajokiranta and Kuuvuori with the average being 2.8 °C, respectively. On December 18th at 09.00 the momentary maximum temperature difference of 5.0 °C was measured between Kuikkulankatu and Kuuvuori.

In December 2024 the regression models for monthly average temperatures have explanatory powers of 0.661 in the CORINE-based regression model and 0.750 in the YKR-based regression model (Table 47). Of the explanatory variables, all except for elevation were statistically significant. The rest had a warming effect with the water body variable being the strongest influencer. However, land cover and the building floor area and population variable also had a quite strong effect. In the case of the monthly averages of daily minimum temperatures the explanatory powers are 0.741 and 0.763 (Table 48). Water bodies, land cover and building floor area and population had a warming effect with the water body variable being the strongest. For the monthly averages of daily maximum temperatures explanatory powers are 0.522 and 0.511 with all but elevation being statistically significant out of the explanatory variables (Table 49). Water bodies had the strongest effect although land cover and building floor area and population had also quite a strong influence. In the case of the momentary maximum temperature range regression models the explanatory powers are 0.653 and 0.602 (Table 50). All explanatory variables were statistically significant and had a warming effect. Water bodies had the strongest warming effect while elevation the weakest.

For December the temperature models look rather similar to one another except for the maximum momentary temperature range model where the limestone quarry in Parainen influenced the temperature range (Figure 58). In all models the coast and the archipelago are the warmest areas while the mainland is cooler. The UHI is not clearly distinguishable in any of the maps but the city centre is slight-

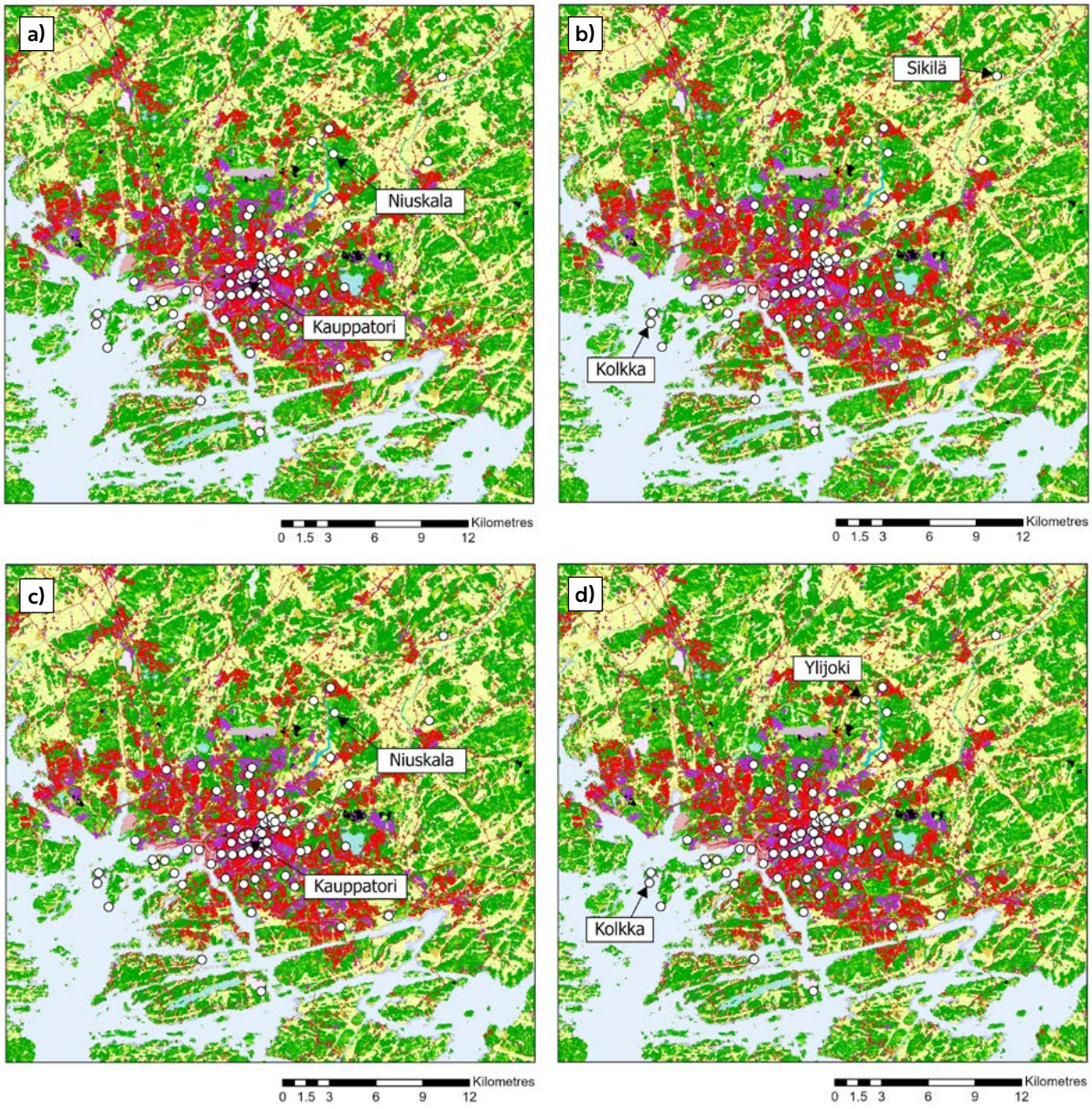

Figure 56. The locations of the logger sites of the highest and lowest a) monthly average temperatures (Kauppatori 1.7 °C, Niuskala -0.3 °C), b) monthly averages of daily minimum temperatures (Kolkka –0.7 °C, Sikilä –3.0 °C), c) monthly averages of daily maximum temperatures (Kauppatori 3.6 °C, Niuskala 2.0 °C) and d) momentary maximum temperature range on December 13th at 05.00 with the difference of 9.1 °C (Kolkka –0.5 °C, Ylijoki –9.6 °C). Background map: CORINE Land Cover 2018. For information on CORINE level 4 classes and respective colours, used in this Figure and subsequent CORINE based Figures, see Suomi et al. 2024, Appendix A.

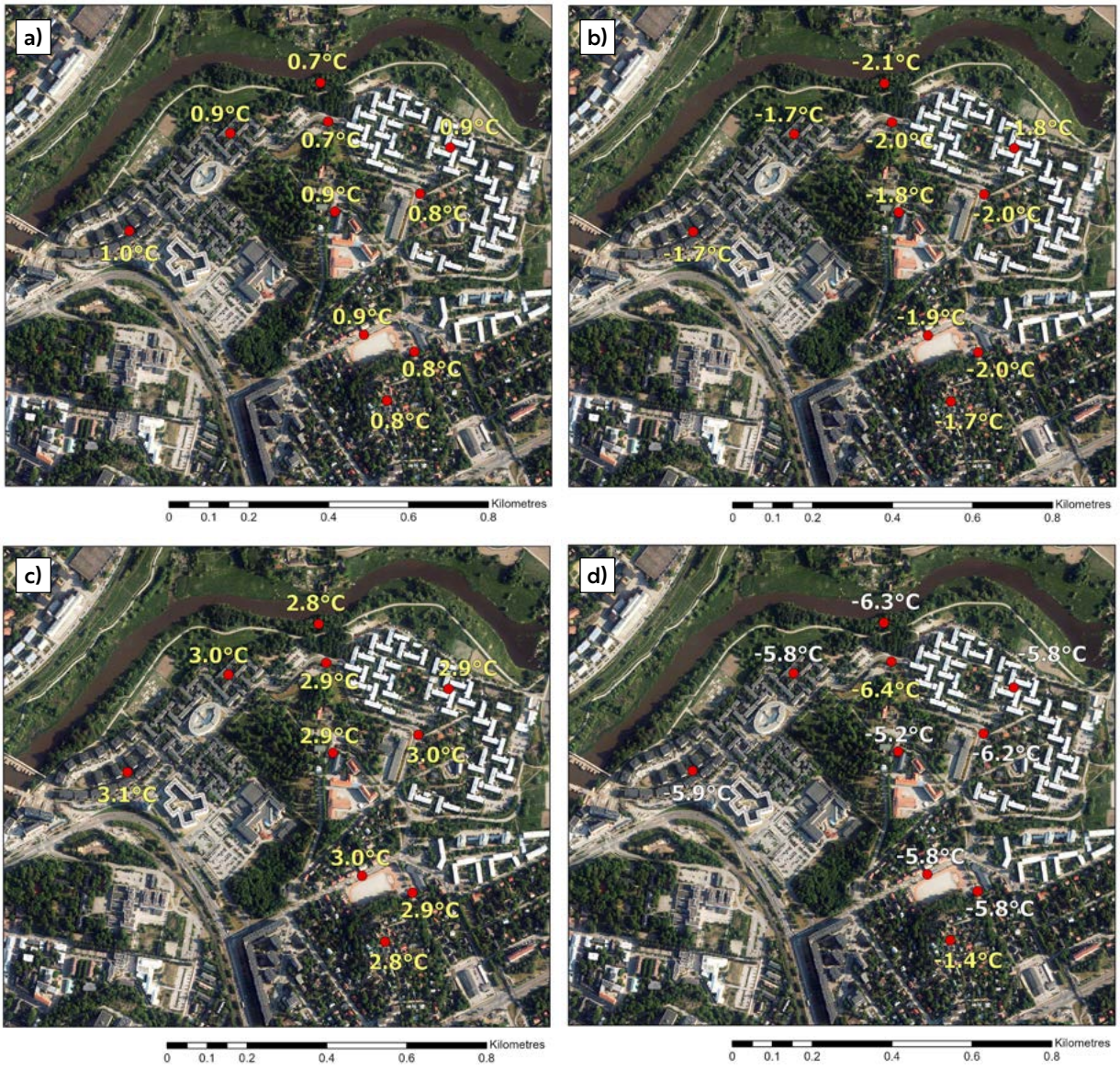

Figure 57. The Student Village logger sites with a) monthly average temperatures, b) monthly averages of daily minimum temperatures, c) monthly averages of daily maximum temperatures and d) the momentary maximum temperature range on December 18th at 09.00 in 2024 with the difference of 5.0 °C between Kuuvuori and Kuikkulankatu. For individual logger site names, see Figure 4.

ly warmer than surrounding areas. The coldest temperature outside of the limestone quarry in the maximum range map is –11.35 °C with the low-lying sites appearing as the coldest areas due to cold air drainage.

Regarding the maximum momentary temperature range in the whole Turku region on the 13th Turku was located on the north-eastern edge of a high pressure ridge (Figure 59). During this the 500 hPa surface pressure height in

Table 47. The regression models for the monthly average temperatures in December 2024.

CORINE-based regression model		
R Square	0.676	
Adjusted R Square	0.661	
Variable	**Standardized Coefficients Beta**	**Significance**
Constant		<0.001
v1_3_5_400m	0.700	<0.001
tkuwaters_5km	0.783	<0.001
relelev_300m	0.048	0.511

YKR-based regression model		
R Square	0.762	
Adjusted R Square	0.750	
Variable	**Standardized Coefficients Beta**	**Significance**
Constant		<0.001
rakvae_5x5	0.778	<0.001
tkuwaters_5km	0.790	<0.001
relelev_300m	-0.038	0.552

Table 48. The regression models for the monthly averages of daily minimum temperatures in December 2024.

CORINE-based regression model		
R Square	0.752	
Adjusted R Square	0.741	
Variable	**Standardized Coefficients Beta**	**Significance**
Constant		<0.001
v1_3_5_400m	0.652	<0.001
tkuwaters_5km	0.825	<0.001
relelev_500m	0.185	0.005

YKR-based regression model		
R Square	0.774	
Adjusted R Square	0.763	
Variable	**Standardized Coefficients Beta**	**Significance**
Constant		<0.001
rakvae_3x3	0.662	<0.001
tkuwaters_5km	0.788	<0.001
relelev_500m	0.137	0.028

Table 49. The regression models for the monthly averages of daily maximum temperatures in December 2024.

CORINE-based regression model		
R Square	0.543	
Adjusted R Square	0.522	
Variable	**Standardized Coefficients Beta**	**Significance**
Constant		<0.001
v1_3_5_400m	0.627	<0.001
tkuwaters_5km	0.723	<0.001
relelev_100m	-0.059	0.498

YKR-based regression model		
R Square	0.532	
Adjusted R Square	0.511	
Variable	**Standardized Coefficients Beta**	**Significance**
Constant		<0.001
rakvae_3x3	0.604	<0.001
tkuwaters_5km	0.673	<0.001
relelev_100m	-0.076	0.394

Table 50. The regression models for the momentary maximum temperature range in December 2024.

CORINE-based regression model		
R Square	0.669	
Adjusted R Square	0.653	
Variable	**Standardized Coefficients Beta**	**Significance**
Constant		<0.001
v1_3_5_700m	0.593	<0.001
tkuwaters_2km	0.743	<0.001
relelev_500m	0.316	<0.001

YKR-based regression model		
R Square	0.619	
Adjusted R Square	0.602	
Variable	**Standardized Coefficients Beta**	**Significance**
Constant		<0.001
rakvae_1x1	0.490	<0.001
tkuwaters_2km	0.599	<0.001
relelev_500m	0.323	<0.001

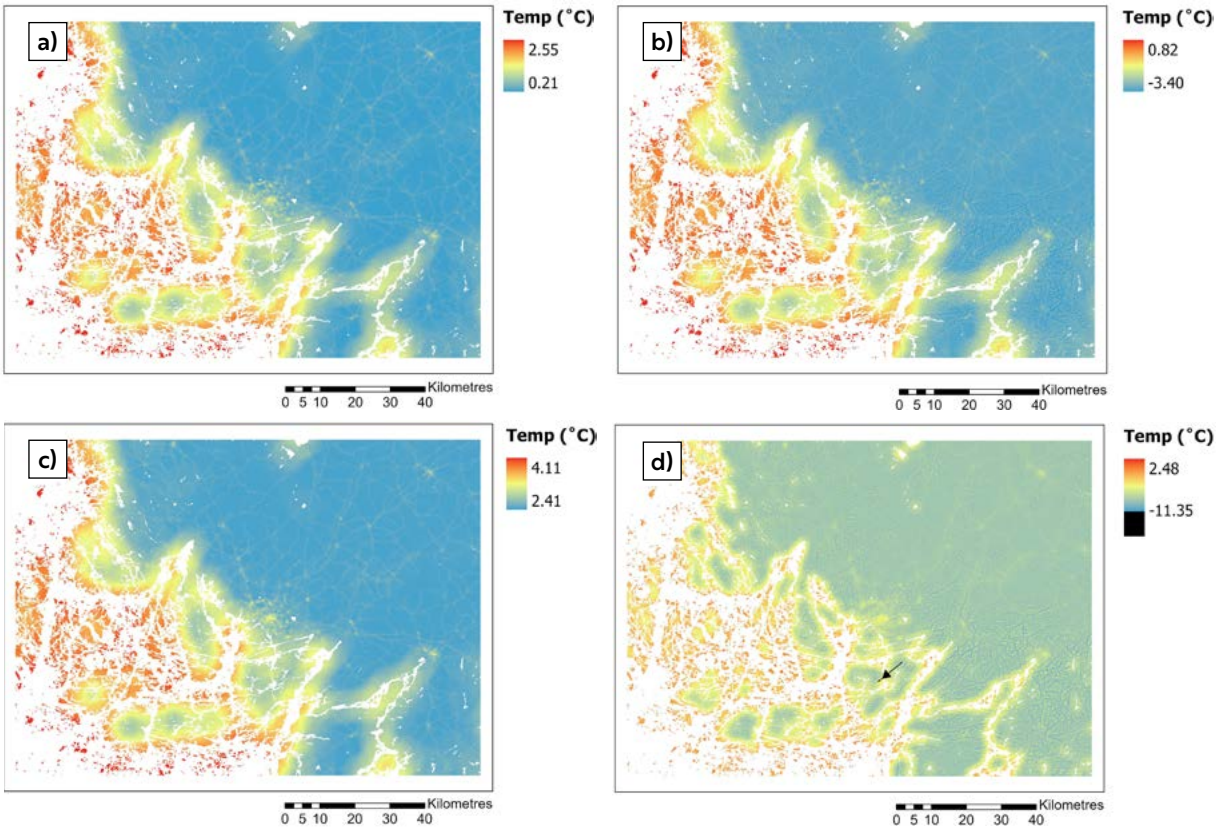

Figure 58. High-resolution (100 m) temperatures based on linear regression model depicting December 2024 a) monthly average temperatures, b) monthly averages of daily minimum temperatures, c) monthly averages of daily maximum temperatures and d) temperatures of momentary maximum temperature range on December 13th, 2024, at 05.00. The abnormally low temperature area in the limestone quarry located in Parainen is marked in black (arrow).

Turku was about 540–548 decametres. The centre of the high-pressure ridge extends greatly over western Europe while low-pressure centres appear over eastern Russia and north-east of the Icelandic coast on the Norwegian Sea. The map is timed at 00.00 UTC. In the case of the maximum temperature difference in the Turku Student Village on the 18th (map is timed 06.00 UTC), Turku is located between multiple low-pressure centres resulting in low air pressure in the Turku area (Figure 60). These low-pressure centres located in eastern Russia, north of the British Isles and in Novaya Zemlya. A weaker low-pressure centre also appeared in northern Finland. The 500 hPa surface pressure height was about 532–536 over Turku during this time. On December 13th at 05.00 at average wind speed measured 0.9 m/s while the average cloudiness was 7 oktas. On the 18th at 09.00, during the maximum difference between the Student Village sites, average wind speed was 0 m/s and average cloudiness 7 oktas.

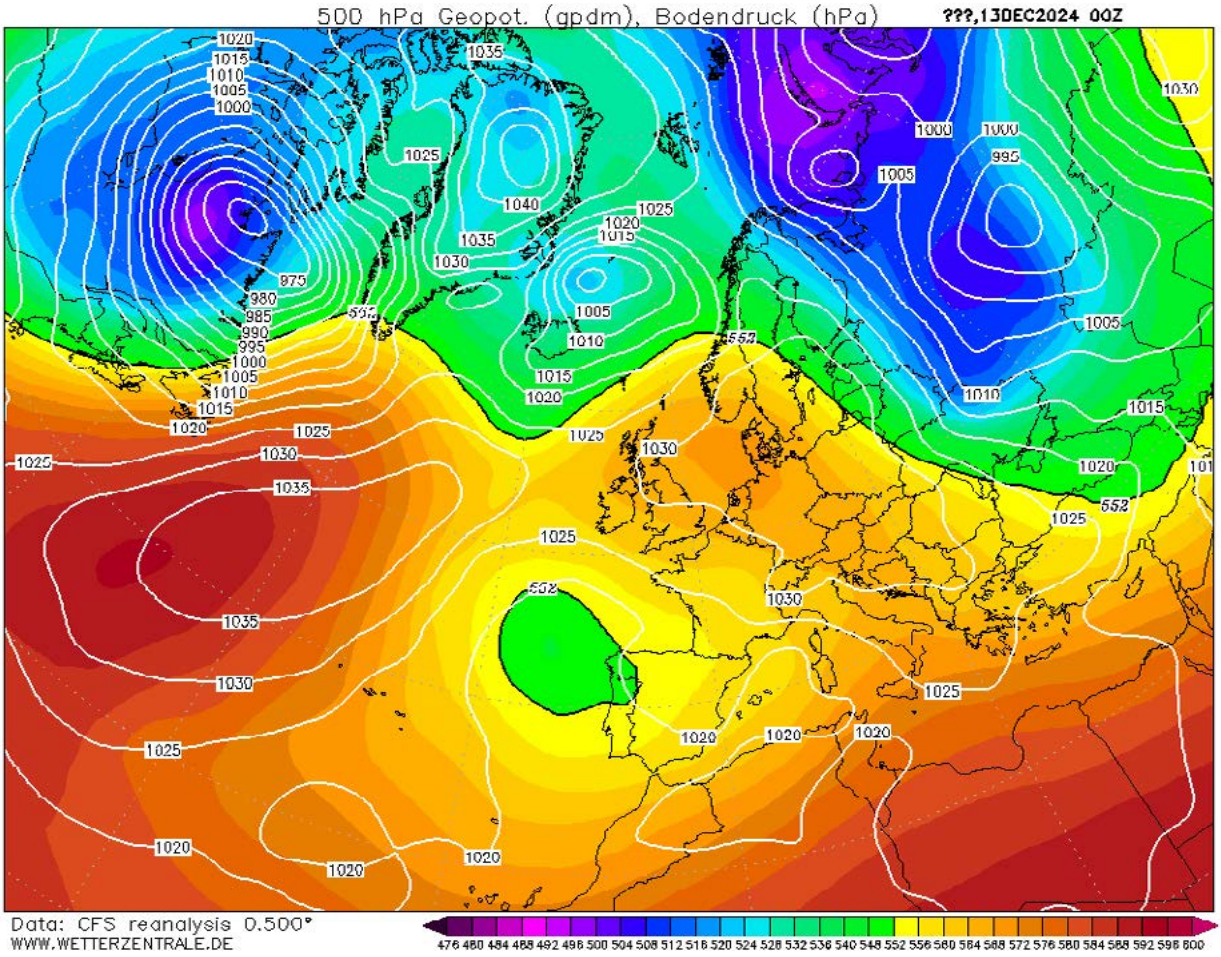

Figure 59. Sea level air pressure (white contours) and height of 500 hectopascal pressure level in decametres (colour ramp) for December 13th at 00.00 UTC. Retrieved from Wetterzentrale (https://www.wetter-zentrale.de/en/reanalysis.php?model=cfsr).

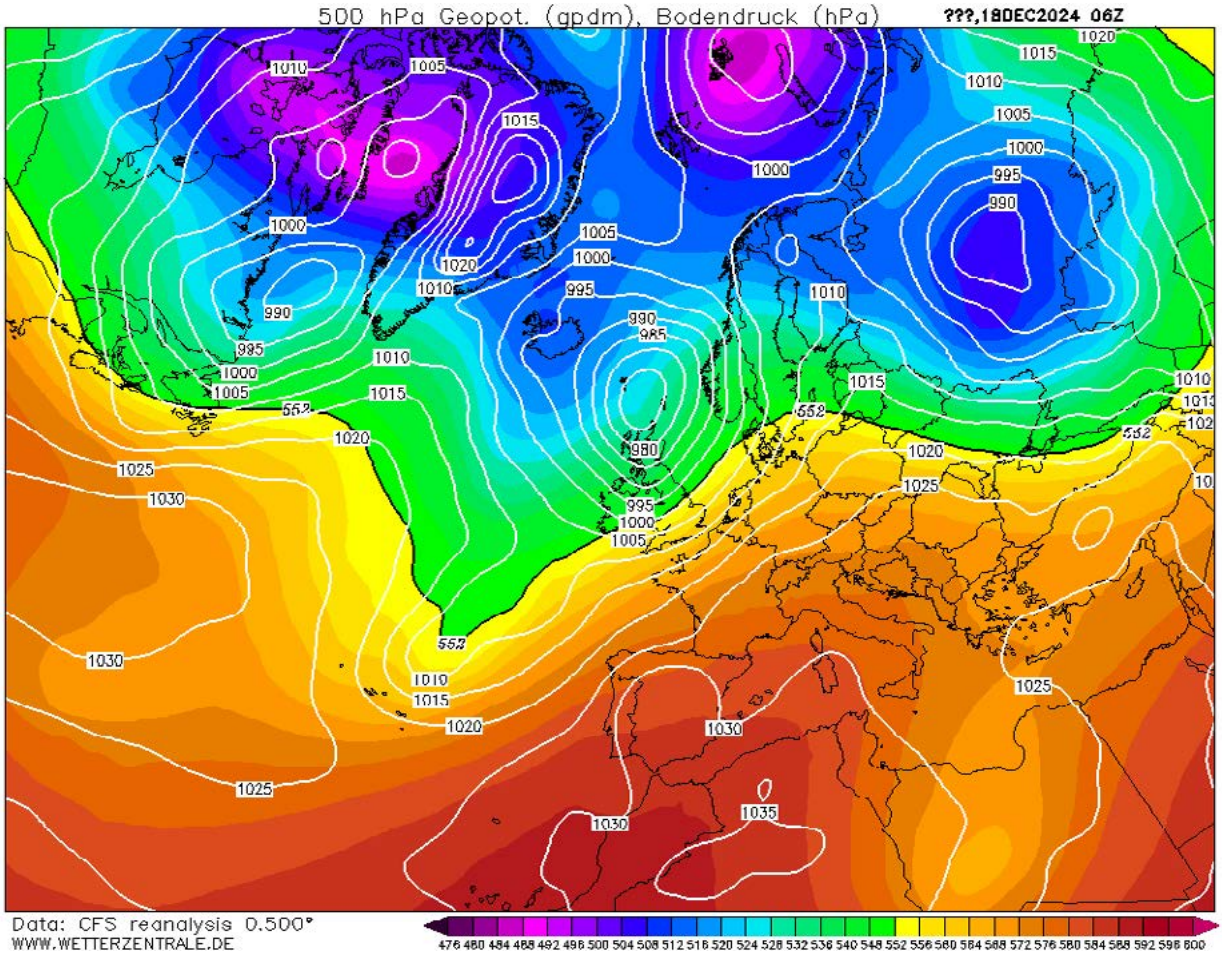

Figure 60. Sea level air pressure (white contours) and height of 500 hectopascal pressure level in decametres (colour ramp) for December 18th at 06.00 UTC. Retrieved from Wetterzentrale (https://www.wetter-zentrale.de/en/reanalysis.php?model=cfsr).

4.2 Annual overview

During the study year 2024, an annual average temperature difference between the on average warmest and coldest observation sites of the Turku region was 2.0 °C. The highest annual average temperature, 8.4 °C, was measured in Kauppatori in the Turku city centre, whereas the lowest respective temperature was measured in forested uninhabited site Niuskala, located approximately 10 kilometres to the NNE of the Kauppatori observation site. For the annual averages of daily minimum temperatures, the highest value was recorded in Betel in the Turku city centre with a temperature of 5.3 °C. The lowest respective temperature of 2.1 °C occurred in Niuskala, resulting in a temperature difference of 3.2 °C. In the case of the annual averages of daily maximum temperatures, the difference of 1.2 °C was recorded between the warmest (11.4 °C) site Kauppatori, and coldest (10.2 °C) site Niuskala.

Regarding the Turku Student Village area, the highest annual average temperature of 7.7 °C was recorded in Pispalantie and the lowest respective temperature of 7.2 °C in Aurajokiranta, resulting in a temperature difference of 0.5 °C. For the annual averages of daily minimum temperatures in the Student Village, the difference of 1.0 °C was recorded between Kuuvuori and Aurajokiranta, based on temperatures of 4.3 °C and 3.3 °C, respectively. Regarding the annual averages of daily maximum temperature, the highest temperature, 11.0 °C, was recorded in Kuuvuori, and the lowest, 10.5 °C, in Aurajokiranta, resulting in a temperature difference of 0.5 °C.

5
SYNTHESIS

Based on the observations recorded in the Turku airport by FMI the coldest month in 2024 was January with an average temperature of –7.6 °C while the warmest month was July with an average temperature of 18.2 °C. Compared to the 30-year climatic reference period 1991–2020, the largest warm anomaly of 2024 was recorded in May, which was on average 3.8 °C warmer than during the reference period. The largest respective cold anomaly was recorded in January, which was 3.8 °C colder than on average.

Regarding the whole observation network, the warmest sites were often Betel and Kauppatori, located in the Turku city centre (Tables 51–54). During couple of months in summer, daily maximum temperatures were warmest in Piispankatu, located approximately 1 km to the NE of the Turku city centre. Kolkka and Kuuva, located in the coastal areas in Ruissalo island, approximately 10 km to the WSW of the Turku city centre, were the warmest sites during autumn months, when the warming effect of sea is clear in the coastal zone. To summarize, the Turku city centre is relatively warm throughout the year, whereas the coldest sites were often rural inland sites Niuskala, Sikilä and Ylijoki. Hiiriluoto manner site, located in the forest in the middle of Ruissalo island, approximately 500 m distance from the sea, and the coastal site Kolkka in the same island, were also coldest sites during some months, mostly during spring and summer, reflecting the cooling effect of sea during those seasons.

Table 51. Highest and lowest monthly average temperatures in the Turku region in 2024.

	Monthly average temperature				
Month	**Highest temp. (°C)**	**Lowest temp. (°C)**	**Difference (°C)**	**Highest temp. site**	**Lowest temp. site**
January	-6.2	-8.2	2.0	Betel	Sikilä
February	-1.7	-3.2	1.5	Kauppatori	Sikilä
March	1.6	0.1	1.5	Betel	Niuskala
April	4.4	3.0	1.4	Kauppatori	Kolkka
May	15.6	13.2	2.4	Kauppatori	Niuskala
June	17.6	15.1	2.5	Puutori	Niuskala
July	19.4	17.3	2.1	Kauppatori	Niuskala
August	18.7	16.2	2.5	Kauppatori	Niuskala
September	15.2	12.8	2.4	Kauppatori	Niuskala
October	9.7	7.3	2.4	Kuuva	Niuskala
November	4.6	2.7	1.9	Kolkka	Niuskala
December	1.7	-0.3	2.0	Kauppatori	Niuskala

Table 52. Highest and lowest monthly averages of daily minimum temperatures in the Turku region in 2024.

Month	Monthly averages of daily minimums				
	Highest temp. (°C)	Lowest temp. (°C)	Difference (°C)	Highest temp. site	Lowest temp. site
January	-9.2	-13.0	3.8	Betel	Sikilä
February	-3.5	-5.6	2.1	Betel	Sikilä
March	-0.8	-3.1	2.3	Betel	Niuskala
April	1.4	-0.8	2.2	Kauppatori	Niuskala
May	9.7	4.4	5.3	Betel	Niuskala
June	13.8	9.2	4.6	Kauppatori	Niuskala
July	16.4	13.4	3.0	Kauppatori	Niuskala
August	15.5	11.3	4.2	Kuuva	Sikilä
September	12.1	8.0	4.1	Kuuva	Ylijoki
October	7.5	3.4	4.1	Kolkka	Niuskala
November	2.9	0.1	2.8	Kolkka	Niuskala
December	-0.7	-3.0	2.3	Kolkka	Sikilä

Table 53. Highest and lowest monthly averages of daily maximum temperatures in the Turku region in 2024.

Month	Monthly averages of daily maximums				
	Highest temp. (°C)	Lowest temp. (°C)	Difference (°C)	Highest temp. site	Lowest temp. site
January	-3.5	-4.9	1.4	Kauppatori	Niuskala
February	0.3	-1.0	1.3	Kauppatori	Sikilä
March	4.4	3.1	1.3	Betel	Kolkka
April	7.6	6.1	1.5	Kauppatori	Kolkka
May	21.1	18.4	2.7	Lieto	Kuuva
June	21.2	19.5	1.7	Piispankatu	Hiiriluoto manner
July	22.8	20.9	1.9	Kauppatori	Niuskala
August	22.3	20.6	1.7	Piispankatu	Niuskala
September	18.9	17.2	1.7	Kauppatori	Hiiriluoto manner
October	12.3	11.2	1.1	Kauppatori	Ylijoki
November	6.3	4.8	1.5	Kauppatori	Niuskala
December	3.6	2.0	1.6	Kauppatori	Niuskala

Table 54. Highest and lowest temperatures of month-specific momentary maximum temperature ranges in the Turku region in 2024.

		Momentary maximum temperature range				
Month	Date and time (GMT+2)	Highest temp. (°C)	Lowest temp. (°C)	Difference (°C)	Highest temp. site	Lowest temp. site
January	21st, 00.00	-11.8	-26.0	14.2	Luostarivuori	Halinen
February	8th, 05.00	-12.9	-19.9	7.0	Betel	Sikilä
March	18th, 22.30	-0.9	-7.5	6.6	Betel	Sikilä
April	29th, 16.00	15.8	7.6	8.2	Kuuva	Sikilä
May	29th, 01.00	19.2	10.3	8.9	Luostarivuori	Ylijoki
June	12th, 18.00	18.9	8.9	10.0	Nummi	Lieto
July	10th, 03.00	16.3	9.0	7.3	Kuuva	Sikilä
August	18th, 05.00	16.0	7.4	8.6	Kolkka	Sikilä
September	30th, 08.00	9.5	-1.3	10.8	Kolkka	Lieto
October	16th, 08.30	9.0	-2.0	11.0	Kuuva	Ylijoki
November	24th, 11.00	3.5	-8.8	12.3	Kuuva	Sikilä
December	13th, 05.00	-0.5	-9.6	9.1	Kolkka	Ylijoki

Regarding the Turku Student Village, the warmest sites were commonly Kuuvuori and Pispalantie (Table 55–58). On some months, multiple sites were warmest having the same average temperatures. In these cases, usually Suntiontie and Yo-kylä itä were also the warmest. Kuuvuori is a hill-top site, located in a detached house area along a gravel road approximately 20–40 m higher than the other observation sites of the Student Village area, while Pispalantie and Suntiontie are located on the sides of asphalted roads, Pispalantie in the block of flat area and Suntiontie in the detached house area. Yo-kylä itä is located in the middle of a densely built block of flat area consisting of 3 to 4 floor buildings. The coldest site was mostly Aurajokiranta, which is a low-lying site on the riverbank of River Aura that is prone to cold air drainage. On some months, there were multiple coldest sites. In most cases, Kuikkulankatu and Kuuvuori kenttä were additionally the coldest sites. Kuikkulankatu is located close to the Aurajokiranta site, while Kuuvuori kenttä site is right next to the higher elevated Kuuvuori, from where the cold air drainage can occur.

Of the explanatory variables used in the month-specific regression models, the urban variables, namely in the CORINE-based regression model the urban land cover variable and in the YKR-based regression model the population and building floor based variable were most commonly statistically significant. In addition, variable reflecting the proximity of water bodies was often statistically significant in both models. High proportion of urban land cover as well as high population density and/or high building floor area meant warming influence throughout the year (Tables 59 & 60). In contrast, the direction of the effect of water bodies shifted depending both on season and time of day: during spring and summer in daytime, water bodies generally produced a cooling effect, while otherwise they mostly had a

Table 55. Highest and lowest monthly average temperatures in the Student Village in 2024. In the cases in which multiple observation sites are either warmest or coldest with 0.1 °C accuracy, the warmest or coldest site, determined by multiple decimal accuracy, is reported. This pattern is followed in this Table and Tables 56–58.

	Monthly average temperature				
Month	Highest temp. (°C)	Lowest temp. (°C)	Difference (°C)	Highest temp. site	Lowest temp. site
January	-7.1	-7.6	0.5	Kuuvuori	Aurajokiranta
February	-2.2	-2.5	0.3	Pispalantie	Aurajokiranta
March	1	0.6	0.4	Pispalantie	Aurajokiranta
April	3.9	3.6	0.3	Pispalantie	Aurajokiranta
May	14.9	14.0	0.9	Yo-kylä itä	Aurajokiranta
June	17.1	16.3	0.8	Yo-kylä itä	Aurajokiranta
July	19.0	18.3	0.7	Pispalantie	Aurajokiranta
August	18.1	17.2	0.9	Pispalantie	Aurajokiranta
September	14.5	13.5	1	Kuuvuori	Aurajokiranta
October	8.7	8.1	0.6	Kuuvuori	Aurajokiranta
November	4.0	3.6	0.4	Pispalantie	Aurajokiranta
December	1.0	0.7	0.3	Pispalantie	Aurajokiranta

Table 56. Highest and lowest monthly averages of daily minimum temperatures in the Student Village in 2024.

	Monthly averages of daily minimums				
Month	Highest temp. (°C)	Lowest temp. (°C)	Difference (°C)	Highest temp. site	Lowest temp. site
January	-10.3	-12.6	2.3	Kuuvuori	Aurajokiranta
February	-4.1	-4.7	0.6	Pispalantie	Aurajokiranta
March	-1.8	-2.3	0.5	Pispalantie	Aurajokiranta
April	0.7	0.1	0.6	Pispalantie	Aurajokiranta
May	8.1	6.5	1.6	Kuuvuori	Aurajokiranta
June	12.5	11.3	1.2	Kuuvuori	Aurajokiranta
July	15.8	15.0	0.8	Pispalantie	Aurajokiranta
August	14.1	12.9	1.2	Kuuvuori	Aurajokiranta
September	10.4	9.1	1.3	Kuuvuori	Aurajokiranta
October	6.2	4.7	1.5	Kuuvuori	Aurajokiranta
November	2.0	1.4	0.6	Kuuvuori	Aurajokiranta
December	-1.7	-2.1	0.4	Pispalantie	Aurajokiranta

Table 57. Highest and lowest monthly averages of daily maximum temperatures in the Student Village in 2024.

	Monthly averages of daily maximums				
Month	**Highest temp. (°C)**	**Lowest temp. (°C)**	**Difference (°C)**	**Highest temp. site**	**Lowest temp. site**
January	-4.1	-4.3	0.2	Pispalantie	Kuikkulankatu
February	-0.4	-0.6	0.2	Suntiontie	Kuuvuori kenttä
March	3.8	3.6	0.2	Pispalantie	Aurajokiranta
April	7.2	7.0	0.2	Suntiontie	Kuuvuori kenttä
May	20.7	19.8	0.9	Kuuvuori	Aurajokiranta
June	21.2	20.3	0.9	Yo-kylä itä	Aurajokiranta
July	22.5	21.8	0.7	Yo-kylä itä	Aurajokiranta
August	22.1	20.9	1.2	Kuuvuori	Aurajokiranta
September	18.6	17.4	1.2	Kuuvuori	Aurajokiranta
October	11.9	11.5	0.4	Suntiontie	Aurajokiranta
November	5.8	5.5	0.3	Suntiontie	Aurajokiranta
December	3.1	2.8	0.3	Pispalantie	Kuuvuori

Table 58. Highest and lowest temperatures of month-specific momentary maximum temperature ranges in the Student Village in 2024.

		Momentary maximum temperature range				
Month	**Date and time (GMT+2)**	**Highest temp. (°C)**	**Lowest temp. (°C)**	**Difference (°C)**	**Highest temp. site**	**Lowest temp. site**
January	21st, 00.00	-13.7	-25.0	11.3	Kuuvuori	Aurajokiranta
February	5th, 07.30	-4.0	-7.9	3.9	Kuuvuori	Aurajokiranta
March	12th, 23.00	-0.1	-3.3	3.2	Kuuvuori	Aurajokiranta
April	9th, 23.30	8.8	3.6	5.2	Kuuvuori	Aurajokiranta
May	28th, 23.30	19.2	14.5	4.7	Kuuvuori	Aurajokiranta
June	28th, 05.00	19.1	15.5	3.6	Suntiontie	Aurajokiranta
July	16th, 22.00	22.5	19.9	2.6	Pispalantie	Aurajokiranta
August	18th, 06.00	14.5	10.2	4.3	Kuuvuori	Aurajokiranta
September	30th, 09.30	9.9	4.4	5.5	Kuuvuori	Yo-kylä länsi
October	16th, 08.30	6.2	-1.0	7.2	Kuuvuori	Aurajokiranta
November	24th, 11.30	1.1	-6.8	7.9	Kuuvuori	Aurajokiranta
December	18th, 09.00	-1.4	-6.4	5.0	Kuuvuori	Kuikkulankatu

warming effect. In late autumn and early winter, this warming effect of water bodies even surpassed that of land cover and population and building floor area. Of the applied variables, elevation was least often statistically significant. When it was, its effect was mostly seen as a proneness of lower-lying areas for cold air drainage. There were, however, also few situations in which the higher relative elevation meant lower temperature.

In the regression-based temperature maps the Turku city centre and other densely built districts mostly appear warmer than their surroundings. One reason behind these UHIs is thermal behaviour of construction materials: buildings and paved surfaces absorb solar heat during the day and release it after sunset, which delays nighttime cooling, resulting in the UHI effect that is often most pronounced during night hours. This mechanism is a key contributor of UHI in summer, when also lower evapotranspiration in urban than in rural areas for its part supports the formation of UHI. In winter, the anthropogenic heat release originated mostly from traffic and heat leakages from buildings is essential factor behind the UHI phenomenon. Of the built-up areas, main roads outside the most densely populated areas appear as warmer stripes relative to their environment.

The regression-based temperature maps also often highlight the archipelago and the coastal zones of mainland as relatively warm regions. In daytime in spring and summer, these same areas appear as the coldest. This twofold impact of water bodies reflects the high thermal inertia of them, caused by the high specific heat capacity of water, which enables heat storage within a deep layer. As a result, land areas both heat and cool more rapidly than surrounding water bodies. This difference is reflected in the daytime coolness of coastal areas in spring and summer, and, conversely, in their relative warmth during autumn and early winter, particularly at night.

In the Turku region, local temperature variation is strongly influenced by both land use and the presence of water bodies. Along the coast, water tends to reduce seasonal and diurnal temperature variability, though in certain situations it can intensify spatial temperature contrasts. The impact of land use is manifested most clearly as the warmness of densely built urban areas, that often form the core of UHI. The UHI has multiple societal consequences; it e.g., worsens heat-related health risks during heatwaves, but, on the other hand, diminishes heating demand during cold weather.

A good localized example of topography-driven thermal effect can be seen in the limestone quarry southwest of the Parainen city centre. Owing to its depth and the unusually large topographic variability compared to the overall topographic variability of the Turku region, the quarry occasionally exerts a pronounced influence on the modelled temperature (see e.g., Figs. 7d and 26d). During inversions that were common at the times of highest momentary temperature difference situations, the modelled temperatures for quarry were suspiciously low. The influence of quarry could also be detected in the modelled minimum temperatures of January, May, June, July, August, September and October.

Table 59. Monthly adjusted R square values and standardized coefficients for each statistically significant ($p \leq 0.05$) explanatory environmental variables (land cover, water bodies, elevation) of the CORINE-based and YKR-based multiple linear regression models applied for the average and averages of daily minimum temperature data of 2024. In this table and table 60, YKR refers to the building floor area and population -based variable.

		Monthly average temperature		Monthly averages of daily minimums	
Month	**Variable**	**Adjusted R Square**	**Standardized coefficients Beta**	**Adjusted R Square**	**Standardized coefficients Beta**
January		0.733		0.737	
	Urban land cover		0.881		0.777
	Water body		0.701		0.547
	Relative elevation		0.131		0.370
		0.684		0.728	
	YKR		0.788		0.721
	Water body		0.560		0.432
	Relative elevation		0.154		0.377
February		0.600		0.728	
	Land cover		0.862		0.942
	Water body		0.627		0.758
	Relative elevation				
		0.583		0.677	
	YKR		0.814		0.841
	Water body		0.535		0.613
	Relative elevation				
March		0.682		0.713	
	Urban land cover		0.911		0.894
	Water body		0.215		0.501
	Relative elevation				
		0.670		0.712	
	YKR		0.851		0.851
	Water body				0.407
	Relative elevation				0.148
April		0.709		0.746	
	Urban land cover		0.790		0.916
	Water body				0.314
	Relative elevation				0.166
		0.733		0.736	
	YKR		0.779		0.875
	Water body		-0.189		0.222
	Relative elevation				0.146
May		0.765		0.692	
	Urban land cover		0.712		0.829
	Water body		-0.198		0.368
	Relative elevation		0.181		0.274
		0.754		0.673	
	YKR		0.677		0.784
	Water body		-0.268		0.282
	Relative elevation		0.167		0.258

		Monthly average temperature		Monthly averages of daily minimums	
Month	**Variable**	**Adjusted R Square**	**Standardized coefficients Beta**	**Adjusted R Square**	**Standardized coefficients Beta**
June		0.615		0.610	
	Urban land cover		0.820		0.690
	Water body		0.304		0.522
	Relative elevation		0.192		0.282
		0.631		0.709	
	YKR		0.840		0.788
	Water body		0.290		0.582
	Relative elevation				0.215
July		0.571		0.643	
	Urban land cover		0.800		0.778
	Water body		0.351		0.599
	Relative elevation				0.215
		0.548		0.660	
	YKR		0.782		0.796
	Water body		0.296		0.588
	Relative elevation				
August		0.600		0.640	
	Urban land cover		0.764		0.657
	Water body		0.489		0.628
	Relative elevation		0.197		0.270
		0.595		0.662	
	YKR		0.758		0.675
	Water body		0.441		0.625
	Relative elevation				0.242
September		0.666		0.636	
	Urban land cover		0.725		0.594
	Water body		0.545		0.622
	Relative elevation		0.296		0.335
		0.619		0.698	
	YKR		0.687		0.652
	Water body		0.479		0.634
	Relative elevation		0.258		0.301
October		0.664		0.670	
	Urban land cover		0.643		0.561
	Water body		0.796		0.712
	Relative elevation		0.172		0.303
		0.658		0.734	
	YKR		0.626		0.623
	Water body		0.747		0.727
	Relative elevation				0.270
November		0.582		0.644	
	Urban land cover		0.644		0.666
	Water body		0.780		0.726
	Relative elevation				0.230

Month	Variable	Monthly average temperature		Monthly averages of daily minimums	
		Adjusted R Square	Standardized coefficients Beta	Adjusted R Square	Standardized coefficients Beta
		0.667		0.750	
	YKR		0.724		0.761
	Water body		0.789		0.750
	Relative elevation				0.143
December		0.661		0.741	
	Urban land cover		0.700		0.652
	Water body		0.783		0.825
	Relative elevation				0.185
		0.750		0.763	
	YKR		0.778		0.662
	Water body		0.790		0.788
	Relative elevation				0.137

Table 60. Monthly adjusted R square values and standardized coefficients for each statistically significant ($p \leq 0.05$) explanatory environmental variables (land cover, water bodies, elevation) of the multiple linear regression models applied for the averages of daily maximum temperature and momentary maximum temperature range data of 2024.

Month	Variable	Monthly averages of daily maximums		Momentary maximum temperature range	
		Adjusted R Square	Standardized coefficients Beta	Adjusted R Square	Standardized coefficients Beta
January		0.500		0.537	
	Urban land cover		0.673		0.492
	Water body		0.662		0.304
	Relative elevation		-0.063		0.515
		0.487		0.549	
	YKR		0.648		0.476
	Water body		0.609		0.238
	Relative elevation				0.516
February		0.327		0.540	
	Urban land cover		0.653		0.784
	Water body		0.360		0.621
	Relative elevation				
		0.350		0.469	
	YKR		0.662		0.687
	Water body		0.322		0.517
	Relative elevation		-0.224		
March		0.171		0.475	
	Urban land cover				0.772
	Water body		-0.430		0.516
	Relative elevation				

		Monthly averages of daily maximums		Momentary maximum temperature range	
Month	**Variable**	**Adjusted R Square**	**Standardized coefficients Beta**	**Adjusted R Square**	**Standardized coefficients Beta**
		0.360		0.441	
	YKR		0.477		0.708
	Water body		-0.284		0.418
	Relative elevation				
April		0.535		0.714	
	Urban land cover		0.292		
	Water body		-0.539		-0.872
	Relative elevation		-0.188		
		0.556		0.717	
	YKR		0.310		
	Water body		-0.573		-0.831
	Relative elevation		-0.181		
May		0.580		0.623	
	Urban land cover				0.605
	Water body		-0.762		0.213
	Relative elevation				0.458
		0.594		0.664	
	YKR				0.646
	Water body		-0.737		0.223
	Relative elevation				0.428
June		0.302		0.223	
	Urban land cover				0.586
	Water body		-0.567		0.332
	Relative elevation				
		0.389		0.140	
	YKR		0.316		0.458
	Water body		-0.452		
	Relative elevation				
July		0.355		0.628	
	Urban land cover		0.445		0.630
	Water body		-0.273		0.629
	Relative elevation				0.279
		0.348		0.689	
	YKR		0.402		0.706
	Water body		-0.348		0.675
	Relative elevation				0.217
August		0.206		0.640	
	Urban land cover				0.561
	Water body		-0.477		0.633
	Relative elevation				0.357
		0.303		0.737	
	YKR		0.335		0.671
	Water body		-0.364		0.693
	Relative elevation				0.296

		Monthly averages of daily maximums		Momentary maximum temperature range	
Month	**Variable**	**Adjusted R Square**	**Standardized coefficients Beta**	**Adjusted R Square**	**Standardized coefficients Beta**
September		0.067		0.647	
	Urban land cover				0.306
	Water body		-0.306		0.729
	Relative elevation				0.388
		0.196		0.701	
	YKR		0.391		0.396
	Water body				0.757
	Relative elevation				0.357
October		0.314		0.564	
	Urban land cover		0.588		0.378
	Water body		0.478		0.737
	Relative elevation				0.242
		0.292		0.550	
	YKR		0.551		0.350
	Water body		0.416		0.700
	Relative elevation				0.224
November		0.462		0.631	
	Urban land cover		0.586		0.378
	Water body		0.697		0.759
	Relative elevation				0.292
		0.503		0.590	
	YKR		0.620		0.303
	Water body		0.675		0.704
	Relative elevation				0.287
December		0.522		0.653	
	Urban land cover		0.627		0.593
	Water body		0.723		0.743
	Relative elevation				0.316
		0.511		0.602	
	YKR		0.604		0.490
	Water body		0.673		0.599
	Relative elevation				0.323

At the times of maximum momentary temperature ranges of spring and autumn and July, the study area was influenced by high-pressure located in southern Finland. In February, the largest momentary spatial temperature range situations were characterized by low-pressures located close to the Turku region in southern Finland. In other cases of maximum momentary temperature ranges, the study area was generally positioned between low- and high-pressure centres, and a pressure gradient in the area was relatively moderate. Average wind speed reached highest values in April, June and autumn months in the case

of the Turku region and in April and October in the case of the Student Village highest momentary temperature ranges (Table 61). Lowest wind speeds occurred in May, September and December. During other times the wind speed averages ranged from 1 m/s to approximately 2 m/s while the lowest values were close to 0 m/s and highest 2.5–4.5 m/s. Cloudiest conditions in the whole Turku region during the momentary maximum temperature ranges occurred in February and May with the average of 5.5 oktas. In the case of the Student Village the cloudiest conditions with the average of 7 oktas occurred in July and December. Yearly averages for average wind speed and cloudiness were 1.79 m/s and 2.29 oktas for the whole Turku region while in the case of Student Village, the respective averages were 1.35 m/s and 1.29 oktas, i.e., the maximum momentary temperature range situations of the Student Village were generally more connected to the wind and cloudiness conditions that support the formation of UHI.

Table 61. The average wind speed and average cloudiness in the FMI's Turku Artukainen station at the times of month-specific momentary maximum temperature ranges of the Turku region and of the Turku Student Village area in 2024. The values represent the averages of previous half-an-hour observations including the observation of the time of the momentary maximum temperature range.

Turku					Student Village				
Moment of maximum temp. range					Moment of maximum temp. range				
Month	Day	Time	Average wind speed (m/s)	Cloud-iness [1/8]	Month	Day	Time	Average wind speed (m/s)	Cloud-iness [1/8]
January	20–21	23.30–00.00	1.85	1.25	January	20–21	23.30–00.00	1.85	1.25
February	8	04.30–05.00	1.175	5.5	February	5	07.00–07.30	1.45	0
March	18	22.00–22.30	0.675	8	March	12	22.30–23.00	1.1	0
April	29	15.30–16.00	4.475	5.5	April	9	23.00–23.30	2.175	0
May	29	00.30–01.00	0.325	0	May	28	23.00–23.30	0.25	0
June	12	17.30–18.00	3.625	0	June	28	04.30–05.00	1.325	0
July	10	02.30–03.00	1.625	0	July	16	21.30–22.00	1.65	7
August	18	04.30–05.00	1.9	0	August	18	05.30–06.00	1.225	0
September	30	07.30–08.00	0.275	0	September	30	09.00–09.30	0.75	0
October	16	08.00–08.30	2.575	0.25	October	16	08.00–08.30	2.575	0.25
November	24	10.30–11.00	2.125	0	November	24	11.00–11.30	1.85	0
December	13	04.30–05.00	0.9	7	December	18	08.30–09.00	0	7
Average			1.79	2.29	**Average**			1.35	1.29

Information on spatial temperature differences supports climate-related urban planning. The UHI effect, a major contributor to heat-related health risks during hot periods, can be mitigated by green infrastructure, e.g., by tree planting and by expanding vegetated areas in the built environment. The choice of construction materials also plays a role: re-

flective, high-albedo surfaces help lower summer heat stress but may have the drawback in the form of elevating energy consumption for heating in colder months. During winter, spatial temperature mapping can help pinpoint locations especially vulnerable to slipperiness, as well as guide assessments of heating demand across different parts of the city. These season-dependent effects and differences highlight the importance of planning, and when implemented carefully, temperature-based planning supports both public health and energy efficiency year-round.

6
CONCLUDING REMARKS

This study examined the spatial and temporal variations in temperature across the Turku region during 2024 by utilising half-an-hour interval temperature observations of altogether 77 temperature and relative humidity (T/RH) loggers together with GIS data on various environmental variables. The analyses were complemented by large-scale atmospheric reanalysis data and data on cloudiness and wind speed. Turku city centre was principally the warmest site in the region. The difference in annual average temperature of 2024 between the warmest observation site, located in the densely built Turku city centre, and the coldest observation site, located approximately 10 km to the NNE of the city centre in an uninhabited forest, was approximately 2.0 °C, which coincides with the respective longer-term average reported in earlier studies (Suomi & Käyhkö, 2012; Suomi, 2014). The respective difference in daily minimum temperatures was 3.2 °C, and in daily maximum temperatures 1.2 °C. Largest momentary spatial temperature difference was 14.2 °C, measured at night in January between the relatively warm high-positioned site in the Turku city centre and the semi-urban site along the River Aura approximately 3 km to the NE of the city centre. The primary drivers of spatial temperature variability in the Turku area are land cover, proximity to water bodies, and topography, of which the impacts of land cover and water bodies are clearly stronger than that of topography.

The main findings of the study are summarised as follows:

- **Urban land cover**, determined based on the CORINE Land Cover dataset, exerted a consistent warming influence throughout the year. Built-up areas, particularly those dominated by blocks of flats and asphalted streets and squares, retained heat effectively during daytime resulting in delayed nighttime cooling, reinforcing the UHI effect.
- **High population density and building floor area,** determined based on the YKR data, also consistently exhibited a warming effect. This influence, almost similar to that of urban land cover, was also present throughout the year and played a notable role in amplifying the UHI.
- **Water bodies** exhibited seasonally varying impacts. Coastal areas were relatively cool in daytime in spring, but, on the contrary, relatively warm in late autumn and early winter, especially at night. This warming effect of water bodies occasionally surpassed the warming influence of the city.
- **Elevation** showed varying and generally weakest effects. Its impact was seen most clearly during nocturnal inversions, when low-lying areas were clearly colder that their surroundings.
- **Large-scale atmospheric conditions**, particularly the locations of high- and low-pressure systems, had a strong influence on the magnitude and timing of spatial temperature differences. High-pressures enhanced

spatial temperature differences via their effects on wind speed and cloudiness, which was seen e.g., during the maximum momentary temperature difference situations in spring and July.

- **Wind speed and cloudiness** showed seasonal variation. Wind speeds were highest in April, June, and at the end of autumn, while lowest values occurred in May, September, and December. Cloudiness peaked in March and December across the region, while the Student Village experiencing the cloudiest conditions in July and December.

These results emphasize the complex interplay between land cover, water bodies, elevation, and atmospheric conditions in shaping local temperature patterns in the Turku region. The UHI effect emerges as a consistent and significant feature, having implications for e.g., public health and energy efficiency. Understanding these spatial dynamics is essential for climate-related urban planning. Based on the experiences of two different urban type variables applied within separate regression models, testing of additional datasets, variables and modelling methods could further enhance the accuracy of temperature modelling. Large temporal VARIABILITY of spatial temperature differences and their dependence on weather conditions, observed in this study, suggests to put enough emphasis on analysing both momentary situations and long-term average conditions. For the purposes of urban planning, it is recommended to consider potential impacts of climate change and urban development on temperature and its spatial variability.

7
ACKNOWLEDGEMENTS

We thank the Geography Division of the University of Turku and Urban Environment Division of the City of Turku for financial support in maintaining the TURCLIM weather observation network. Funding for this research for Juuso Suomi and Krista Väätäinen was granted by the European Union's Horizon 2020 research and innovation programme under the Grant Agreement number 957751.

8
REFERENCES

Jokinen, P., Pirinen, P., Kaukoranta, J., Kangas, A., Alenius, P., Eriksson, P., Johansson, M. & Wilkman, S. (2021) Tilastoja Suomen ilmastosta ja merestä 1991–2020. Ilmatieteen laitoksen raportteja 2021:8. https://helda.helsinki.fi/items/d7ce3a4f-bf47-4453-be76-2a0de738c59a

Kuttler, W. & Weber, S. (2023) Characteristics and phenomena of the urban climate. *Meteorologische Zeitschrift, 32(1),* 15–47. https://doi.org/10.1127/metz/2023/1153

National Land Survey of Finland (2019) Elevation model 2019, 10 m × 10 m, TIFF. CSC—IT Center for Science. http://urn.fi/urn:nbn:fi:csc-kata00001000000000000622 (accessed 22 Jul 2024)

National Land Survey of Finland (2020) SLICES 2010, 10 m × 10 m, generalized raster, ETRS TM35FIN. National Land Survey of Finland. CSC—IT Center for Science Ltd. http://urn.fi/urn:nbn:fi:csc-kata00001000000000000262 (accessed 22 May 2024)

Oke T.R. (1987) Boundary Layer Climates, 2nd edition. 435 pp. Routledge, London.

Reinwald, F., Thiel, S., Kainz, A. & Hahn, C. (2024) Components of urban climate analyses for the development of planning recommendation maps. Urban Climate, 57, 102090. https://doi.org/10.1016/j.uclim.2024.102090

Statistics Finland (2023) YKR-aineisto. Statistics Finland. https://stat.fi/tup/ykraineistot/index.html (accessed 20 Dec 2024)

Suomi, J. & Käyhkö, J. (2012) The impact on environmental factors on urban temperature variability in the coastal city of Turku, SW Finland. International Journal of Climatology, 32(3), 451-463. https://doi.org/10.1002/joc.2277

Suomi, J. (2014) Characteristics of urban heat island (UHI) in a high latitude coastal city - a case study of Turku, SW Finland. PhD thesis. University of Turku, Faculty of Mathematics and Natural Sciences, Department of Geography and Geology. https://urn.fi/URN:ISBN:978-951-29-5912-9

Suomi, J., Saranko, O., Partanen, A., Fortelius, C., Gonzales-Inca, C. & Käyhkö, J. (2024) Evaluation of surface air temperature in the HARMONIE-AROME weather model during a heatwave in the coastal city of Turku, Finland. Urban Climate, 53, 101811. https://doi.org/10.1016/j.uclim.2024.101811

Syke (2024) Corine maanpeite 2018. Finnish Environment Institute (Syke). https://ckan.ymparisto.fi/dataset/corine-maanpeite-2018 (accessed 21 August 2024)

Wetterzentrale (2025). Top Karten. CFS reanalysis 0.500°. Wetterzentrale. https://www.wetter zentrale.de (accessed 11 Aug 2025)

UNIVERSITY OF TURKU
MAANTIETEEN JA GEOLOGIAN LAITOS
DEPARTMENT OF GEOGRAPHY AND GEOLOGY

TURUN YLIOPISTON MAANTIETEEN JA GEOLOGIAN LAITOKSEN JULKAISUJA
PUBLICATIONS FROM THE DEPARTMENT OF GEOGRAPHY AND GEOLOGY, UNIVERSITY OF TURKU

No. 6. Jussi S. Jauhiainen: Asylum seekers in Lesvos, Greece, 2016–2017. 2017

No. 7. Jussi S. Jauhiainen: Asylum seekers and irregular migrants in Lampedusa, Italy, 2017. 2017

No. 8. Jussi S. Jauhiainen, Katri Gadd & Justus Jokela: Paperittomat Suomessa 2017. 2018.

No. 9. Jussi S. Jauhiainen & Davood Eyvazlu: Urbanization, Refugees and Irregular Migrants in Iran, 2017. 2018.

No. 10. Jussi S. Jauhiainen & Ekaterina Vorobeva: Migrants, Asylum Seekers and Refugees in Jordan, 2017. 2018.

No. 11. Jussi S. Jauhiainen: Refugees and Migrants in Turkey, 2018. 2018.

No. 12. Tua Nylén, Harri Tolvanen, Anne Erkkilä-Välimäki & Meeli Roose: Guide for cross-border spatial data analysis in Maritime Spatial Planning. 2019.

No. 13. Jussi S. Jauhiainen, Lutz Eichholz & Annette Spellerberg: Refugees, Asylum Seekers and Undocumented Migrants in Germany, 2019. The Case of Rhineland-Palatinate and Kaiserslautern. 2019.

No. 14. Jussi S. Jauhiainen, Davood Eyvazlu & Bahram Salavati Sarcheshmeh: Afghans in Iran: Migration Patterns and Aspirations. 2020.

No. 15. Jussi S. Jauhiainen & Ekaterina Vorobeva: Asylum Seekers and Migrants in Lesvos, Greece, 2019–2020. 2020.

No. 16. Salla Eilola, Petra Kollanen ja Nora Fagerholm: Vehreyttä ja rentoa oleskelutilaa kaivataan Aninkaisten konserttitalon kortteliin – Raportti 3D-näkymiä pilotoivan asukaskyselyn tuloksista ja käyttökokemuksesta. 2021.

No. 17. Jussi S. Jauhiainen, Sanni Huusari & Johanna Junnila: Asylum Seekers and Undocumented Migrants in Lesvos, Greece, 2020–2022. 2022.

No. 18. Jussi S. Jauhiainen, Heidi Ann Erbsen, Olha Lysa & Kerly Espenberg. Temporary Protected Ukrainians and Other Ukrainians in Estonia, 2022. 2022.

No. 19. Liliana Solé, Katri Väänänen, Johanna Kostamo ja Nora Fagerholm: Saaristomeren maisema-arvot ja tulevaisuuden kehitystoiveet. 2023.

No. 20. Joni Mäkinen, Kari Kajuutti & Juulia Kautto: Mannerjäätikön alaisten sulamisvesireittien ja murtoo-maaperä--muodostumien luontotyyppi, hyödyntämismahdollisuudet ja suojelutarve. MurtooVarat -hankkeen loppuraportti. 2023.

No. 21. Jussi S. Jauhiainen, Olha Mamchur & Mart Reimann: Return Migration of Ukrainians from the European Union to Ukraine, 2022–2024. 2024.

No. 22. Jussi S. Jauhiainen & Oiva Tuominen(†) ja Mauno Mielonen(†): Maantiede Turun yliopistossa 1924–2024. 2024.

No. 23. Nora Fagerholm, Salla Eilola, Ulrika Stevens Laura Kivirinne, Ville Rummukainen ja Veera Kangasniemi: Urban Biodiversity Parks hankkeen alkukartoitus pilotti-alueille Halinen ja Jyrkkälä. Nykyiset luontoarvot ja potentiaaliset alueet luonnonmonimuotoisuutta lisääville toimenpiteille. Urban Biodiversity Parks -hankkeen julkaisu 2025.

No. 24. Juuso Suomi, Krista Väätäinen & Jukka Käyhkö: Seasonal and diurnal characteristics of spatial temperature variability in Turku, SW Finland – a case study of 2021. 2025.

No. 25. Juuso Suomi, Krista Väätäinen & Jukka Käyhkö: Interaction of weather, air quality and urban heat island in the city of Turku, SW Finland – a case study of 2021 and 2023. 2025.

No. 26. Juuso Suomi, Krista Väätäinen & Jukka Käyhkö: Characteristics of spatio-temporal temperature variability in relation to population and various environmental parameters – A case study of Turku, SW Finland. 2025.

ISBN ISBN 978-952-02-0383-2 (PDF) ISSN 2324-0369 (PDF)